AGRICULTURAL UNIVERSITY OF ATHENS
SCHOOL OF APPLIED BIOLOGY AND BIOTECHNOLOGY

MSc. in Systems Biology

Biomedical Systems Laboratory. School of Mechanical Engineering,
National Technical University of Athens

Master Thesis

Single-cell Spatial Proteomics of Chronic Kidney Disease Tissue samples

Maria I. Chrysopoulou

Supervisor:
Chatzopoulos Polydefkis, Professor AUA
Alexopoulos Leonidas, Associate Professor NTUA

Athens
2020

AGRICULTURAL UNIVERSITY OF ATHENS

SCHOOL OF APPLIED BIOLOGY AND BIOTECHNOLOGY

Biomedical Systems Laboratory, School of Mechanical Engineering,

National Technical University of Athens

Master Thesis

Single-cell spatial proteomics of Chronic Kidney Disease Tissue Samples

"Μελέτη της χρόνιας νόσου των νεφρών μέσω πρωτεομικής τοπολογικής και single-cell ανάλυσης ιστολογικών δειγμάτων"

Maria I. Chrysopoulou

Chatzopoulos Polydefkis, Professor AUA (supervisor)

Alexopoulos Leonidas, Associate Professor NTUA (supervisor)

Douni Eleni, Associate Professor AUA

Single-cell Spatial Proteomics of Chronic Kidney Disease Tissue Samples

School of Applied Biology and Biotechnology

Biomedical Systems Laboratory, School of Mechanical Engineering, National Technical University of Athens

ABSTRACT

Chronic kidney disease (CKD) constitutes a multifactorial systemic disease that covers a wide range of renal pathological conditions, with multiple initial causes and subsequent mechanisms. Since CKD diagnostics lack accurate prognostic and diagnostic markers, the CKD research should focus on system-wide approaches and the investigation of its underlying molecular paths. In the current research, the Multiple Iterative Labeling by Antibody Neodeposition (MILAN) protocol was optimized and applied in formalin-fixed paraffin-embedded (FFPE) kidney tissue samples. In addition, a set of 20 CKD-related proteins was tested in samples from healthy and CKD renal tissue including G2 and G3 CKD stages. Furthermore, a new method of image processing was employed, using open-source software that permitted the investigation of the proteins' spatial distribution in different renal compartments. The changes in the relative expression of 15 proteins between the healthy and CKD condition was evaluated as statistically significant and was following previous findings. Some of them were decreased in the initial CKD stage G2 and increased in the advanced CKD Stage G3. The expression of other proteins was more rapidly reversed in the glomeruli than the renal tubules between the two CKD stages. The results verified the involvement of several proteins in the regulation of cell proliferation, tissue inflammation, glomerular filtration, and fibrosis. The molecular pathways that were generally represented from this set of proteins are the AGE-RAGE and the TGFβ signalling pathways, which have already been connected to the CKD progression. In conclusion, this research inserted a novel method in CKD research with a great perspective for the future. Nevertheless, further research is required for the detailed investigation of the underlying mechanisms of CKD.

Scientific area:

Human Systemic Diseases

Keywords:

Chronic Kidney Disease, Multiplex Immunofluorescence, Proteomic Analysis, Spatial analysis, Single-cell analysis, Image processing

Μελέτη της Χρόνιας Νόσου των νεφρών μέσω πρωτεομικής τοπολογικής και single-cell ανάλυσης ιστολογικών δειγμάτων

Τμήμα Βιοτεχνολογίας

Εργαστήριο Βιοϊατρικών Συστημάτων, Σχολή Μηχανολόγων Μηχανικών, Εθνικό Μετσόβιο Πολυτεχνείο

ΠΕΡΙΛΗΨΗ

Η χρόνια νόσος των νεφρών αποτελεί μία πολυπαραγοντική συστημική ασθένεια που περιλαμβάνει ένα εύρος παθολογικών καταστάσεων των νεφρών, με πολλαπλές αρχικές αιτιολογίες και υποκείμενους μηχανισμούς. Η έγκαιρη διάγνωσή της, απαιτεί ακριβείς προγνωστικούς και διαγνωστικούς δείκτες, γι αυτό η έρευνα στρέφεται πλέον σε συστημικές προσεγγίσεις και τη διερεύνηση των μοριακών μηχανισμών της ασθένειας. Στην παρούσα εργασία, βελτιστοποιήθηκε και εφαρμόστηκε το πρωτόκολλο πολυπλεκτικού ανοσοφθορισμού Multiple Iterative Labeling by Antibody Neodeposition (MILAN) σε τομές ιστών νεφρών μονιμοποιημένες σε φορμαλίνη και παραφίνη, από υγιή άτομα και ασθενείς των σταδίων 2 και 3 της νόσου. Έπειτα, αναπτύχθηκε μια σειρά βημάτων επεξεργασίας των εικόνων με χρήση προγραμμάτων ελεύθερου λογισμικού, η οποία ανέδειξε πληροφορίες ως προς την έκφραση και τη χωρική τους κατανομή σε διαφορετικές νεφρικές περιοχές. Συνολικά, ελέγχθηκε η ταυτόχρονη έκφραση και τοπολογική κατανομή 20 πρωτεϊνών που σχετίζονται με την ασθένεια. Σε 15 από αυτές βρέθηκε στατιστικά σημαντική διαφορετική έκφραση μεταξύ των δειγμάτων από υγιείς και ασθενείς επιβεβαιώνοντας προηγούμενα σχετικά βιβλιογραφικά δεδομένα. Ορισμένες πρωτεΐνες, εμφάνισαν μειωμένη έκφραση στο στάδιο 2 και αυξημένη έκφραση στο στάδιο 3 της ασθένειας κυρίως στα σπειράματα. Οι πρωτεΐνες αυτές έχουν συσχετιστεί με κυτταρικές διαδικασίες όπως συμμετοχή στη ρύθμιση του πολλαπλασιασμού των κυττάρων, τη ρύθμιση της φλεγμονώδους αντίδρασης του ιστού, τη σπειραματική διήθηση και τη νεφρική ίνωση. Επίσης, επιβεβαιώθηκε η σημαντικότητα των σηματοδοτικών μονοπατιών AGE-RAGE και TGFβ, τα οποία έχουν σχετιστεί με την ασθένεια και σε προηγούμενες μελέτες. Η παρούσα εργασία εισήγαγε μια καινοτόμα ερευνητική προσέγγιση με υψηλές δυνατότητες εξέλιξης στην έρευνα για τη χρόνια νόσο των νεφρών. Ωστόσο, απαιτείται μελλοντικά περαιτέρω μελέτη για την πληρέστερη διερεύνηση των υποκείμενων μηχανισμών της χρόνιας νεφρικής νόσου.

Επιστημονικη περιοχή:

Συστημικές Ασθένειες Ανθρώπου

Λέξεις Κλειδιά:

Χρόνια Νόσος των νεφρών, Ιστολογική μελέτη, Πολυπλεκτικός Ανοσοφθορισμός, Πρωτεομική Ανάλυση, Τοπολογική Ανάλυση, single-cell ανάλυση, ανάλυση εικόνας

Acknowledgments:

The current thesis was conducted in the Biomedical Systems Laboratory, School of Mechanical Engineering, National and Technical University of Athens, under the supervision of Associate Professor Leonidas Alexopoulos. I would like to thank all the people who contributed to the successful completion of this thesis.

I would like to express my gratitude to Mr. Leonidas Alexopoulos for allowing me to work on such an interesting scientific project and supporting me throughout this period.

I also wish to acknowledge the Ph.D. candidates, Danae Zareifi and Christos Fotis, and the graduate student Nikos Meimetis during this demanding year.

I would also like to thank Dr. Giorgio Cattoretti, Associate Professor at the University of Milano Bicocca for training us in the MILAN protocol and Rafael Kramann, Christoph Kuppe, and Julio Saez-Rodriguez, RWTH Aachen University for supplying us with tissue samples.

Finally, I would like to thank my family and friends for the encouragement and support I have received all these years.

Contents

I. Introduction

i) Chronic Kidney Disease

Chronic Kidney Disease (CKD) is a term related to a wide spectrum of pathological states of the kidney, roughly characterized by the progressive damage of kidney and/or partial loss of kidney function, persistent for 3 months at least, that affects the patients' general health condition (Zoccali et al., 2017), ("KDIGO 2017 Clinical Practice Guideline Update for the Diagnosis, Evaluation, Prevention, and Treatment of Chronic Kidney Disease–Mineral and Bone Disorder (CKD-MBD)," 2017). The final stage of CKD, irrelevant to the initial cause and CKD-type, is renal failure and it is described by the term End-Stage Renal Disease (ESRD).

Epidemiological Data

CKD is considered a common disease worldwide. The percentage of the world's population affected by CKD is estimated to 10% and only in Europe and the United States the number of CKD patients that progress to ESRD is increasing by 5-10% every year. Millions of people die every year due to a lack of early diagnosis methods, inadequate care, and limited access to renal replacement therapies (International Society of Nephrology (ISN), McCullough et. al., 2019).

CKD was the 12th cause of mortality in 2017 with 1.23 million deaths according to the Institute for Health Metrics and Evaluation, increased by 41.5% since 1990. Further, CKD resulted in 35,8 million disability-adjusted life-years (DALYs) in 2017 (Bikbov et al., 2020).

However, according to Hill et al., (2016), the numbers of CKD prevalence in different countries show high variability owing to different CKD assessment criteria, mostly in low- and middle- income countries, in which the accessibility to CKD treatment is restricted and these cases are not registered. As a result, CKD prevalence could be over- or underestimated and further research is required to get an accurate epidemiological overview of Chronic Kidney Disease worldwide (Romagnani et al., 2017, Glassock et al., 2017, Stanifer et al., 2016, Saran et al., 2017).

Diagnosis and CKD classification

The Kidney Disease Improving Global Outcomes (KDIGO) initiative defines several CKD stages to describe the progression of the disease based on the glomerular filtration rate (GFR), the albuminuria levels and the possible initial cause ("KDIGO 2017 Clinical Practice Guideline Update for the Diagnosis, Evaluation, Prevention, and Treatment of Chronic Kidney Disease–Mineral and Bone Disorder (CKD-MBD)", 2017, Figure 1).

GFR:

GFR indicates the efficacy of renal excretory function as a meter of the flow of plasma from the glomerulus into Bowman's space over a specified period. About 1 litre per minute of oxygenated blood reaches glomeruli via the afferent arteriole and exiting through the efferent arteriole. Plasma is the only blood component that can cross glomeruli and contains organic and inorganic solutes that can be freely filtered in Bowman's space. In the healthy state, the renal plasma flow (RPF) is approximately 600 to 720 ml per minute and GFR is approximately 120 ml per min (Kaufman et al., 2020, Fattah et al., 2019, Asmar et al., 2019, Yavuz et al., 2019). Although GFR is only one of the components of excretory function, it is considered a general indicator of

kidney function as numerous CKD structural or functional abnormalities are mirrored to the GFR decrease (Levin et al., 2013).

Renal excretory function depends on the total number of nephrons, the structural and functional units of the kidney, and single nephron's effectiveness in the filtration procedure. As a result, GFR is described by the equation:

$GFR_{(total)} = GFR_{(single-nephron)}$ *x number of nephrons* (expressed in ml/min/1.73 m^2)

that clarifies that GFR can be unaltered when the total number of nephrons increases their efficiency whereas the decrease in $GFR_{(total)}$, that characterizes CKD, is due to loss of functional nephrons (Romagnani et al., 2017). GFR could either be estimated (eGFR) or measured (mGFR). The GFR-based CKD stages are classified as G1-G5. The CKD starting GFR value is 90 ml/min/1.73 m^2 and follows a decreasing trend in parallel with kidney dysfunction up to 15 ml/min/1.73 m^2 that characterizes ESRD.

Albuminuria:

Albuminuria is the pathological condition that refers to the presence of excessive albumin in the urine. In the healthy state, albumin, a major plasma protein, is barely found in urine, whereas in kidney diseases its presence is notably increased. Albuminuria is a type of proteinuria; nonetheless, CKD clinical assessment emphasizes on albuminuria rather than proteinuria because albumin is the predominant urinary protein, and its quantity is highly correlated to the glomerular injury and risk of cardiovascular disease. These proteins are not excreted in terms of physiology but the evaluation of their presence has been established to be expressed in relation with the urinary loss rate: albumin/protein excretion rate (AER/PER). The values given constitute a ratio of albumin/protein to serum creatinine (expressed in mg/g). The value of 10 mg/g in 24 hours is considered normal. In CKD patients this value increases from 10 to 30 mg/g (CKD A1 stage). In advanced CKD this value can reach 300 mg/g (A2 stage) or get over it (A3 stage).

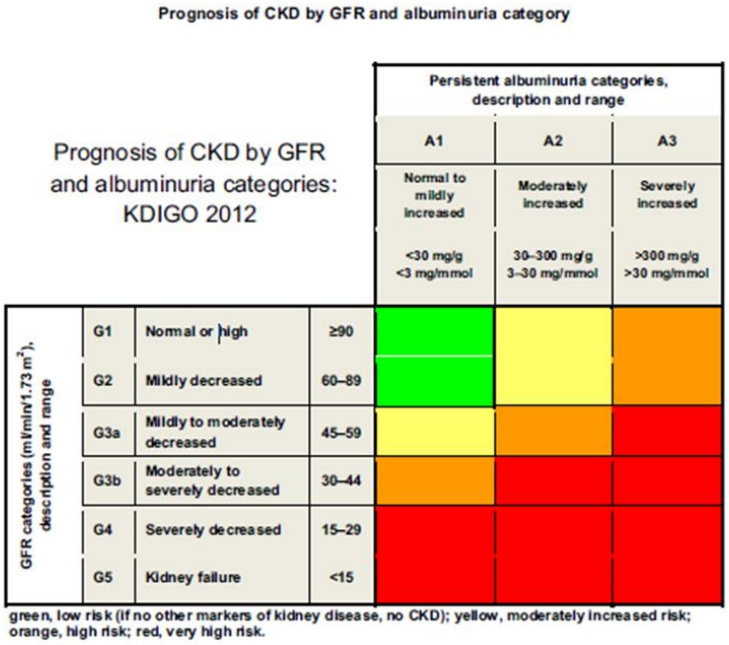

Figure 1 CKD stages according to GFR and albuminuria levels, indicating the risk of CKD progression (Levin et al., 2013)

Initial Cause:

Additional to KDIGO basic classification and risk assessment of CKD patients, the connection to existing contributing factors and the investigation of the primary causes is highly recommended. The clinical management of CKD patients is undoubtedly a complicated and demanding task as it requires the consideration of the patients' complete clinical image. ("KDIGO 2017 Clinical Practice Guideline Update for the Diagnosis, Evaluation, Prevention, and Treatment of Chronic Kidney Disease–Mineral and Bone Disorder-CKD-MBD", 2017).

Age and gender are the basic factors that should be taken into consideration. People older than 65 years old are more vulnerable to develop CKD, however, if younger people get affected with CKD, they deal with a higher risk of progression to ESRD. Besides, CKD is more frequent in female patients but male patients are prone to relapse to ESRD (Hill et al., 2016). Furthermore, preterm birth of babies with birth weight less than 2.5 kg has been associated with the development of CKD later in life due to incomplete kidney development (Brenner et al., 1988, The Low Birth Weight and Nephron Number Working Group, 2017, Hirano et al., 2016, Ruggajo et al., 2016). Nephrons are generated between 3 and 9 months of gestation and no new nephrons can be created after birth. So, the restricted number of nephrons in people of preterm birth and the augmented function of the available nephrons to compensate for the organism's requirements, increase the risk of early kidney damage and dysfunction that lead to CKD.

About the subjacent diseases that are associated with kidney deterioration, it is a fact that they differ between higher- to middle-income countries' population and middle- to lower-income countries' populations (LMICs). In the first case, CKD is linked to diabetes mellitus and hypertension. Patients with diabetes mellitus are predisposed to microvascular diseases which are also correlated to CKD. In LMICs, the possible underlying pathological condition involves infectious diseases, glomerulonephritis (glomeruli inflammation) and improper use of remedies that may contain nephrotoxins, nonsteroidal anti-inflammatory drugs (NSAIDs) and other substances that could be proven toxic to the nephrons (Jha et al., 2013, Stanifer et al., 2017). It is also possible, though, that in LMICs, diabetes and obesity will become the major risk factor of CKD in the next few years (Charlton et al., 2014, Khalsa et al., 2016, Bertram et al., 2011, Hostetter et al., 1981).

There are also genetic and environmental factors that lead to CKD and they have been identified in specific populations of the world such as the Aboriginal Australians, African Americans, and others (Komenda et al., 2016). Endemic environmental causes related to climate and daily agricultural routine, have also been correlated with CKD in agricultural populations in many regions of the world (Gifford et al., 2017, Glaser et al., 2016, Jayasumana et al., 2016).

CKD Pathophysiology

Fundamental renal function: renal reserve

In humans, the average number of nephrons per kidney is estimated at around 950.000. They are formed between the 3rd and 9th month of gestation (Bertram et al., 2011). After birth, no new nephrons can be generated and the existing nephrons increase in size to compensate the organism's needs. The fundamental renal function is called "renal reserve" and relies on the capability of nephrons to increase the single-nephron GFR without structural changes to deal with temporary increment in filtration rate, as required in the daily food intake (Hostetter et al., 1981).

Nephron Hypertrophy

However, in persistent increments in body mass, like in pregnancy and obesity, or cases of reduction of the total number of nephrons due to ageing, injury, donation, etc., a reparative

mechanism is activated that enlarges the glomerular tuft, Bowman's capsule and the proximal tubule leading to nephron hypertrophy.

The mechanism involves the expression of transforming growth factor-a (TGF-a) and epithelial growth factor receptor (EGFR) due to glomerular hypertension (increased filtration force) and glomerular hyperfiltration (Ruggenenti et al., 2012, Laouari et al., 2011). The expression of these factors promotes nephron hypertrophy but reduces glomerular hypertension because of the expansion of the filtration surface (Helal et al., 2012). Nephron hypertrophy maintains the augmented single-nephron GFR that further attenuates the nephron capacity and results in nephron loss. Besides, beyond a certain level, augments the shear stress on podocytes and evokes various pathological conditions, such as podocyte detachment, focal segmental glomerulosclerosis (FSGS), global glomerulosclerosis, and nephron atrophy. (Benghanem Gharbi et al., 2016, Ruggenenti et al., 2012, Helal et al., 2012, Denic et al., 2017, Hodgin et al., 2015, Kriz and Lemley, 1999, Kriz and Lemley, 2015).

Glomerulal Hyperfiltration

Glomerular hyperfiltration is a state characterized by excessive production of pro-urine by the glomerular filtration process. The causes of glomerular hyperfiltration vary including afferent arteriolar vasodilation as seen in patients with diabetes and/or by efferent arteriolar vasoconstriction owing to activation of the renin-angiotensin-aldosterone system (RAS system), thus leading to glomerular hypertension. Glomerular hypertrophy and glomerular hyperfiltration might be both a cause and a consequence of renal injury (Cachat et al., 2015, Helal et al., 2012).

Wound-healing responses lead to renal fibrosis

In conditions of nephron loss or general renal injury, the organism reacts with general wound-healing responses that usually lead to interstitial fibrosis. Fibrosis is the final common pathway for most renal diseases resulting in ESRD, describing a generalized decay of the renal tissue. The principle mechanism of fibrosis is the Epithelial to Mesenchymal Transition (EMT) of tubular epithelial cells which are transformed into mesenchymal fibroblasts migrating to adjacent interstitial parenchyma along with the persistent cytokine exposure and the accumulation of inflammatory cells. Interstitial fibrosis can bring the remnant nephrons in a steady condition, in which though, they are in risk of secondary injury (anaerobic metabolism, intracellular acidosis and endoplasmic reticulum stress) or further deteriorate them because of progression to renal ischemia (Ruggenenti et al., 2012, Schnaper, 2017, Kaissling et al., 2013, Peired et al., 2013).

Glomerular and Podocytes injury

The first part of the nephron consisting of a network of capillaries and the Bowman's capsule is called "glomerulus". Around the capillaries, podocytes form foot processes ("pedicels") that extend across the whole capillaries' surface and create spaces, known as filtration slits or slit diaphragms (Reiser and Altintas, 2016). The main cell-surface proteins of the slit diaphragm are nephrin and podocin that form a complex. Blood gets filtered through these slits, as they constitute one of the main components of the glomerular blood filtration barrier. Therefore, a podocyte injury or a filtration slits' damage directly leads to impaired kidney function (Martin and Jones, 2018, Vivarelli et al., 2017). Podocyte injury is considered a major reason for the pathogenesis of proteinuria and glomerulosclerosis and is observed in many pathological states of CKD (Lal and Patrakka, 2018, Asanuma, 2015, Reiser and Sever, 2013).

Genetic factors as the primary cause of CKD

The most prevalent genetic abnormalities associated with CKD are the congenital anomalies of the kidney and urinary tract (CAKUT). People with such congenital abnormalities appear with weak epithelial integrity, irregular function, a load of unfiltered metabolic waste and glycoproteins that lead to a low number of functional nephrons, kidney hypodysplasia, nephrocalcinosis and generation of cysts (Oliveira et al., 2016, Trautmann et al., 2015, Eckardt et al., 2015, Nicolaou et al., 2015, Cain et al., 2010, Uy and Reidy, 2015). There have been also found

specific gene variants that raise the possibility of CKD, such as uromodulin (UMOD) and apolipoprotein (APOL1). APOL1 influence autophagy and endosomal function and advance nephron loss and glomerulosclerosis in CKD patients (Köttgen et al., 2009, Kruzel-Davila et al., 2017).

Pathological conditions associated with CKD development

Diabetes

Hyperglycaemia in patients with diabetes drives the sodium/glucose cotransporter 2 (SGLT2)-related reabsorption of sodium in the proximal tubules that disables the tubule-glomerular feedback and triggers the RAS system at the macula densa of the renal tubules. As a consequence, the afferent arteriole is expanded stably and the efferent arteriole is constricted ending up to single- and total-GFR increase (Anders et al., 2016, Vallon, 2015, van Bommel et al., 2017).

Acute Kidney Injury (AKI)

Acute Kidney Injury can occur due to pre-, intra- or post-renal dysfunction. The main consequence of such an injury is nephron loss. The subsequent storage of toxins and other metabolic waste creates uraemic pathology and can be harmful to other organs, as well (Bellomo et al., 2012).

Systemic Complications of CKD

CKD leads to severe systemic complications. In the first stages of CKD, patients present with low serum 25-hydroxyvitamin D and 1,25-dihydroxyvitamin D_3 and high levels of serum parathyroid hormone (PTH) and fibroblast growth factor 23 (FGF23). These hormones are fundamental in mineral homeostasis and bone integrity, so CKD patients are prone to develop mineral bone disorder (Portale et al., 2014). In addition, fluid and electrolyte abnormalities, such as hypervolemia and hyperkalemia are common in CKD patients due to the imbalanced exchange of Na^+ and K^+ in the distal tubules. The accumulation of serum bicarbonate also reduces the minerals in bones, and muscles are damaged leading to metabolic acidosis. Another inevitable consequence is the excessive loss of blood along with the low production of erythropoietin and the restricted absorption of iron by hepcidin that results in anaemia. Moreover, the accumulation of uric acid in blood leads to hyperuricemia and uremia. The uremic acid affects also lipid particles in the blood and together with imbalanced lipid metabolism, dyslipidemia can occur.

Many of the factors mentioned above, contribute to the increase of arterial hypertension and the endocrine dysfunction. The most severe consequence though, that usually develops, is cardiovascular disease (CVD). CVD involves various atherosclerotic processes, vascular wall degeneration, systolic/ diastolic dysfunction, and can end up to ischemia that can be proven fatal.

End-Stage Renal Disease (ESRD)

The final pathological condition of CKD, known as ESRD, is defined by excessive renal fibrosis: glomerular sclerosis and interstitial fibrosis. The procedure that leads to ESRD involves numerous mechanisms such as extracellular matrix formation, cytokine secretion, energy

metabolism, podocyte injury, cell proliferation and differentiation, endoplasmic reticulum stress, autophagy, infiltration of inflammatory cells and activation of fibroblasts (Humphreys, 2018).

Molecular Mechanisms of CKD

CKD is a multifactorial disease that covers a broad range of renal pathological conditions. As a consequence, numerous molecular mechanisms are associated with CKD, concerning pre-renal, intrinsic renal, or post-renal processes. Some of them are mentioned below.

- MAPK pathway (p38 Mitogen-Activated Protein Kinase pathway):

MAPK pathway is an intracellular signal transduction pathway that has been associated with CKD progression and is regarded to play an essential role in inflammation, apoptosis, and tubulointerstitial fibrosis (Ma et al., 2014). MAPK pathway is involved in the production of proinflammatory and profibrotic mediators and the fibrosis-related extracellular matrix synthesis, in which the contribution of p38a isoform is regarded as the most important mediator (Sugiyama et al., 2012, Yang et al., 2014). According to Lee et al., (2019), MAPK activation increases along with JNK pathway activation after the development of renal fibrosis, mainly in the tubular and the interstitial area, and possibly interacts with TGF-β pathway. The degree of renal fibrosis advances in parallel with p38 activity as its inhibition has been found to suppress TGF-β-related fibrosis. Apoptosis signal-regulating kinase 1 (ASK1) is regarded as a possible upstream MAPK activator (Lin et al., 2015).

- TGF-β/Smad pathway (Transforming Growth Factor β/ Smad pathway)

Transforming growth factor-β (TGF-β) signalling cascade is significant in renal fibrosis development (Kalluri and Neilson, 2003, Liu, 2010, Loeffler and Wolf, 2014). TGF-β intracellular signalling is initiated when TGF-β binds to its specific receptors and activates downstream signalling pathways, including both SMAD-dependent and SMAD-independent pathways (Ding and Choi, 2014, Kalluri and Neilson, 2003, Loeffler and Wolf, 2014, Zavadil et al., 2004). Receptor-regulated SMADs (R-SMADs) activated by TGF-β receptor type 1, forms a complex with SMAD4 and translocates into the nucleus, where it regulates target genes encoding proteins involved in the fibrotic process (Kalluri and Neilson, 2003, Loeffler and Wolf, 2014, Zavadil et al., 2004). Specifically, TGFβ-1 is considered the main modulator of the EMT mechanism through the Smad pathway, and probably by cooperation with hypoxia-inducible factors (HIFs) such as Hepatocyte Growth Factor (HGF) and Bone Morphogenetic Factor-7 (BMF-7) that are known fibrosis inhibitors (Seo et al., 2016).

- MAPK/ERK pathway (Mitogen-Activated Protein Kinase/ Extracellular signal-regulated Kinase pathway):

MAPK/ERK pathway has been associated to congenital kidney diseases as it participates in the early renal differentiation, defining the final size, shape, and nephron number of the kidney as well as the nephrogenesis (Boucherat et al., 2015, Ihermann-Hella et al., 2018, Newbern et al., 2008). Its activation derives from the glial cell line-derived neurotrophic factor (GDNF)-induced RET signaling and fibroblast growth factor (FGF) signaling, whose binding to their cognate receptors causes receptor tyrosine kinase (RTK) dimerization, autophosphorylation, and activation of intracellular signaling cascades, including the MAPK/ERK pathway (Costantini, 2010, Walker et al., 2016).

- RAS system pathway:

RAS system (Renin-angiotensin system) regulates blood pressure and fluid balance in the organism and it is well associated with the development of CKD by mechanisms relevant or irrelevant to blood-pressure (Cao et al., 2013, 2015, Crowley and Coffman, 2012, Ibrahim et al., 2013, Lima Santos et al., 2012, Rüster and Wolf, 2011, Sparks et al., 2014, Zhou et al., 2015a). The main components of the RAS system include the angiotensinogen (AGT), renin, angiotensin-converting enzyme (ACE) and angiotensin II (Ang II) type 1 and type 2 receptors (AT1 and AT2). AGT is transformed into the active enzyme Ang II from the renin and ACT enzymes activity and afterwards, binds to the receptor AT1 and AT2 to mediate biological functions, such as vasoconstriction, endothelial dysfunction, atherosclerosis, inflammation, fibrosis, and apoptosis (Axelsson et al., 2015, Hsu et al., 2011, Lanz et al., 2010, Srinivasa et al., 2015).

Numerous factors regulate the RAS system including hyperglycemia, high-salt, albumin overload, reduced availability of nitric oxide, increased uremic toxin, and oxidative stress signalling (Cao et al., 2015, 2013, 2011, Saito et al., 2014). Klotho anti-ageing protein is required for RAS activation, as well (Zhou et al., 2015b). In proximal tubules, ROS generation and p38 MAPK activation induce AGT expression (Hsieh et al., 2002). Albumin (ALB) acts as a RAS activator, as well, via interaction with endocytic receptor megalin/cubilin and a protein kinase C and NADPH oxidase-dependent pathway (Cao et al., 2011). Other oxidation proteins contribute to RAS components activity through the class B scavenger receptor of CD36 and activation of protein kinase C-a, NADPH oxidase, NF-kB/AP-1 signalling, Stat3 and cyclooxygenase-2 pathway (Cao et al., 2013, Saito et al., 2014, F. Wang et al., 2014).

Regarding CKD, renal Ang II synthesis is augmented after kidney injury and its binding to AT1 evokes multiple harmful effects, including elevated intraglomerular pressure, water and solute retention, cell proliferation and hypertrophy, inflammatory responses in glomerular and tubulointerstitial compartments, insulin resistance, and renal fibrosis (Axelsson et al., 2015, Dikalov and Nazarewicz, 2013, Srinivasa et al., 2015). Also, in patients with diabetes-related CKD, hyperglycemia drives the sodium/glucose cotransporter 2 (SGLT2)-related reabsorption of sodium in the proximal tubules that disables tubule-glomerular feedback and triggers the RAS system at the macula densa of the renal tubules.

The role of Ang II and its mechanistic target of rapamycin (mTOR) signalling is important in podocyte hypertrophy and glomerular hyperfiltration. Angiotensin II propels vasoconstriction and aldosterone secretion. Aldosterone restrains the expression of nephrin, a podocyte protein located in the slit diaphragm important to the maintenance of the glomerular filtration barrier (Benigni et al., 2004). Angiotensin II may be also responsible for the glomerular FSGS lesions through the absence of podocytes replacement and the clinical assessment of proteinuria (Rizzo et al., 2013, Clark et al., 2011, Abbate et al., 2006, Ruggenenti et al., 2012). In podocytes, Ang II induces cell apoptosis by a mechanism involving TGF-β1 (Yuan et al., 2012). Ang II-TGF-β1 actions may be a positive-feedback-loop process.

Besides, renin directly participates in mesangial hypertrophy, glomerulosclerosis renal fibrosis through binding to its membrane receptor PRR, that is mainly localized in the mesangium of glomeruli and the collecting duct via stimulation of TGF-β1 and an Ang II-independent matrix gene expression (Huang et al., 2006, Zhang et al., 2012).

- RAS system-PI3K/Akt/NF-κB pathway:

Ang II contributes to podocytes injury via the PI3K/Akt/NFκB pathway, the CASP9 upregulation and the involvement of nephrin and podocin proteins, as well (Cardoso et al., 2018, Yang et al., 2017, Yu, 2016, L. Zhang et al., 2016, Zhao et al., 2018, Wang et al., 2019). It is known that the PI3K pathway activates the Akt pathway leading to resistance of podocytes to apoptosis (Ren and You Yu, 2016, Wang et al., 2014, Yu-Shengyou and Li, 2013, Zhang et al., 2018). NFκB and CASP9 are

critical molecules to the apoptotic process (Druskovic et al., 2006, Markó et al., 2016, Silva et al., 2011, Sun et al., 2018) and Akt regulates both of them in this direction (Liu et al., 2009, Tang et al., 2016). On the other hand, nephrin suppresses cell death but it is also a PI3K subunit and as such, it is capable of activating Akt (Huber et al., 2001, Liu et al., 2018, Yang et al., 2016, Zhu et al., 2008). Nephrin can also influence Akt activation by its upstream position. Concerning the above, Ang II seems to promote podocyte apoptosis by hindering the activation of PI3K/Akt/NFκB pathway partially due to nephrin downregulation and CASP9 upregulation.

Finally, there is evidence that Ang II participates in the interstitial fibrosis, by regulating the epithelial-mesenchymal transition of tubular epithelial cells via inactivation of the PI3K/Akt pathway (Lin et al., 2013, Yang et al., 2004).

- Wnt/β-catenin signaling and RAS system

Wnt/β-catenin signalling is an upstream RAS system regulator. It regulates cell proliferation and EMT (epithelial-mesenchymal transition) during embryogenesis and is silenced in the adult kidney (Angers and Moon, 2009, Clevers and Nusse, 2012, MacDonald et al., 2009). However, in CKD condition Wnt/β-catenin pathway is reactivated and participates in renal fibrosis (Seo et al., 2016). In CKD kidneys, Wnts get activated and bind to numerous receptors promoting a series of downstream intracellular signaling events with final the dephosphorylation of b-catenin (Cox et al., 2010, Dai et al., 2009, Hwang et al., 2009, Wang et al., 2014). This renders stabilization and nuclear translocation of b-catenin, where it activates transcription factors of the T-cell factor (TCF) and lymphoid enhancer-binding factor (LEF) families to stimulate the transcription of RAS genes among others (Rao and Kühl, 2010).

- RAP pathway-MAGI2 (Ras Proximate pathway-Membrane-Associated Guanylate kinase Inverted 2):

RAP1 is a small GTPase of the RAS-like small GTP-binding protein superfamily that regulates cell adhesion, migration, proliferation, and cell survival in the kidney (Boettner and Van Aelst, 2009). RAP1 is also essential to signal transduction in podocytes. RAP1 activity depends on the balance between the active guanosinetriphosphate (GTP)–bound form and the inactive guanosinediphosphate–bound form. This balance is tightly regulated by upstream factors including guanine nucleotide exchange factors (GEFs), which turn on signaling by catalyzing the exchange of guanosine diphosphate to GTP, and GTPase activating proteins, which terminate signaling by hydrolyzing GTP to guanosinediphosphate (Kooistra et al., 2007). MAGI2 belongs to the MAGUK family of scaffolding proteins, exclusively expressed at the slit diaphragm of the podocytes, that forms a complex with the Rap1 guanine nucleotide exchange factor (RapGEF2) and is required for the RAP1 activation and the Rap1-mediated downstream signaling (Ihara et al., 2012, Lehtonen et al., 2005, Zhu et al., 2019). The complex MAGI2-RapGEF2 has been proven essential to normal podocyte function (Balbas et al., 2014, Ihara et al., 2014, Lefebvre et al., 2015, Shirata et al., 2017). In the case of MAGI2 mutation, there is spontaneous glomerulosclerosis, abnormalities of podocytes cellular morphology, dramatic loss of the actin cytoskeletal organization that will lead to podocyte injury and mediate FSGS. MAGI2 expression is one of the most dramatically downregulated of all podocyte-expressed genes in parallel with Rap1 in human proteinuric kidney diseases, including diabetic nephropathy and idiopathic FSGS (Potla et al., 2014).

The other isoform of RAP protein, RAP1b, plays a different role in the diseased kidney. In Diabetic Nephropathy the mitochondrial electron transport system is overloaded in the proximal tubular cells due to the constant uptake of glucose metabolic intermediaries. As a consequence, intracellular oxidative stress is enhanced and tubular cells are prone to damage (Kanwar et al., 2008). Moreover, the mitochondrial-mediated pathway leading to apoptosis is

one of the most severe cell death signaling pathways that cause the release of mCyto C and activation of caspases 9 and 3, accelerating the apoptotic process (Yang and Cortopassi, 1998).

In these cases, RAP1b has been observed as severely decreased. According to Xiao et al., (2014), the mechanism involves the downregulation of PGC-1a via the ERK1/2–C/EBP-b pathway and the phosphorylation of Drp-1 protein. As a result, there is an imbalance between mitochondrial fission and fusion proteins, which is followed by a series of events leading to ROS overproduction and apoptosis of tubular cells. The fact that RAP1b overproduction reverses this process, indicates that the role of RAP1b is protective regarding the mitochondrial function of proximal tubules.

- mTOR pathway (mammalian Target of Rapamycin pathway):

The mTOR pathway has a central role in the regulation of cell metabolism, growth, and proliferation. mTOR pathway is activated by growth factors and cytokines via the PI3K/Akt pathway and the formation of phosphatidylinositol (3,4,5) triphosphate (PIP3) and the 3-phosphoinositide-dependent protein kinase-1 (PDK1) (Fantus et al., 2016).

In the kidney, the mTOR pathway contributes to renal homeostasis, metabolism, and autophagy. In renal diseases, it may participate in the development of glomerular diseases, polycystic kidney disease (PKD), acute kidney injury (AKI), and kidney transplant rejection. In CKD, mTOR pathway enhances the development of interstitial fibrosis and the expression of fibrosis-related genes (Bonegio et al., 2005, Jain et al., 2001, Jolicoeur et al., 2003, Krämer et al., 2008, Rangan and Coombes, 2007, Wu et al., 2006).

- HIF-1 pathway (Hypoxia-induced Factors pathway):

Hypoxia-induced Factors are transcription factors responsible for gene expression in hypoxia, a pathological condition characterized by the insufficient supply of oxygen in cells (Matsumoto et al., 2004, Ohashi et al., 2002, Semenza, 2001). When an organ deals with limited availability of oxygen, cells increase the expression of HIFs, that regulate the transcription of a great range of genes, including erythropoietin (EPO), vascular endothelial growth factor (VEGF), and glucose transporter-1 (GLUT1) to restore tissue homeostasis by stimulating various adaptive mechanisms (Haase, 2006, Wenger et al., 2005).

Kidneys are prone to show hypoxia due to the high oxygen demand of the renal tubules, mostly in pathological conditions like CKD (Fu et al., 2016, Higgins et al., 2007, Hirakawa et al., 2017). Hypoxia accelerates CKD progression by hindering the tubular epithelial cell growth and impelling dedifferentiation, extracellular matrix transition, dedifferentiation, inflammation, and apoptosis. HIFs' role in this process is ambiguous. Concerning cell death, HIFs are protective via interaction with Bcl-2 family genes, p53, and mitochondrial enzymes (Sendoel and Hengartner, 2014). HIFs also, inhibit mesenchymal stem cell proliferation via the upregulation of cell cycle inhibitor p27 and inflammation via downregulation of NF-κB and other pro-inflammatory factors. On the other hand, HIFs promote tubular and glomerular cell proliferation through the regulation of tissue repair genes, such as erythropoietin (EPO) and SDF-1 (Johnson et al., 2006). Finally, their role in fibrosis can be protective or deleterious, as they interact with fibrogenic genes and pro-fibrotic signalling pathways such as TGF-β, NF-κB, Notch, and PI3K/Akt pathways and they influence epigenetic factors and the EMT process (Liu et al., 2017).

- TNFa-FGF23 pathway (Tumor Necrosis Factor-Fibroblast Growth Factor 23 pathway):

In CKD, mineral metabolism gets severely imbalanced and ends up as a factor of morbidity and mortality (Block et al., 2004, Isakova et al., 2011). In early CKD stages, FGF23 increase has been

associated with phosphate and vitamin D3 homeostasis maintenance (Gutiérrez, 2010, Quarles, 2012). However, high FGF23 levels are connected to mortality independently to phosphate levels (Gutiérrez et al., 2008). FGF23 binds to the aKlotho protein FGF receptors and restrain phosphate reabsorption while decreases the Vitamin D3 levels (Hu et al., 2013, Urakawa et al., 2006). FGF23 activity is regulated by many factors, such as parathyroid hormone (PTH), insulin, aldosterone, erythropoietin, adipokines, and calcitriol (Bär et al., 2018, Daryadel et al., 2018, Hu et al., 2013, Kuro-O and Moe, 2017, Zhang et al., 2016).

Also, there is evidence that FGF23 is an important factor in the inflammation process, as it has been positively correlated to IL-6, IL-12, CCL5, and TNF (Mendoza et al., 2012, Wallquist et al., 2018). Finally, there is a positive correlation between FGF23, inflammation, and hypoxia, as there is HIF-1-mediated FGF23 upregulation that depends on IL-1β and erythropoietin (Clinkenbeard et al., 2017, Daryadel et al., 2018, David et al., 2016, Flamme et al., 2017). TNF (plasma tumour necrosis factor) is increased in CKD and contributes to the disease progression (Amdur et al., 2016, Feng et al., 2018, Mendoza et al., 2012). According to Egli-Spichtig et al., (2019), TNF is crucial in FGF23 stimulation in renal and other inflammatory diseases. TNF-α receptors are increased in CKD, as well. TNFR2 contributes to cell proliferation and cell survival with a potential role in the antiapoptotic and inflammatory process (Mizoguchi et al., 2002, Piva et al., 2006, Ramesh and Reeves, 2002). Lee et al., (2017) showed that NF-κB activates TNFR2 and that TNF-α inhibits NF-κB upstream regulator IκB and activates NF-κB. Therefore, TNF-a-induced kidney injury is possibly mediated via a TNFR2-NF-κB complex. This mechanism stimulates the expression of Apolipoprotein-A4, which has been found associated with many renal diseases (Boes et al., 2006, Graversen et al., 2008, Lee et al., 2017).

- IL-17 pathway (Interleukin-17 pathway):

IL-17a is the main effector of Th17 cells. The past few years, it has been shown that IL-17 plays an important role in hypertension diseases and CKD participating mainly in the inflammation process via stimulation of pro-inflammatory cytokines, chemokines, adhesion molecules, and matrix metalloproteases (Cortvrindt et al., 2017, McMaster et al., 2015, von Vietinghoff and Ley, 2010).

In CKD IL-17 activates the tubular epithelial cells, vascular smooth muscle cells, endothelial cells, and fibroblasts to release a large array of proinflammatory mediators, including chemokines, such as MCP-1, RANTES, CXCL1, IL6, TNF-a, CCL2, CXCL10, TGF-β, and CXCL8, which, in turn, may recruit inflammatory cells such as T cells and macrophages (Gaffen, 2009, Pietrowski et al., 2011, Van Kooten et al., 1998, Zhang et al., 2013). According to Orejudo et al., (2019), MCP-1 is considered the main mediator of IL-17 signalling in renal inflammation. The inflammatory responses of IL-17 involve ROS production, modulation of nitric oxide levels, and activation of protein kinases, including RhoA/Rho-kinase, the MAPK cascade and the regulation of Smad-Akt pathways (Karbach et al., 2014, Pietrowski et al., 2011, Wu et al., 2016, Xing et al., 2013, Zhang et al., 2013).

IL-17 could be protective against fibrosis because of a decrease in metalloproteinase-2 via kallikrein-kinin-system-regulated process or direct interaction between IL-17 and kallikrein-1 in the kidney (Ramani et al., 2016). Other activities of IL-17 include the expression and activity of sodium transporters along the nephron and increase in blood pressure (Norlander et al., 2016, Orejudo et al., 2019).

- JAK/STAT pathway (Janus kinase/signal transducer and transcriptional activator pathway):

The JAK/STAT signaling pathway is a central molecular pathway mediating fundamental cellular processes including cell growth, proliferation, differentiation, migration, apoptosis,

and immunomodulation. It consists of numerous cytokines and growth factors focused on cell signalling transduction. Therefore, it is essential in the process of growth, development, and homeostasis, including hematopoiesis, immune cell development, stem cell maintenance, and organism growth (Sun et al., 2020).

JAK/STAT is a crucial signalling pathway in CKD development and progression, mainly in Diabetic Nephropathy (Brosius and He, 2015, Ghoreschi et al., 2009, Matsui and Meldrum, 2012, Villarino et al., 2017). In injured kidney cells, there is a higher expression of JAKs 1,2,3 and STATs 1,3 in glomeruli and the tubule-interstitial compartment and the JAK/STAT pathway stimulates excessive cell proliferation, enhanced production of TGF-β1, collagen IV, and fibronectin, contributing to the glomerulosclerosis and other renal pathological conditions (Berthier et al., 2009, Bienaimé et al., 2016, Chuang and He, 2010, Marrero et al., 2006, Nechemia-Arbely et al., 2008, Wang et al., 2002).

STAT3 appears to be a key molecule of the JAK/STAT pathway in CKD. STAT3 is found to be localized primarily in epithelial cells of collecting ducts and interstitial cells in normal and CKD kidneys (Kuratsune et al., 2007). Its expression has been associated with increased deposition of extracellular matrix proteins driving the progression of renal fibrosis (Pang et al., 2010).

- Hippo-Salvador pathway:

The Hippo-Salvador signalling pathway constitutes a kinase cascade implicated in the regulation of organ size, cell proliferation, cell death, tissue regeneration, and tumorigenesis (Pan, 2010, Zhao et al., 2011). The Hippo signalling pathway has been shown to interact with the TGF-β and Wnt/β-catenin signalling pathways, through a variety of mechanisms to regulate fibrosis in CKD (Attisano and Wrana, 2013, Azzolin et al., 2014, Seo et al., 2016, Varelas et al., 2010, 2008, Wrighton et al., 2008).

- AGE-RAGE pathway:

AGEs (Advanced glycation end products) constitute molecules formed by the nonenzymatic reaction of reducing sugars with proteins and amino acids via the glycation process. They can be harmful because they include modification of functional domains of proteins leading to protein inactivation or dysfunction. In the case of increased AGEs formation, the tissue deals with dicarbonyl stress, which is considered crucial to CKD development (Giacco et al., 2014). The key component in the dicarbonyl stress is the restricted expression of the Glo1 enzyme of the cytosolic glyoxalase system in response to hypoxia-inducible factor-1a and inflammatory signalling conflicting with transcription factor Nrf2 and the increased proteolysis. The overexpression of the AGEs receptor (RAGE) has been connected with glomerular hypertrophy, increased albuminuria, mesangial expansion, advanced glomerulosclerosis, and increased serum creatinine (Rabbani and Thornalley, 2018, Yamamoto et al., 2001).

The signal transduction of the AGE-RAGE pathway is induced by the formation of a complex between RAGE and heparan sulfate, regulated by the AGE-modified albumin, the high-mobility group protein 1 (HMGB1), and the S100 proteins (Xu et al., 2013). Its downstream targets include the extracellular regulated kinase-1 and -2 and p38 MAPK pathway linked to endothelial permeability, inflammation, extracellular matrix expansion, and renal fibrosis (Borbiev et al., 2004, Feliers and Kasinath, 2011, Stambe et al., 2004, Yang et al., 2014). On the other hand, RAGE downregulation has been associated with decreased podocyte production of monocyte chemoattractant protein-1 (MCP-1), decreased monocyte recruitment, glomerulosclerosis, extracellular matrix accumulation, albuminuria, and decline in renal function (Che et al., 2010, Chow et al., 2006, Gu et al., 2006, Rabbani and Thornalley, 2018, Wendt et al., 2003).

A major AGE is serum albumin (ALB) that undergoes glycation and produces the AGE glycoalbumin. In the normal kidney, ALB inhibits the TNFa-induced VCAM1 production and

protects against inflammation. In CKD, though ALB is significantly reduced partly due to glycation.

CKD Diagnosis Problems and Deadlocks

CKD is asymptomatic in its early stages and can be detected only when the injury is advanced. Current CKD diagnostics involves the measurement of eGFR and proteinuria. eGFR assessment requires the estimation of serum creatinine (sCr) in the plasma, which is concentrated in plasma in case of renal malfunction, otherwise is secreted in the urine. The international guidelines (Risk-Injury-Failure-Loss-End-Stage Kidney Disease (RIFLE), Acute Kidney Injury Network (AKIN), or Kidney Disease, Improving Global Outcomes (KDIGO) annotate that an observable increase in sCr, even a small one, indicate the presence of renal injury, known as Acute Kidney Injury (AKI) and represent the initial condition of a CKD patient (Bellomo et al., 2012, Kellum et al., 2012, Kiryluk et al., 2018, Mehta et al., 2007). AKI symptoms are usually transient and kidney function returns to normal. When these symptoms persist for more than 3 months, the renal pathological condition is characterized as CKD.

Besides the broad usage of sCr in CKD diagnosis, sCr remains a less accurate marker, as sCr levels in the plasma may rise due to irrelevant to CKD reasons or stay unaltered in the initial kidney damage and become observable when the renal mass is decreased about 50%. Therefore, sCr-based diagnosis lacks specificity and sensitivity or leads to late diagnosis. Finally, given that CKD is a multifactorial, complex, and heterogeneous disease, its prognosis, early diagnosis, and targeted treatment require information about the initial aetiology, that sCr cannot offer.

Nowadays, a definite diagnosis requires a renal biopsy but there are additional difficulties in this procedure (L'Imperio et al., 2016, Prikryl et al., 2017), the most serious being the fact that biopsy is an invasive process and that there is an absence of molecular biomarkers indicative of the aetiology and the spatial characteristics of the renal damage (Kiryluk et al., 2018).

In the past few years, researchers have turned their focus on less-invasive methods and samples easily available, such as urine and blood, in which the analysis relies on "second generation" biomarkers (L'Imperio et al., 2016). The so-called "second generation" biomarkers involve gene expression in tissue and presence of proteins in urine that can be more specific and predictive of the system imbalance (Fassett et al., 2011). Some of them are the neutrophil gelatinase-associated lipocalin (NGAL), and kidney injury molecule-1 (KIM-1), that enhance diagnosis specificity but they still fail to differentiate the subjacent causes of CKD and determine the CKD subcategories (Fassett et al., 2011, Xu et al., 2017). The main reason for this failure is that complex diseases as CKD, cannot be identified by changes in single molecules and they need the identification of coordinated changes in functionally correlated molecules. The identification of such changes requires a systemic approach to the disease and deep knowledge of the underlying mechanisms. This approach can lead to the molecular-based classification of renal diseases and research worldwide has already started to invest in it.

ii) Contemporary Approaches in CKD Research and Diagnostics

Systems Biology in CKD research

The field of Systems Biology focuses on a holistic description of the systems, opposing to the "traditional" approach that focuses on the study of single elements. So, the study of the CKD proteome through systems biology methodologies is considered a promising way to study the CKD underlying mechanisms. CKD proteomics can contribute to the identification of the early pathological modifications and the molecular changes related to disease progression.

Immunostaining in CKD research and diagnostics

Immunostaining refers to protein detection via selective antibody binding to specific antigens. It is used as a basic diagnostic method in pathology and has been established as a common tool in several fields of life sciences research, as well. The process of detection involves the use of antibodies towards antigens of interest upon a tissue section, live cells or fixed cells and staining with a chromogen (Immunohistochemistry-IHC) or a fluorophore (Immunofluorescence-IF). The main difference between IF and IHC is the use of light, which is absorbed in IHC and emitted in IF (Bolognesi et al., 2017). IF methods are divided into two main categories: direct and indirect. In the direct IF, the primary antibodies that detect the protein of interest are already conjugated with a fluorochrome. Indirect IF relies on the use of secondary antibodies that are specific to the species in which the primary antibody has been raised in and carry the fluorophore.

The routine process in formalin-fixed paraffin-embedded (FFPE) tissue samples allowed only one stain per section so far. In the past few years though, the interest has been focused on multiplexing, a term that defines the application of several antibodies in the same FFPE tissue samples (Bolognesi et al., 2017). The number of antibodies that can be applied per round is defined by the number of the different secondary antibodies available. Due to the restricted number of species that can be used to produce antibodies, multiplexing calls for repetition of the experimental rounds, that require an intermediate treatment of the tissue. In this intermediate step, the antibodies used in the previous rounds should be inactivated, so a new set of antibodies can then be applied. The intermediate step can be:

a) Inactivation of directly conjugated primary antibodies after each round (Adams et al., 2016, Gerdes et al., 2013, Lin et al., 2015, Schubert et al., 2006)

Antibody inactivation has been performed by exposure to ultraviolet (UV) light (Schubert et al., 2006), alkaline solutions (Lin et al., 2015), or sodium borohydride ($NaBH_4$) (Adams et al., 2016). However, this approach reveals numerous disadvantages. The cost and waste of the antibodies, the specificity required, the restriction or damage of the antigens, the limited number of staining can be considered some of them. Finally, the restriction that steric hindrance may evoke has not been examined yet (Clarke et al., 2014, Gerdes et al., 2013, Remark et al., 2016, Schubert et al., 2014, 2006).

b) Restriction of access to previous antibody layer (Lechago et al., 1979)

Insoluble and hydrophobic precipitates such as diaminobenzidine (DAB) when applied in a stained tissue section, hinder the contact between the two layers of antibodies according to the precipitate concentration. Also, Fab monomeric fragments were used in high concentrations some years ago for the same reason but this option is considered unwise due to the high cost and the dubious efficacy (Lu and Partridge, 1998, Negoescu et al., 1994, Nielsen et al., 1987).

c) Antibody removal from the tissue after image acquisition (Gendusa et al., 2014, Glass et al., 2009, Kim et al., 2012, J.-R. Lin et al., 2015, Pirici et al., 2009, Tramu et al., 1978, Zrazhevskiy and Gao, 2013)

Considerable effort has been made to investigating methods for effective antibody removal and the ability to restain the same tissue. Mild boiling in an antigen retrieval solution has been tested but regarded insufficient (Gendusa et al., 2014, Tornehave et al., 2000, Tóth and Mezey, 2007). Other substances that have been used on this purpose include an acidic glycine buffer (Zrazhevskiy and Gao, 2013), strong chemicals (Tramu et al., 1978), proteases (Lin et al., 2015) and a mixture of strong reducing agents and a detergent (Gendusa et al., 2014, Kim et al., 2012).

Antibody removal can be performed in both IHC and IF methods, each one with different restricting factors that can offer around ten staining rounds in each tissue section, (Gendusa et al., 2014, Kim et al., 2012, Pirici et al., 2009). In multiplexing IHC alcohol-soluble precipitates and sequential single-colour rounds are required. Multiplexing IF, though, can take advantage of spectral deconvolution to use more than the standard four colours (4'6-diamidino-2-phenylindole dihydrochloride-DAPI, fluorescein isothiocyanate-FITC, tetramethylrhodamine isothiocyanate-TRITC, Cy5) (Mansfield, 2014, Stack et al., 2014). In the past few years, multiplexing in the same tissue or cell gains more and more attention and numerous protocols have been developed for this purpose.

Multiplex IHC and IF methods

Multiepitope-ligand cartography (MELC) is a multiplexed IHC method based on sequential rounds of antibody staining and photobleaching of each layer of fluorophores. The procedure is fully automated creating maps that depict protein organization and interactome networks. However, some of its disadvantages include the long duration of the process and the expensive robotic set up that requires. It is a fact, though, that hundreds of different proteins can be detected in every sample (Murphy, 2006, Schubert, 2003, Schubert et al., 2006, Zhou and Veenstra, 2006).

Glass et al., (2009) developed a technique called SIMPLE (Sequential Immunoperoxidase labelling and erasing method). SIMPLE requires fixed samples that get counterstained and an image is acquired. Afterwards, there is an AR step to remove the counterstain, and staining is performed with alcohol-soluble red peroxidase substrate 3-amino-9-ethylcarbazole (AEC). An image of the stained sample is acquired, as well. The AEC precipitate is removed by washing in 95% ethanol, and the antibody is removed in an elution solution. This process is repeated, and a final single composite image with pseudocolours can be generated. However, it is limited to the testing of five antibody labels per section.

Multiplexed fluorescence microscopy method (MxIF) was introduced in 2013 (Gerdes et al., 2013) for the quantitative analysis of multiple markers. FFPE tissue samples are directly immunostained and fluorophores are inactivated through alkaline oxidation chemistry, which quickly eliminates cyanine-based dye fluorescence (US patent 7,741,045). Stained and background images are acquired in every cycle and the experimental procedure is repeated for all the antibodies available. Then, the images are processed and analyzed. This technique offers the analysis of numerous different proteins in single tissue samples (Gerdes et al., 2013).

Cyclic Immunofluorescence (CycIF) shares the same principles with MxIF but with the use of standard reagents and open-source software. Fluorophore inactivation is performed by oxidation (with hydrogen peroxide), alkaline pH, and light, and a final washing step. Several 4-channel rounds can be performed. An innovation of CycIF is that it can be combined with live-cell imaging. t-CycIF is an extension of CycIF applicable to fixed tissues, developed in 2018. It is considered an easily accessible and applicable method to a wide variety of contexts (Gaglia et al., 2020, Lin et al., 2015, Lin et al., 2018, 2016).

Lim et al., (2018), developed a protocol for multiplex Immunofluorescence incorporating tyramide signal amplification in an automated Leica Bond Max diagnostic tissue stainer to produce high-quality 7-colour mIF slides.

iii) Multiple Iterative Labeling by Antibody Neodeposition (MILAN)

MILAN is an Immunofluorescence (IF) protocol of four main steps: dewaxing of the FFPE tissue sections, antigen retrieval, sequential staining with primary and secondary antibodies incubation, and removal of the antibodies via disulfide cleavage. Staining and stripping can be repeated as many times as the tissue quality allows. The images obtained per slide are then digitally processed. Image pre-processing involves image registration, autofluorescence subtraction, and the combination of every antibody staining in a final image. In the final composite image, the expression of all proteins is combined and can be further quantified and analyzed in spatial and single-cell levels upon the tissue.

Dewaxing and Antigen Retrieval (AR):

A tissue section contains thousands of crosslinked proteins, sugars, and nucleic acids with methylene bridges (Fox et al., 1985). The FFPE samples are tissue samples that have been dehydrated with a graded alcohol series, partially extracted by terpenic solvents and embedded in paraffin. This process causes the masking of many epitopes, meaning that numerous conformational changes have been made due to loss of water and the contact between active formalin-induced binding sites, resulting in an irreversible, high-energy misfolding of the proteins (Boi et al., 2016, Fowler et al., 2007). This effect can be reversed by enzymatic action or a process involving high temperature and calcium presence, known as antigen retrieval (AR) after paraffin extraction through dewaxing and gradual rehydration (Shi et al., 1991, Shin et al., 1991).

AR processes rely mostly on the duration of heat exposure and the chemical composition of the AR solution buffer (Boenisch, 2005). The AR buffer is based on the typical Laemmli buffer that selectively breaks disulfide bonds and denatures the proteins while making them soluble (Laemmli, 1970). In the MILAN AR step, the Laemmli buffer is somehow modified, containing SDS of 0.5% concentration and 2-ME in half of the Laemmli's buffer concentration (Scalia et al., 2016).

The AR process is temperature-dependent and results in the optimal maintenance of tissue integrity and antigen unmasking. The only epitopes that fail to get unmasked are epitopes with very strong bonds that require energy similar to that of protein and tissue degradation (Fowler et al., 2007, Scalia et al., 2016).

Stripping:

Primary antibodies survive in harsh conditions such as low pH, temperatures above 60°C, and various chaotropic agents. Their retention upon the tissue becomes even stronger when they are paired with secondary antibodies due to an increased affinity of the primary antibody or augmented stability of the antibody chain complexed with the antigen, the binding of one molecule of secondary antibody to neighbouring primary antibodies, or the local macromolecular crowding effect of neighbouring Ig molecules (Ellis, 2001, Gendusa et al., 2014, Oda, 2004). Therefore, an efficient antibody removal requires the destruction of the intramolecular disulfide bridges.

Antibodies removal in MILAN is based on the 2-mercaptoethanol/ Sodium Dodecyl Sulfate (2ME/SDS) method that changes the chemical structure of primary and secondary antibodies by altering the thermodynamic equilibrium of the disulfide bonds of the antibodies. 2ME is a strong reducing agent with a selective action on disulfide bonds making the thermodynamic equilibrium to move towards the unbound form. SDS is a detergent that facilitates the disconnection of the Ig heavy chains. The combination of these agents in

temperature sufficient for the tissue solubilization ends up removing the paratope from the epitope even in case of high-affinity between them and irrelevant to the content on disulfide bonds (Gendusa et al., 2014, Gupta et al., 2016, Scalia et al., 2016). This process is efficient for proteins of molecular weight greater than 25 kDa. Proteins with smaller molecular weight, cross-linked in the tissue usually fail to be removed.

Besides, 2ME/SDS treatment may act as an additional antigen unmasking agent in combination with AR and it is observed to reduce the levels of tissue autofluorescence (AF) due to a quenching effect or disassociation of small soluble AF compounds that are not very steadily cross-linked in the tissue and getting removed gradually across striping repetitions (Gendusa et al., 2014).

The 2ME/SDS protocol, combined with disaccharide protection does not affect the antigens after extensive repetitions of staining and stripping rounds and is proven more reproducible than other buffers tested, such as glycine/SDS buffer, a buffer of high molar urea or a KMnO4/ H2SO4 elution buffer (Bolognesi et al., 2017, Gendusa et al., 2014, Glass et al., 2009, Pirici et al., 2009). The only restriction factor in the method reproducibility is the tissue damage after coverslip removal (Gendusa et al., 2014).

Staining:

MILAN protocol proposes indirect immunostaining with pairs of primary and secondary antibodies. The choice of the secondary antibodies fluorophores is such to avoid overlay of their emission spectra according to the slide scanner filters combination and the visualization of one not to affect the visualization of the others (Buscone et al., 2014, Gendusa et al., 2014, Sternberger and Joseph, 2017). Also, given that secondary antibodies are species-specific, it is crucial to avoid cross-reaction between primary and secondary antibodies, when they are used simultaneously or in sequence (Mason et al., 2000). The concentration of primary antibodies should be between 1-2 ug/ml and that of secondary 5 ug/ml (Bolognesi et al., 2017).

Protection from drying:

Non-freezable water constitutes a small amount of protein-associated water that does not freeze directly to maintain the physical and enzymatic properties of proteins. Drying of the tissue would remove this residual water and destroy the properties of the protein defined by the protein tertiary structure and vanish its immunoreactivity (Crowe et al., 1990). Accordingly, dehydration affects antibody staining and stripping and the reproducibility of a protocol or the diagnostic reliability of individual preparations (Bussolati and Leonardo, 2008, Dabbs, 2013, Lin and Prichard, 2015, Taylor et al., 2013).

However, sugars act in the same way as water and are considered “water substitutes” in the absence of non-freezable water. Hydrogen bonding between the -OH groups on the disaccharide and the polar groups on the protein preserve the conformation of the protein (Crowe et al., 1990, Liao et al., 2002). Therefore, sugars and particularly disaccharides, are required during the dehydration process and storage for the protection of antigens’ immunoreactivity as they protect the whole Ig including the paratope (Carpenter and Crowe, 1989). Their effect depends on their concentration and is transient as removal of the sugar or prolonged storage at room temperature evokes epitope re-masking (Dráber et al., 1995).

In the MILAN protocol, sucrose is preferable to lactose in the storage solution, as lactose is less soluble in alcohol and water, it undergoes crystallization upon drying, and interacts with lysine residues and causing glycation (Andya et al., 1999, Whittier, 1925).

iv) MILAN in CKD research

Beyond the efficacy of multiplexing methods in the proteomic analysis, there are many obstacles in their wide application, such as high costs of antibodies and instruments, low throughput, and deficiency of specialized facilities (Bolognesi et al., 2017). However, MILAN is remarkably advantageous compared to other IF protocols.

Firstly, the materials required are common in every laboratory and of low cost. The materials include routinely used FFPE tissue sections, primary and secondary antibodies largely available, basic chemicals, and widely available fluorescent slide scanners.

Beyond this, the groundbreaking efficiency of the protocol in antibodies removal allows numerous rounds of staining and stripping with the antigens to remain unaffected. So, a great number of antibodies can be tested. Even antibodies that interact and create steric hindrance can be tested in two separate cycles. In addition, mistakes in the staining procedure can be surpassed by stripping and restaining with the same antibody. This way, the protocol allows staining with up to 50 different antibodies. So, the FFPE tissue sections can be widely reclaimed, which is very significant in cases of very few samples available. Besides, the repetitive use of the materials reduces considerably the cost and multiplies the data obtained (Cattoretti et al., 2019).

Furthermore, the images can be processed with open-source image analysis software freely available to all researchers. Image processing of every tissue can reveal information for spatial tissue analysis, in situ characterization of different groups of cells, and/or reach the single-cell level.

Finally, this protocol may be an important aid in the daily clinical assessment of CKD tissue samples allowing the test of numerous antibodies in the very same slide preventing the waste of tissue slides, whenever there is a limited amount of tissue or slides. MILAN also offers the advantage of the experimental repetition to cross-validate the antibodies' expression (Gendusa et al., 2014).

In CKD research, MILAN protocol can be used to gather information on CKD proteome and enlighten the underlying mechanisms of the disease. The fact that the same tissue can be stripped and restained up to 50 times could reveal information about the spatial characteristics of the disease and reach the single-cell level.

II. Aim of the research

The current research aimed at the optimization of the multiplex immunofluorescence protocol MILAN in kidney samples. Alfterwards, a set of CKD-related proteins was applied in healthy and CKD tissue samples in order to examine whether there is a difference in their relative expression between the two states and different CKD stages. Further, a new image processing pipeline was applied to evaluate differences in the proteins' spatial distribution in the renal tissue. This information was combined to reveal correlations of the proteins with molecular pathways, which are already linked to the CKD progression. Finally, it was tested whether the current experimental procedure can reveal information regarding the 9 renal cell types and the perspective for a single-cell-level analysis in CKD.

III. Materials & Methods

i) Immunofluorescence protocol – MILAN

Experimental procedure:

The experimental procedure was based on the multiplex Immunofluorescence protocol entitled MILAN (Multiple Iterative Labeling by Antibody Neodeposition), developed by Cattoretti et al., (2019). MILAN was applied to FFPE kidney tissue samples, after the standardization of the protocol in the laboratory conditions and equipment. Every round consists of four main steps: dewaxing, antigen retrieval, staining, and stripping (Figure 2).

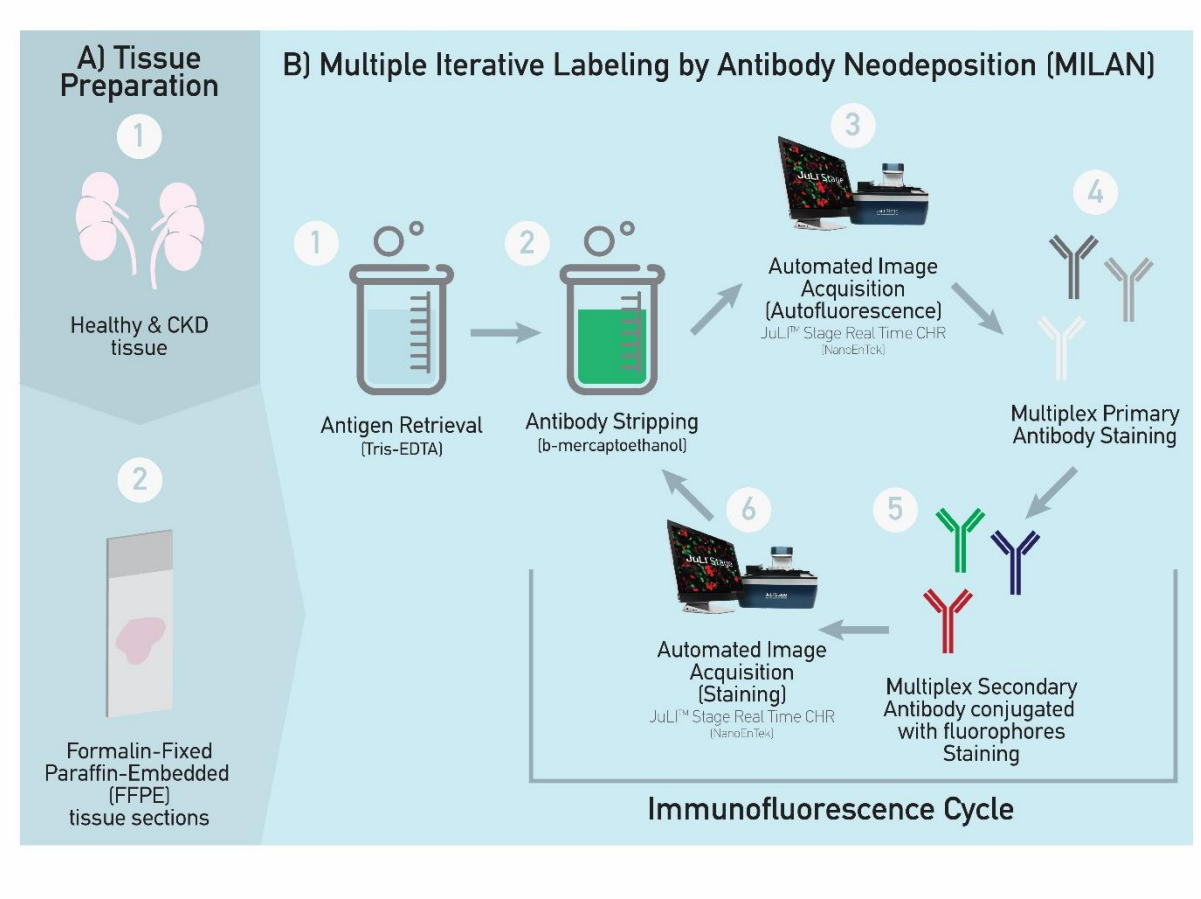

Figure 2 The experimental procedure.

1. Dewaxing:
   FFPE tissue slides were placed for ten minutes successively in two mailers with 20ml of Xylene for paraffin extraction. Then, the slides were transferred in mailers with gradually reduced alcohol concentration: 99%, 95%, 70%. In each one of them, slides remained for ten minutes so the tissue section was gradually rehydrated. The last part of rehydration involved a ten-minute immersion of the slides in a mailer with distilled H_2O.

2. Antigen Retrieval:

When tissue rehydration was completed, the glass slides, placed horizontally inside a glass beaker with 800ml of 10mM EDTA-Tris buffer (1:100) pH 8 were inserted into a microwave oven. The power was set to 100% for 10 minutes and then the power was reduced to 20% for 30 minutes. Afterwards, the slides should remain in environmental conditions to cool until the liquid temperature reached 50°C or below to allow antigen refolding. The temperature was being watched by a kitchen thermometer. Then, the slides could be transferred to the washing buffer (TBS-Ts).

The washing buffer contained Tris that buffers the solution, salt to attenuate molecular interactions not required, Tween-20 to reduce surface tension and hydrate the tissue and sucrose to avoid tissue dehydration.

3. IF Staining with primary and secondary antibodies:

In every round, two unconjugated primary antibodies of different host species were selected and diluted in antibody diluent. The final concentration was figured out for each antibody independently and ranged between 1-3 ug/ml. The secondary antibodies (Alexa Fluor 488, R-Phycoerythrine) were species-specific and were chosen based on their excitation and emission spectra to follow the features of the microscope. In the case of biotinylated primary antibodies, streptavidin (SAPE) was used for their detection. The final concentration of the secondary antibodies and streptavidin is specified to 5 ug/ml as in higher concentration has been noticed that there is no signal increase due to self-quenching (Cattoretti et al., 2019).

Glass slides were placed horizontally in light-shielded chambers. In each slide, a 20-40 ul-droplet of every diluted primary antibody was specifically applied on top of the tissue section. The droplets came from a stock in which antibodies were diluted in double concentration than the one required. The chambers were further placed inside an insulating foam rubber box with iceboxes to keep the temperature around 4°C, ensure the light shield needed for the IF protocol, and the horizontal placement of the slides to avoid any antibody solution slipping.

The primary antibodies stayed upon the tissue for an overnight incubation and then the slides were washed with TBS-Ts buffer for 10 minutes twice. Afterwards, 20-40 ul droplets of secondary antibodies were applied upon the tissue section for one hour in the same conditions. Slides were washed with TBS-Ts twice for 10 minutes to get rid of the excess of the secondary antibodies and reduce the secondary antibody aggregations, which may have been formed. Finally, the same quantity of Streptavidin (SAPE) and DAPI was applied in the tissue section for 30 and 15 minutes respectively to amplify the R-PE signal and stain the nuclei. Finally, the slides were washed again twice in TBS-Ts for 10 minutes.

4. Stripping:

Glass slides were placed in Tris-buffer pH 7.5 for 10 minutes to remove the disaccharides from the mounting fluid, used for image acquisition, and then they were transferred to pre-heated slide mailers with stripping buffer at 56°C inside a water-bath.

Stripping buffer contained 20 ml 10% w/v SDS with 12.5 ml 0.5 M Tris-HCl, pH 6.8, and 67.5 ml ultra-pure water. Under a fume hood, 0.8 ml 2-ME was added to the solution.

The slides remained inside the water-bath for 40 minutes and then they were washed in washing buffer for 1 hour at least with several changes of the buffer in the first 15 minutes.

In the first round of every slide, stripping was additionally performed after AR. This step is not included in the basic MILAN protocol. However, during the procedure of protocol

standardization in our lab equipment, it was found that Stripping reduces the levels of tissue autofluorescence.

From that point on, 10 rounds of staining and stripping went on with different sets of antibodies. Every experimental step was followed by image acquisition to monitor the condition of the tissue and the success of the experimental step.

Image Acquisition:

Glass slides were mounted with mounting fluid and covered by a coverslip for observation and image acquisition. The mounting fluid was wisely selected among others, to prevent antigen refolding (Bolognesi et al., 2017).

Image acquisition performed after every experimental step, with JuLI Stage high-content screener (x10 lens) in brightfield ("BRIGHT") and three fluorescence channels: "GFP", "RFP", "DAPI". RFP channel excites at 525/50 nm and emits light at 580LP, GFP channel excites at 466/40 nm, and emits at 525/50 nm and DAPI channel excites at 390/40 nm and emits at 452/45 nm.

With regards to the fluorescent channels, images were acquired in the highest value of LED power (value = 10) and the lowest D-Phase (value = 1) and in two different Exposure times (140 and 250 msec). Brightness was chosen specifically for each channel: DAPI value = 12, GFP value = 22, RFP value = 30. In the BRIGHT channel, one image per experimental step was acquired in Exposure time = 15 msec, Brightness = 6, LED Power = 3, and D-Phase = 1.

After image acquisition, glass slides were placed vertically to the direction of the slide holder positions inside a container with TBS-Ts washing buffer so as the coverslip to be removed gently without the risk of scratching the tissue.

Storage:

The slides could be stored at any step in the storage buffer at 4°C for up to 3 days. In case of a larger period of not use, they were transferred at -20°C in storage buffer.

FFPE tissue slides:

The experimental procedure was repeated in two groups of FFPE kidney tissue samples. The first one included samples from healthy kidney tissue and the other one samples from patients with CKD. The latter included samples from two CKD patients. The first patient was 55 years old with GFR at 85 ml/min that is characterized as CKD Stage G2 GFR and the second patient was 75 years old with GFR at 60ml/min, who just progressed in CKD Stage G3. The FFPE slides were offered by Rafael Kramann's laboratory, RWTH Aachen University.

Buffers-Chemicals:

Buffers were created according to MILAN protocol with the chemicals mentioned below:

- Tris ultrapure (ApplichemPanreac, A1086,1000)
- Tween 20 (ApplichemPanreac, A4974,0500)
- Sodium chloride (ApplichemPanreac, A2942,0500)
- Sucrose (Sigma, S9378)
- NaN3 (MP biomedicals, 26628-22-8)
- Trehalose (MP biomedicals, 6138-23-4)
- Glycerol (EMD Millipore, 356350)
- n-propyl gallate (MP biomedicals, 121-79-9)
- BSA (VWR, 421501J)
- PBS (Gibco, 10010015)

- SDS (ApplichemPanreac, A1112,0500)
- HCl (ApplichemPanreac, 131020,1212)
- 2-mercaptoethanol (Santa Cruz Biotechnology, 202966)
- Hoechst (Thermo Fisher Scientific, 33042)

Primary Antibodies:

The primary antibodies that were tested, are mentioned in the table below.

#	Name	Supplier	Catalog #	Host Species	Cst (mg/ml)	Cf (ug/ml)
1	GAPDH	HyTest	5G4_4G5	Mouse	5.6	1
2	TMEM174	Cusabio	CSB-PA023755LA01HU	Rabbit	4	2
3	PODXL	Cusabio	CSB-PA13447A0Rb	Rabbit	3	2
4	AREG	R&D Systems	BAF262	Goat-biotin	0.136	2
5	NOX4	Cusabio	CSB-PA015961LA01HU	Rabbit	0.0035	2
6	PDGFRA	Thermofisher Scientific	14-1401-82	Rat	0.5	2
7	CMBL	Cusabio	CSB-PA846604LA01HU	Rabbit	0.5	2
8	CDH11	LifeSpan Biosciences	LS-C149887	Mouse	0.1	2
9	ROMK1	Cusabio	CSB-PA012047LA01HU	Rabbit	3	2
10	SMOC2	R&D Systems	BAF5140	Sheep-biotin	0.05	2
11	AKT1	Cell Signaling Technology	4060S	Rabbit	1.6	2
12	MMP9	R&D Systems	DY911	Mouse	1	2
13	MK12	Cell Signaling Technology	8690BP	Rabbit	1.9	2
14	TSP2	R&D Systems	BAF1635	Goat-biotin	0.05	2
15	JUN	Cell Signaling Technology	9165BF	Rabbit	1.6	2
16	ANXA2	R&D Systems	DYC-3928-2	Mouse	0.75	2
17	IFI44	Cusabio	CSB-PA011014LA01HU	Rabbit	3	2
18	ALB	HyTest	4T24_14E7	Mouse	0.00487	2
19	NETO2	Cusabio	CSB-PA818759LA01HU	Rabbit	2	2
20	LYN	R&D Systems	DYC3936	Mouse	1	2

Secondary Antibodies:

	Name	Supplier	Catalog #	Host Species	Reactivity	Cst	Cf
1	Alexa Fluor 488 IgG	ThermoFisher Scientific	A32731	Goat	anti-Rabbit	1 mg/ml	5 ug/ml
2	R-Phycoerythrin	Santa Cruz	sc-516141	Goat	anti-Mouse	1 mg/ml	5 ug/ml

Selection of fluorophores based on microscope channels excitation and emission spectra

The selection of fluorophores was made via ThermoFisher Scientific's Fluorescence Spectra Viewer, based on the fluorescent channels of the JuliStage™ high-content screener. JuliStage™ provides the following fluorescence channels: an RFP channel with spectra Ex. 525/50 | Em. 580/LP, a GFP channel with spectra Ex. 466/40 | Em. 525/50 and a DAPI channel with spectra Ex. 390/40 | Em. 452/45. R-Phycoerythrin (PE) was chosen as a fluorophore for the secondary antibodies for the RFP channel, and AlexaFluor 488 was considered an appropriate secondary antibody for the GFP channel.

a) Alexa Fluor 488 – JuLI Stage channels

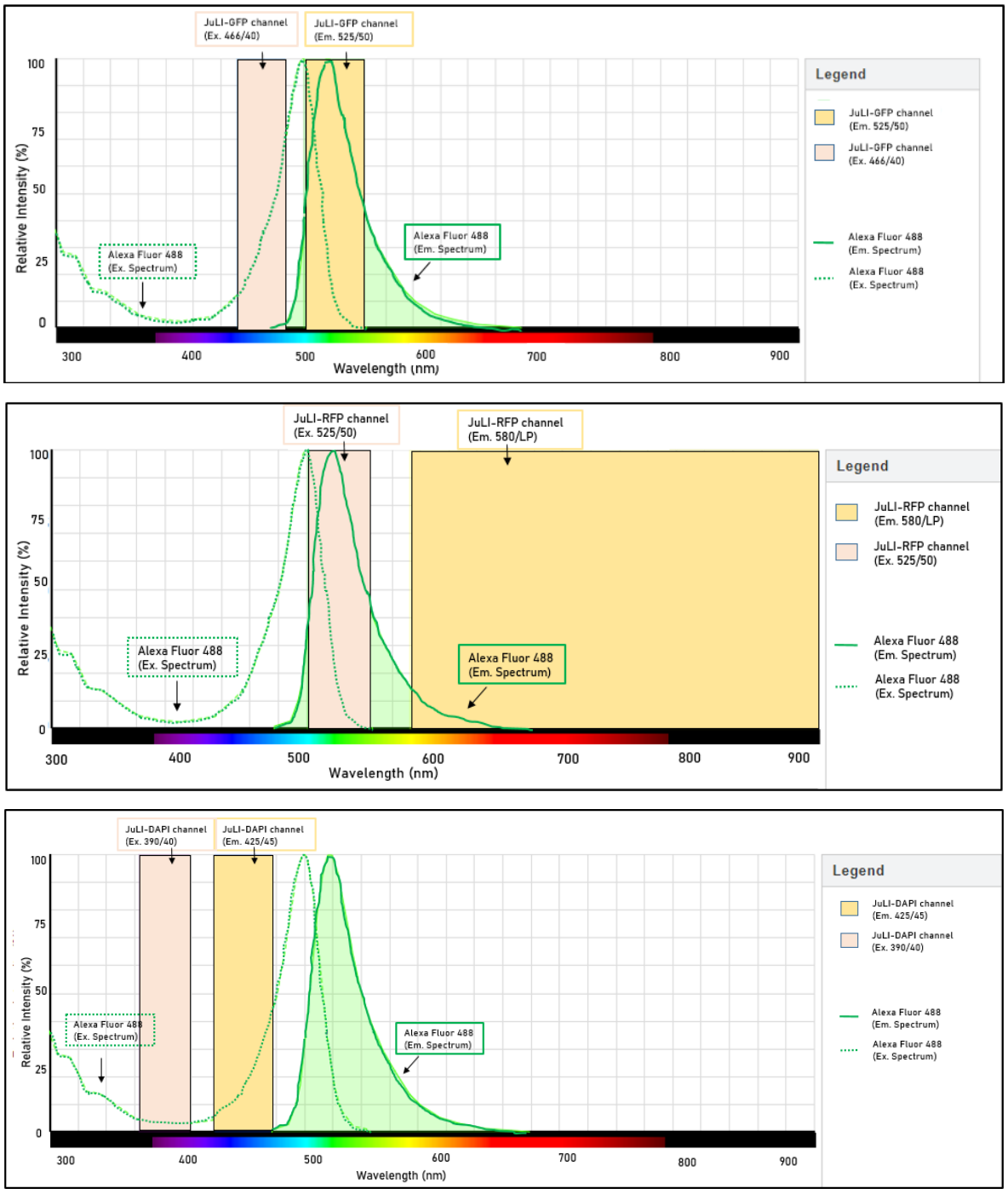

Figure 3 Excitation and emission spectra of Alexa Fluor 488 and JuLI Stage channels. The GFP channel covers 10-75% of the excitation spectrum of Alexa Fluor 488 and their emission spectra coincide 100%. The RFP channel excites Alexa Fluor, as well, but it cannot emit it. The excitation and emission spectra of the DAPI channel and Alexa Fluor 488 are completely distinct.

Figure 1 shows the excitation and emission spectra of Alexa Fluor 488 and JuLI Stage GFP, RFP, and DAPI channels. The GFP channel of JuLI Stage excites Alexa Fluor between 10-75% of its relative intensity and emits 100% of its fluorescence. Alexa Fluor 488 can be excited by the RFP channel, as well, but it gets emitted, only by the small percentage of 10%. Regarding the DAPI channel, Alexa Fluor spectra are completely separated. Alexa Fluor 488 was considered a suitable fluorophore for the GFP channel of JuLI Stage in immunofluorescence protocols.

b) R-Phycoerythrine (R-PE)– JuLI Stage channels

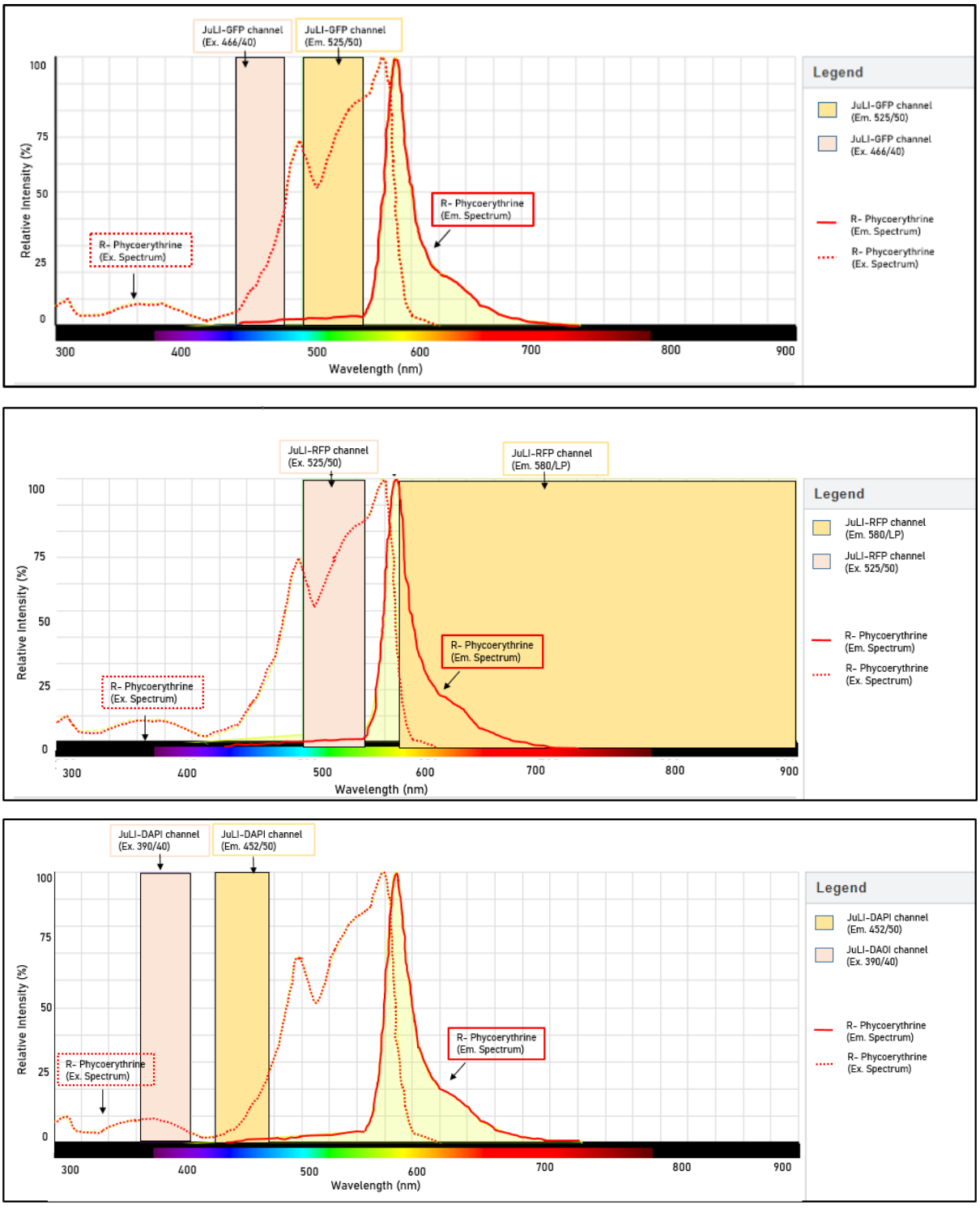

Figure 4 Excitation and emission spectra of the R-Phycoerythrine (R-PE) and JuLI Stage channels. RFP channel covers around 80% of the excitation spectrum of R-PE and their emission spectra coincide 100%. GFP excites R-PE around 45% but it cannot emit it. DAPI channel excites R-PE around 10% but their emission spectra do not coincide at all.

Figure 2 shows the excitation and emission spectra of R-PE in comparison with the JuLI Stage channels spectra. R-PE gets excited around 20-45% of its relative intensity in GFP and DAPI channels but it cannot be emitted. In the RFP channel, R-PE gets excited around 90% and is emitted in its whole spectrum. So, the use of R-PE was considered sufficient for the RFP channel.

c) Kidney autofluorescence spectra coincide with JuLI Stage channels spectra

Renal tissue yields high autofluorescence (AF) levels which produce considerable noise in the application of immunofluorescence protocols. The renal AF include the spectra Ex. 543/5 | Em. 630/70 for the red channel, and Ex. 458/5 | Em. 545/65 for the green channel .

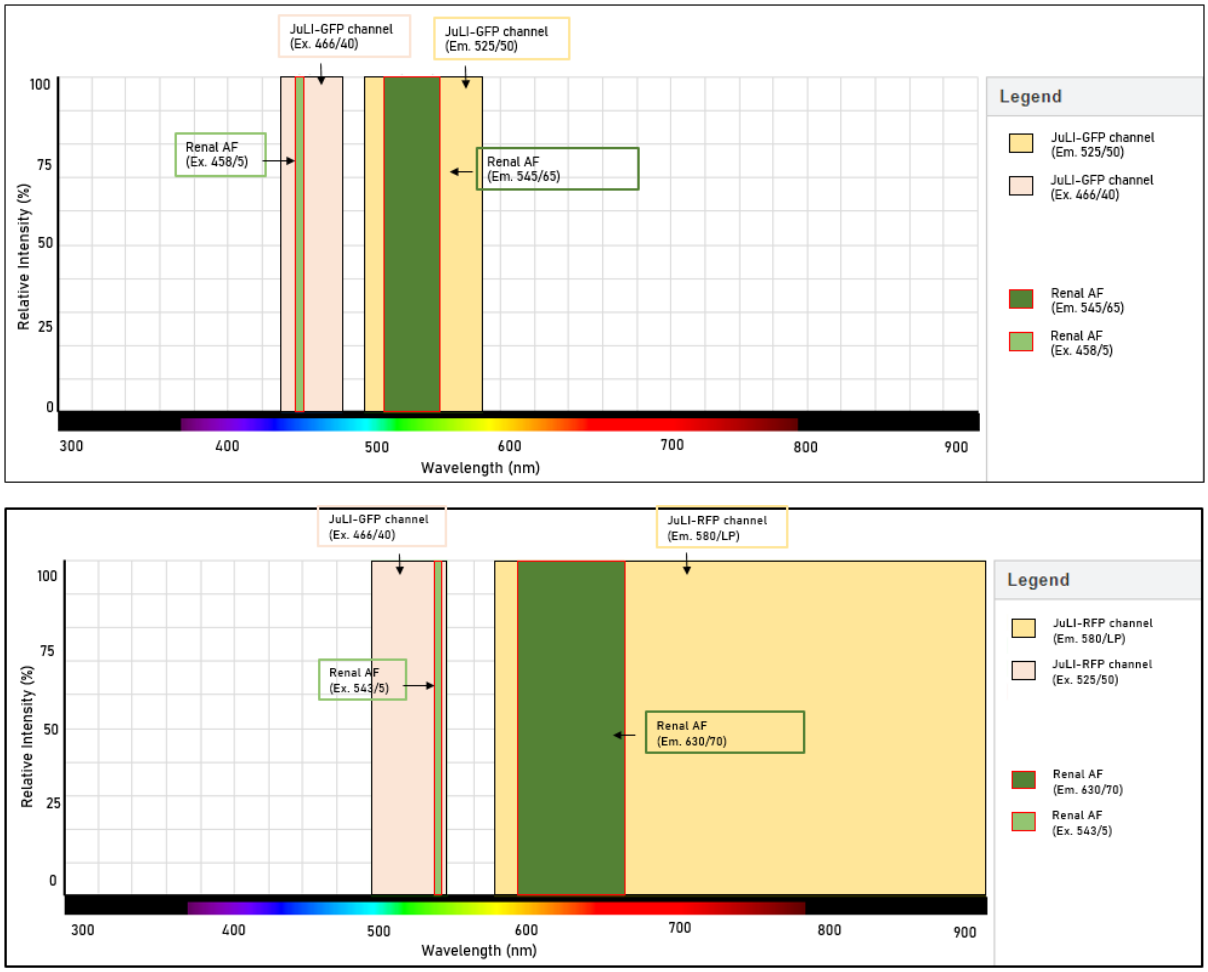

Figure 5 Excitation and emission spectra of renal autofluorescence (AF) and JuLI Stage channels spectra. Both GFP and RFP channels excite and emit the renal AF.

Renal tissue excited between 455.5-460.5 and/or 541,5-545,5 nm, emits autofluorescence between 512.5-577.5 and/or 595-665nm, respectively (Zhang et al., 2018). These ranges completely overlay with the excitation and emission spectra of the GFP and RFP channels. So, renal AF will be present in the images obtained with the GFP and RFP channel and it should be subtracted during the image processing.

ii) Image Processing

Images from three different areas per slide were acquired in every experimental round in GFP, RFP, and DAPI channels via JuLI Stage high-content screener. The areas of the first round were defined as reference images and were captured across the rest of the experimental rounds.

Image analysis was performed with the open-source software ImageJ (Schindelin et al., 2012) and QuPath (Bankhead et al., 2017). The first part of the analysis was performed with ImageJ, wherein images from all rounds were combined in one final composite image.

FIJI software Analysis

The images acquired from every slide after 10 rounds of the experimental procedure were processed with FIJI software. FIJI software offers a great variety of tools for image processing, such as images registration, cropping, illumination correction, etc. To automate the procedure, a script was written in Jython programming language in ImageJ editor that could be further applied in all areas sequentially. The commands included in the script are described below:

- Alignment of GFP, RFP and DAPI images per round, via Elastix plugin (Klein et al., 2010, Shamonin et al., 2013, Tischer, 2019)
- Alignment of all images per channel, via MultiStackReg plugin (Miura, 2019, Thévenaz et al., 1998)
- Cropping of black margins in all images per channel
- Illumination correction of all images per channel, via BaSiC plugin (Peng et al., 2017)
- Subtraction of stripping from staining in pairs for all images and channels
- Combination of all subtracted images in one stack and deletion of all DAPI images except for DAPI image of the first round
- Cropping of black margins in the final stack
- Application of a different LUT in every image of the final stack
- Creation of a composite image depicting the expression of all makers upon the tissue

Using this script, the images were firstly registered and cropped in equal dimensions (Fig. 6).

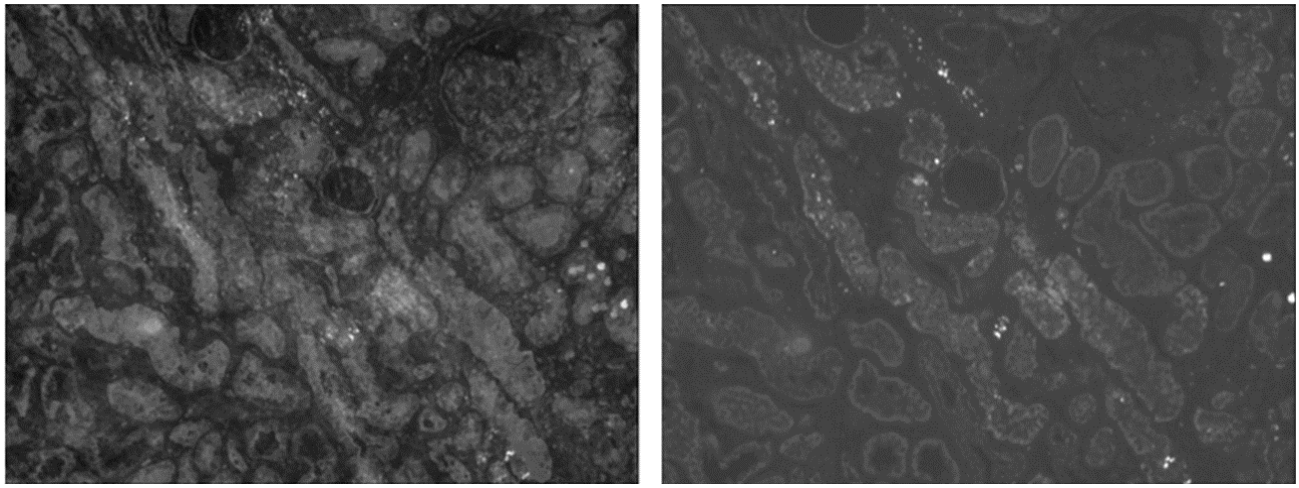

Figure 6 Composite image of 10 images before and after registration. Image registration was performed with the Elastix FIJI plugin. Right: a composite image of unregistered images. Left: a composite image after image registration and cropping in equal dimensions.

Then, in every pair of staining-stripping images, the stripping image was subtracted from the staining image to remove the intensity that corresponds to the tissue autofluorescence (Fig 7).

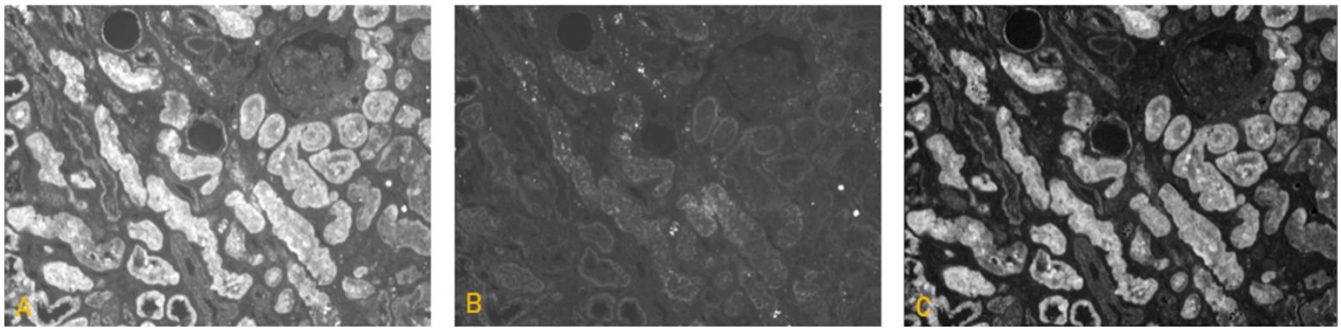

Figure 7 Subtraction of Autofluorescence. The autofluorescence removal resulted from the subtraction of stripping image (B) from the staining image (A) with the FIJI tool Image Calculator. A. Staining image with CMBL protein. B. Stripping image. C. Result of image subtraction.

Finally, the images were gathered in a stack that included 20 images of antibodies staining and the DAPI image of the first round. In these stacks, a different colour (LUT) was applied in every channel corresponding to a different antibody staining (Fig. 8).

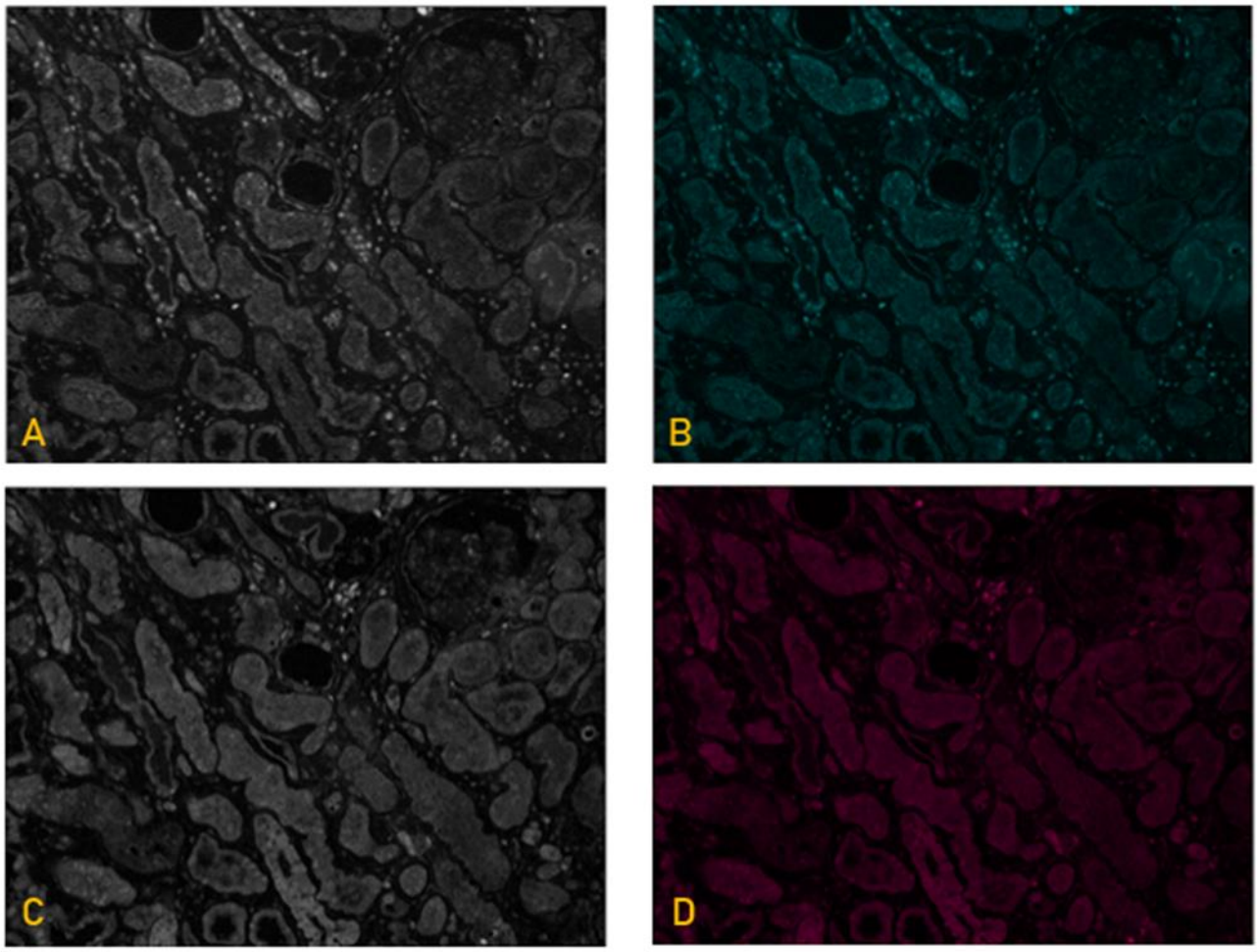

Figure 8 Application of different LUTs in each antibody staining. A-B. JUN staining in grayscale (A) and after LUT application (B). C-D MK12 staining in grayscale (C) and after LUT application (D).

Finally, all of the images were projected in one final composite image (Fig. 9).

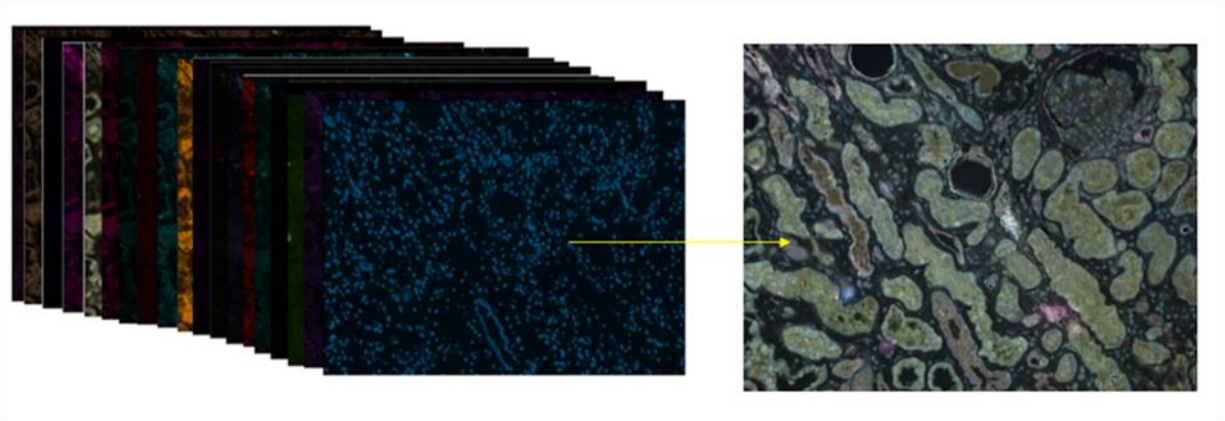

Figure 9 The final stack is converted to the final composite image. All the images with the different colors of the final stack are combined in a final image.

QuPath software Analysis

The final stack contained images with different LUTs, one for every marker, and was transferred to QuPath software (Bankhead et al., 2017). QuPath software is specific for pathology images analysis and it was used to detect tissue areas and quantify the markers' expression upon them.

The final images were transferred to QuPath software (Fig. 10) and channels were renamed according to the antibodies and assigned as classifiers. In addition, images were preprocessed for histogram adjustment to remove the underlying noise.

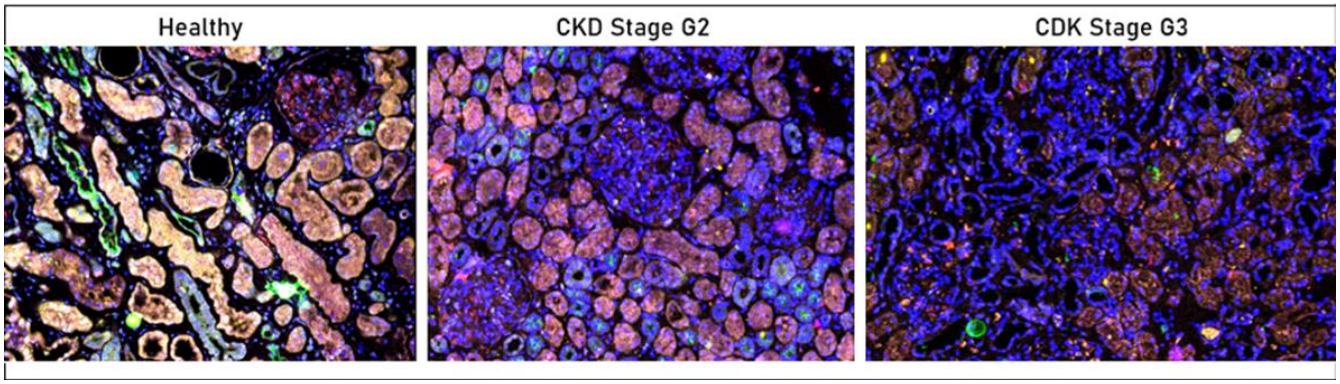

Figure 10 Composite image of different antibodies staining in Healthy and CKD tissue samples. Composite images after FIJI processing were transferred to QuPath software. The images include the antibodies: LYN, CDH11, IFI44, MK12, ROMK1, CMBL, NOX4, TMEM174, and DAPI.

Afterwards, cell detection was performed via the «dsb2018_heavy_augment» Stardist model (Schmidt et al., 2018) that has been incorporated in QuPath and tissue areas of interest were manually annotated and labelled as proximal/distal tubules, glomeruli, or others.The label "Others" was used for areas with dubious identification. Then, the cells were classified according to the presence of each antibody-marker in each one of them (Fig. 11).

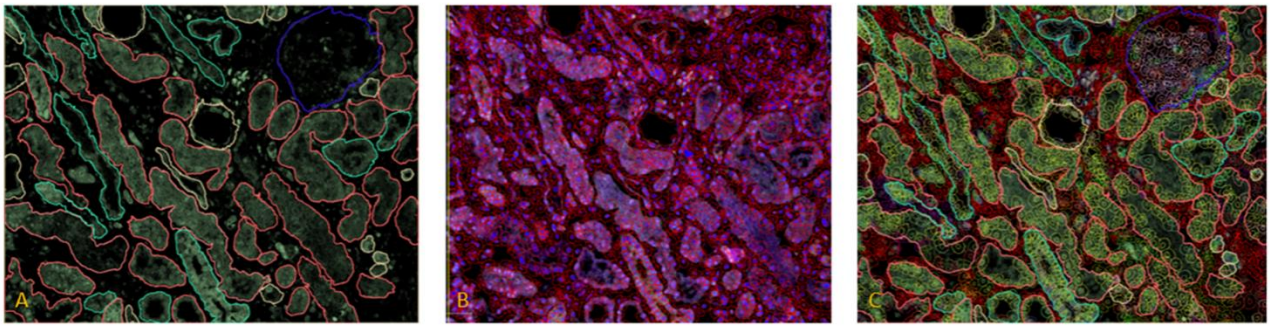

Figure 11 QuPath analysis. A. The images were annotated for characteristic tissue areas such as tubules and glomeruli, B. Cell detection via the Stardist plugin, C. Classification of cells according to the marker-classifier intensity level.

The results of cell classification were exported in a results table, which contained information about the tissue area in which every cell is located and statistical measurements for all the markers present in the cell. This table was used for further statistical analysis.

iii) Statistical Analysis

The total intensity of each protein in every cell of the areas of interest was exported, thus protein expression for every area was quantified as median±SEM of total intensity. One-way ANOVA was performed for the statistical comparison of protein expression, using GraphPad Prism 8.4.3 software.

t-distributed stochastic neighbour embedding (t-SNE) algorithm was employed for visualization of the cells' populations in the R programming language. t-SNE is an unsupervised nonlinear dimensionality reduction method, for visualizing high dimensional data in a low 2-dimensional space. The n-dimensional plot is constructed such that if two points/cells are close, they are most likely to be close in the higher dimensional space as well, while if two points are farther apart they are likely to also be farther apart in the original higher-dimensional space. Only the relative distances between points matter - the two axes are arbitrary and do not have any specific interpretation.

IV. Results

i. MILAN Protocol Standardization

a) Renal AF in healthy and CKD kidneys

Several studies have confirmed the presence of autofluorescence of the renal tissue, mainly in the glomeruli, the tubules, and the blood vessels . There is also evidence that renal AF increases in cases of renal injuries, such as Ischemic Renal Injury and renal tumours. In these pathological conditions, AF levels can be used to indicate the degree of renal damage (Bellini et al., 2008, Patil et al., 2016, Schuh et al., 2016, Tirapelli et al., 2009). AF is increased in CKD tissue samples compared to the normal tissue, as well (Fig. 12). AF levels of healthy and CKD tissue samples were calculated by the whole image intensity after dewaxing and antigen retrieval (AR) for every fluorescence channel. Data are presented as mean±SEM of at least 3 biological replicates.

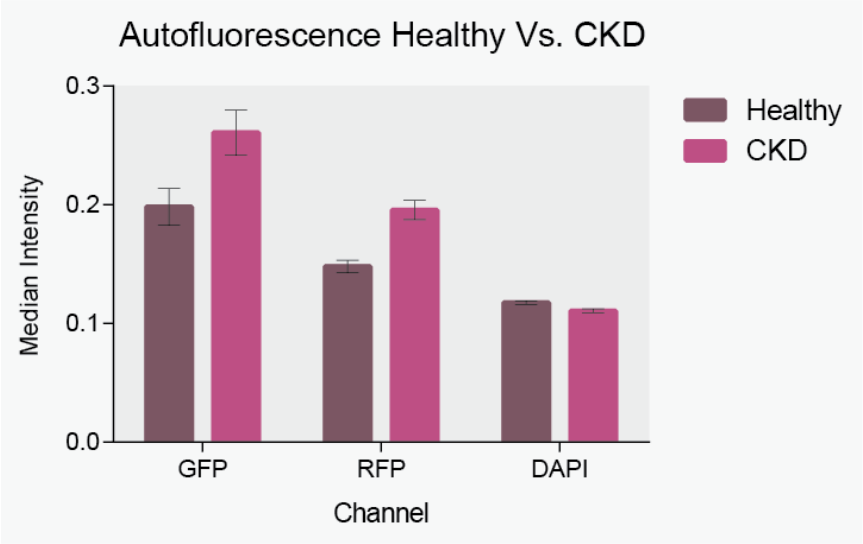

Figure 12 Autofluorescence (AF) levels in healthy and CKD samples in GFP, RFP, and DAPI channel. Autofluorescence is increased in CKD tissue samples, mainly in the GFP and RFP channels. In the DAPI channel, AF is slightly increased compared to the healthy AF levels.

b) MILAN protocol preserves tissue integrity

The tissue loss across several experimental rounds of the MILAN was calculated via FIJI image analysis software. The images of 15 experimental rounds were registered and then the total number of cell nuclei stained with Hoechst 33342 was calculated. The data are presented as mean±SEM of at least 3 biological replicates. The reduction was not found statistically significant. MILAN prevents tissue damage for a minimum of 15 repetitions of the experimental procedure (Fig. 13).

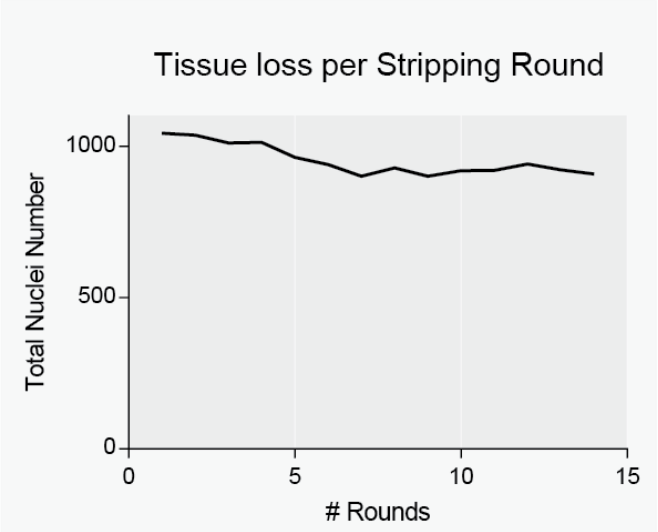

Figure 13 Tissue loss across 15 experimental rounds of MILAN. The number of nuclei in the tissue after 15 repetitions is slightly decreased. The reduction is not statistically significant. The data obtained by FIJI software, are presented as mean±SEM of at least 3 biological replicates.

c) Intensity evaluation across the experimental steps

The verification of increased intensity only due to staining was performed by application only of the antibody diluent and secondary antibodies and image acquisition in increasing exposure times (5-250 msec) and maximum LED power. Whole image intensity was calculated using FIJI software after image registration and cropping in equal dimensions. The comparison of the slopes via linear regression fitting of the data revealed a statistically significant difference between staining and the rest of the experimental conditions. The data are presented as mean±SEM of at least 3 biological replicates.

Maximum intensity is observed in the staining step with a significant difference from the following one that corresponds to the tissue intensity after the antigen retrieval in RFP and DAPI channels. In the GFP channel, the difference is smaller but the highest intensity is observed to the staining step, as well. The secondary antibodies and the Ab diluent do not increase the intensity that appears similar to the intensity after stripping (Fig. 14).

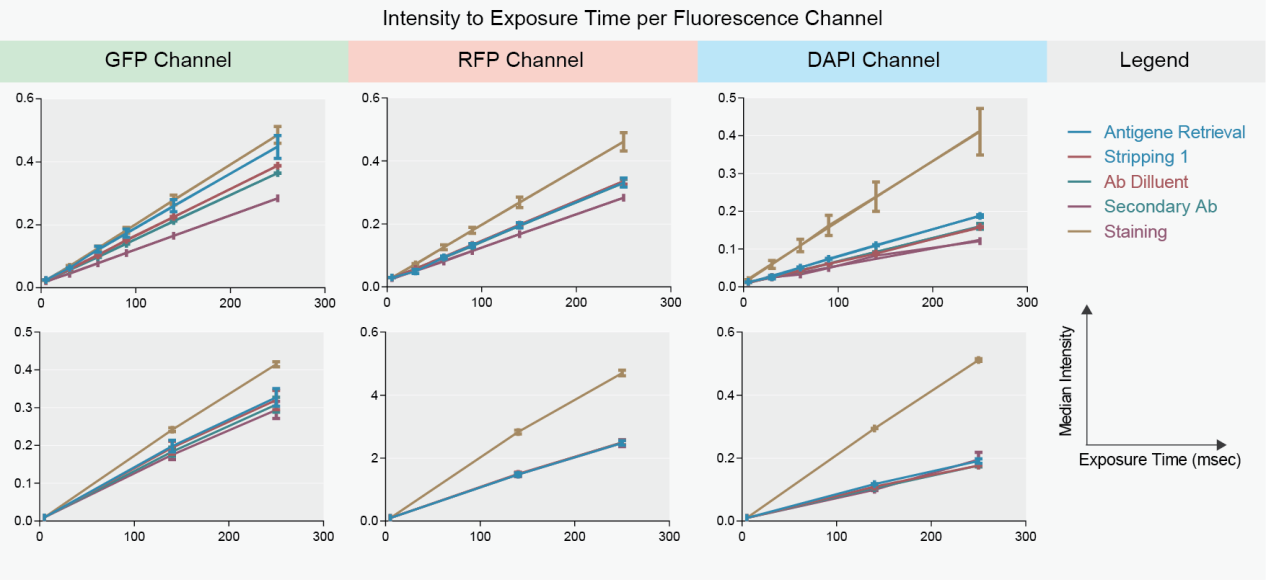

Figure 14 Intensity evaluation across the experimental conditions of MILAN protocol. Staining reveals the highest intensity, in which the antibody diluent and secondary antibodies do not contribute. Images were acquired after the application of the different experimental conditions in increasing exposure times and maximum LED power. The slopes comparison revealed a statistically significant difference between staining and the rest experimental conditions. The data are presented as mean±SEM of at least 3 biological replicates.

d) An additional Stripping step after Antigen Retrieval reduces the levels of Autofluorescence

During the protocol standardization, it was observed that an additional Stripping step, after the Antigen Retrieval reduces the levels of initial autofluorescence in GFP, RFP, and DAPI channel (Figure 7). The highest reduction is observed in the GFP channel.

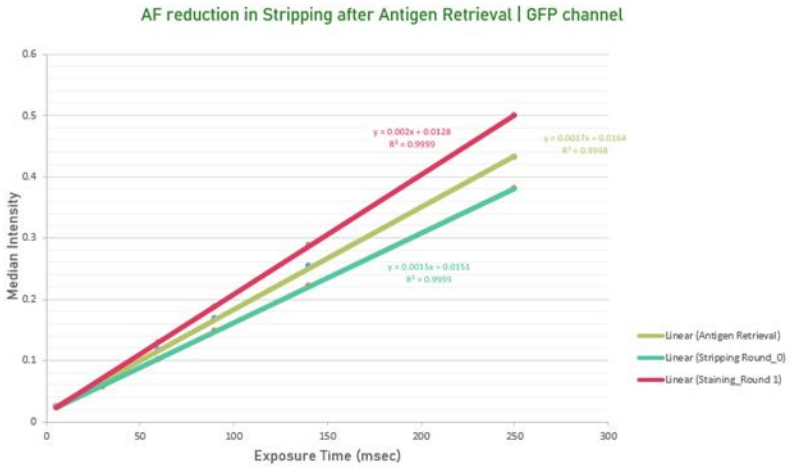

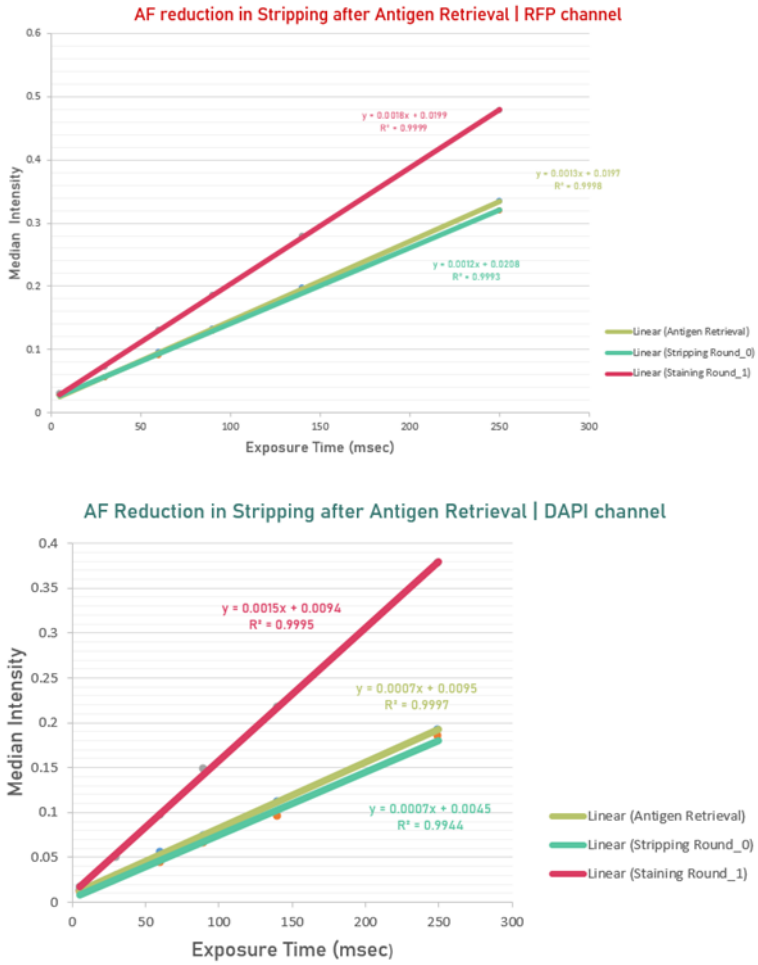

Figure 15 Stripping after Antigen Retrieval reduces the levels of autofluorescence in GFP, RFP, and DAPI channels. The tissue intensity (AF) is reduced if there is an additional stripping step after antigen retrieval, mainly in the GFP channel.

e) Antibody Staining in Healthy and CKD tissue Samples

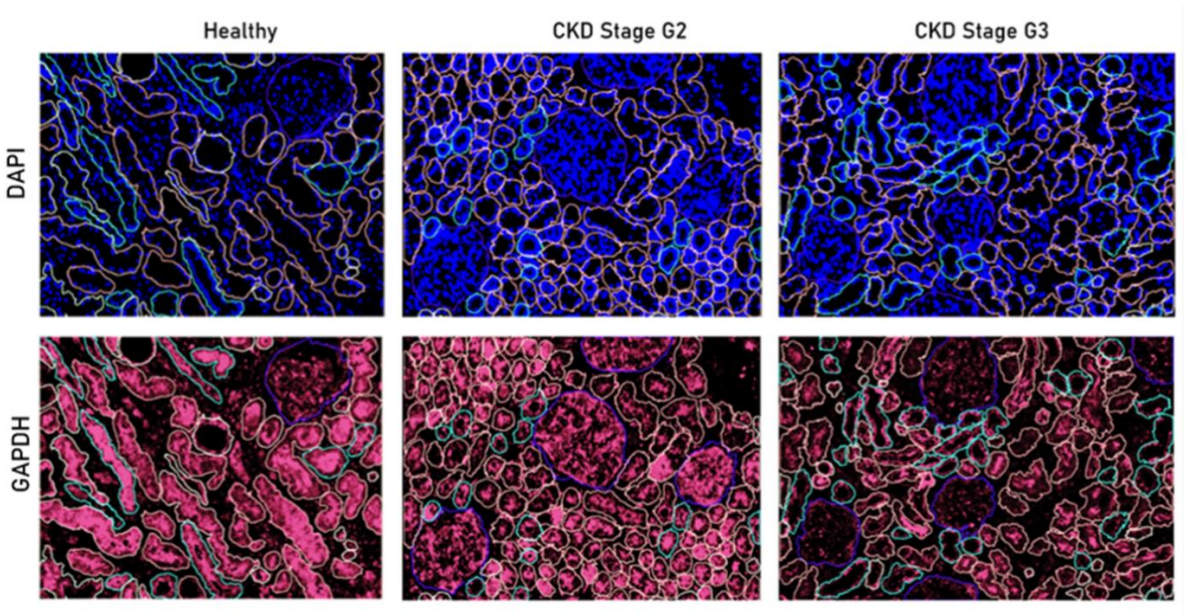
Healthy
CKD Stage G2
CKD Stage G3
DAPI
GAPDH

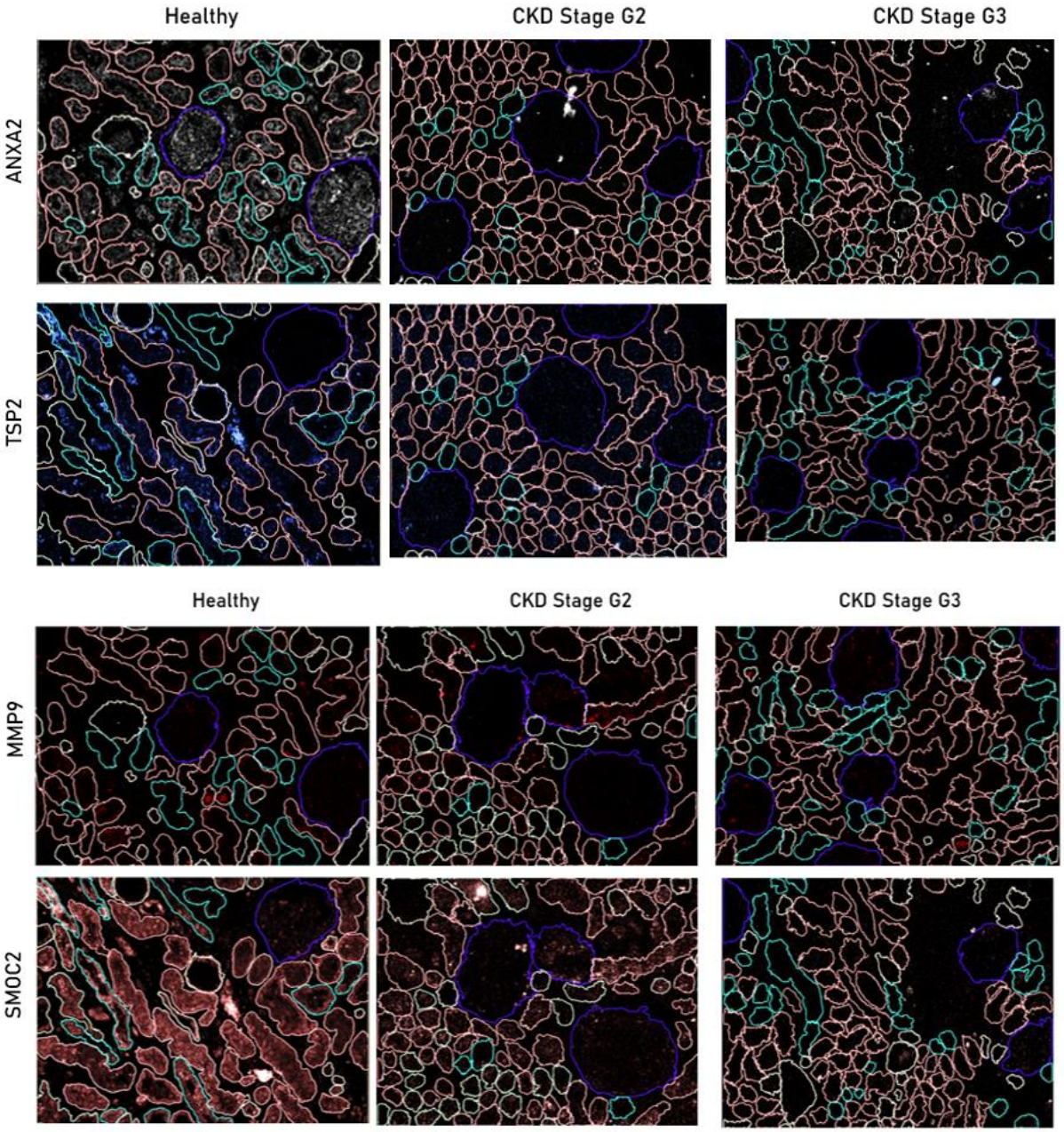
Healthy
CKD Stage G2
CKD Stage G3
ANXA2
TSP2
Healthy
CKD Stage G2
CKD Stage G3
MMP9
SMOC2

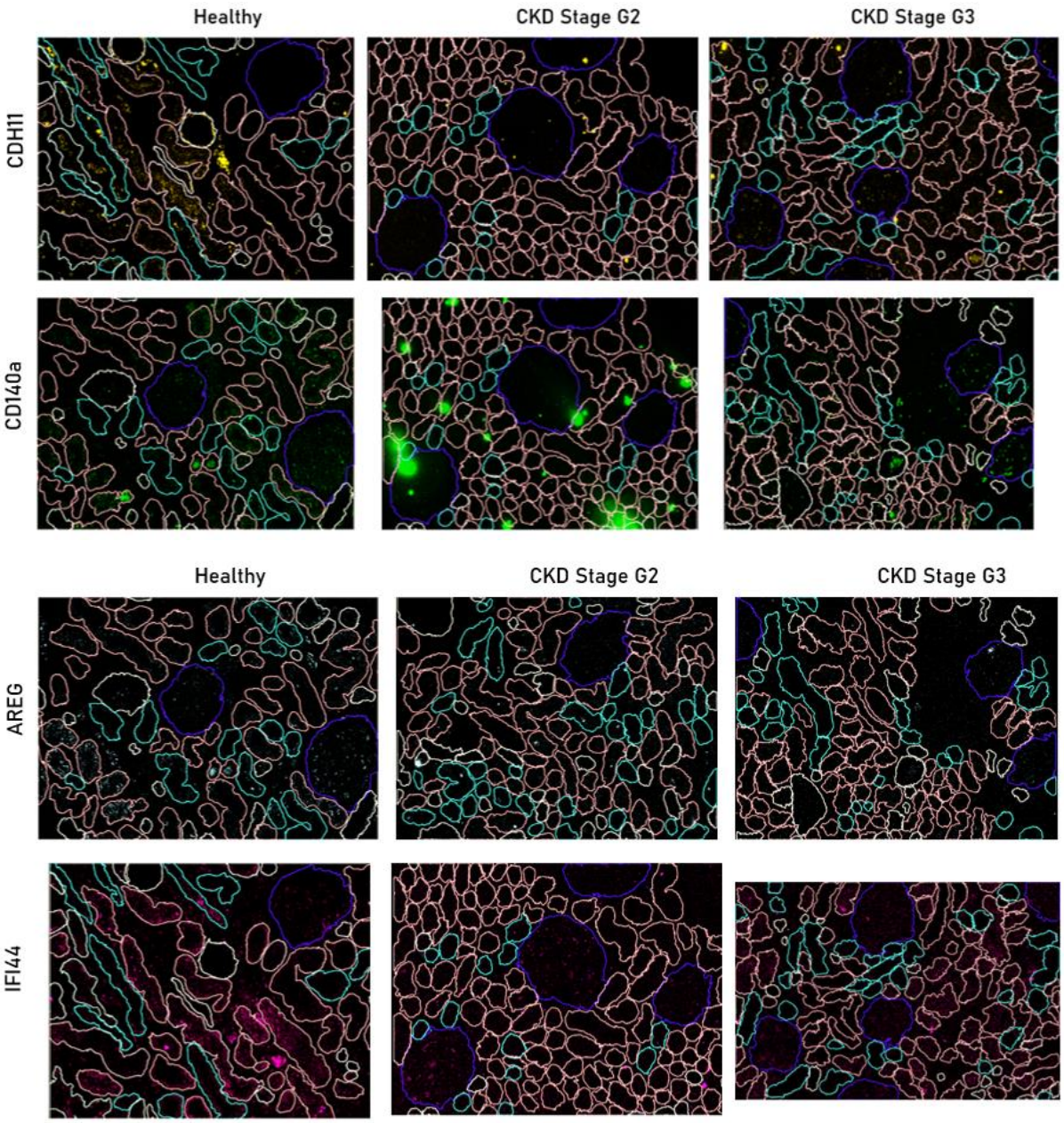
Healthy
CKD Stage G2
CKD Stage G3
CDH11
CD140a
Healthy
CKD Stage G2
CKD Stage G3
AREG
IFI44

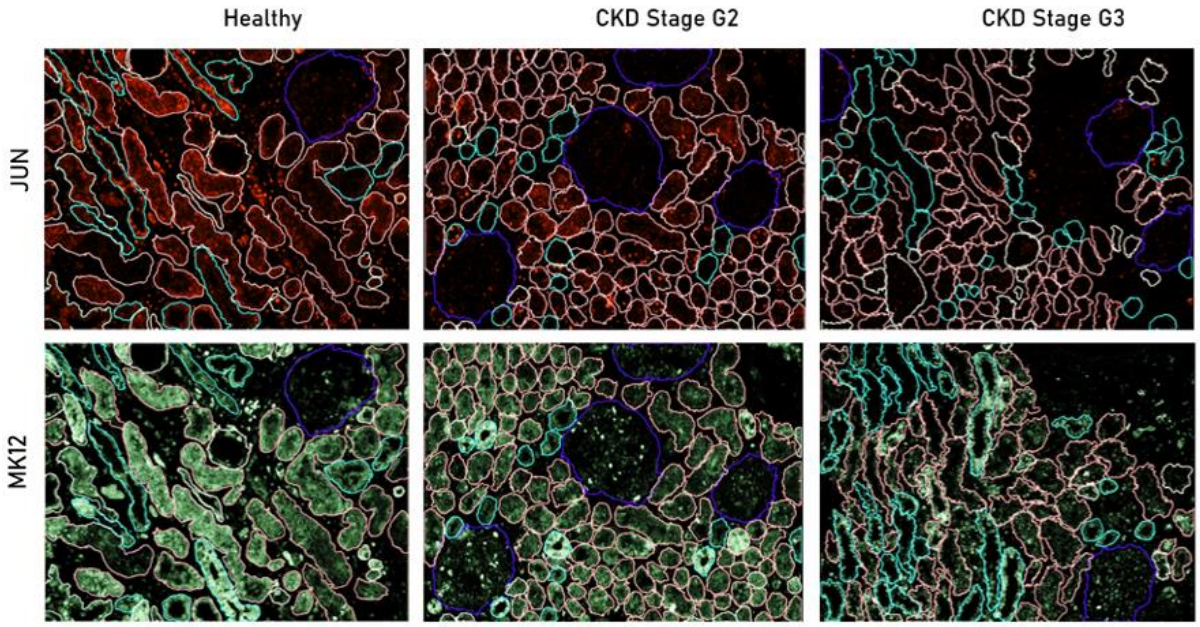
Healthy
CKD Stage G2
CKD Stage G3
JUN
MK12

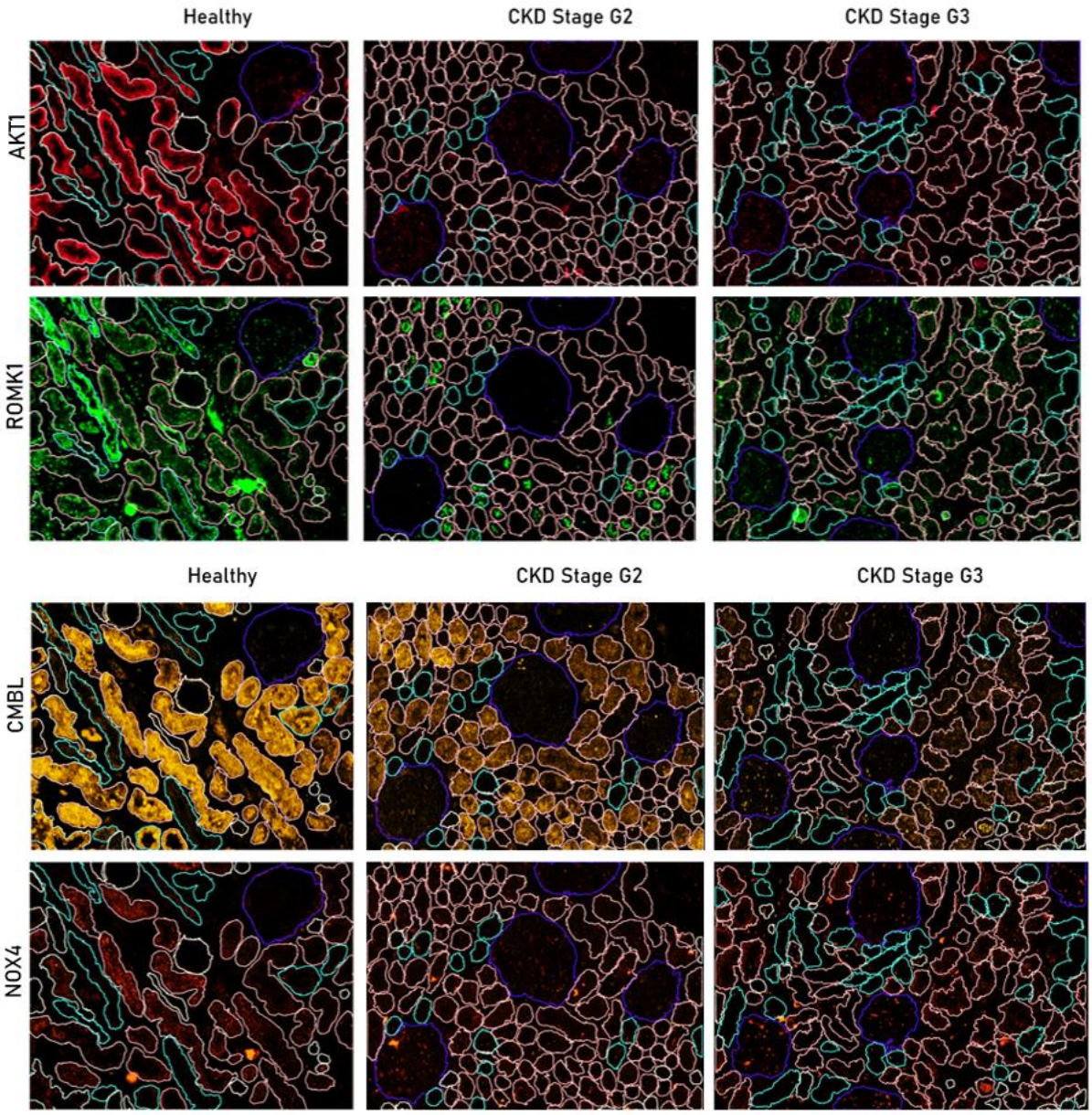
Healthy
CKD Stage G2
CKD Stage G3
AKT1
ROMK1
Healthy
CKD Stage G2
CKD Stage G3
CMBL
NOX4

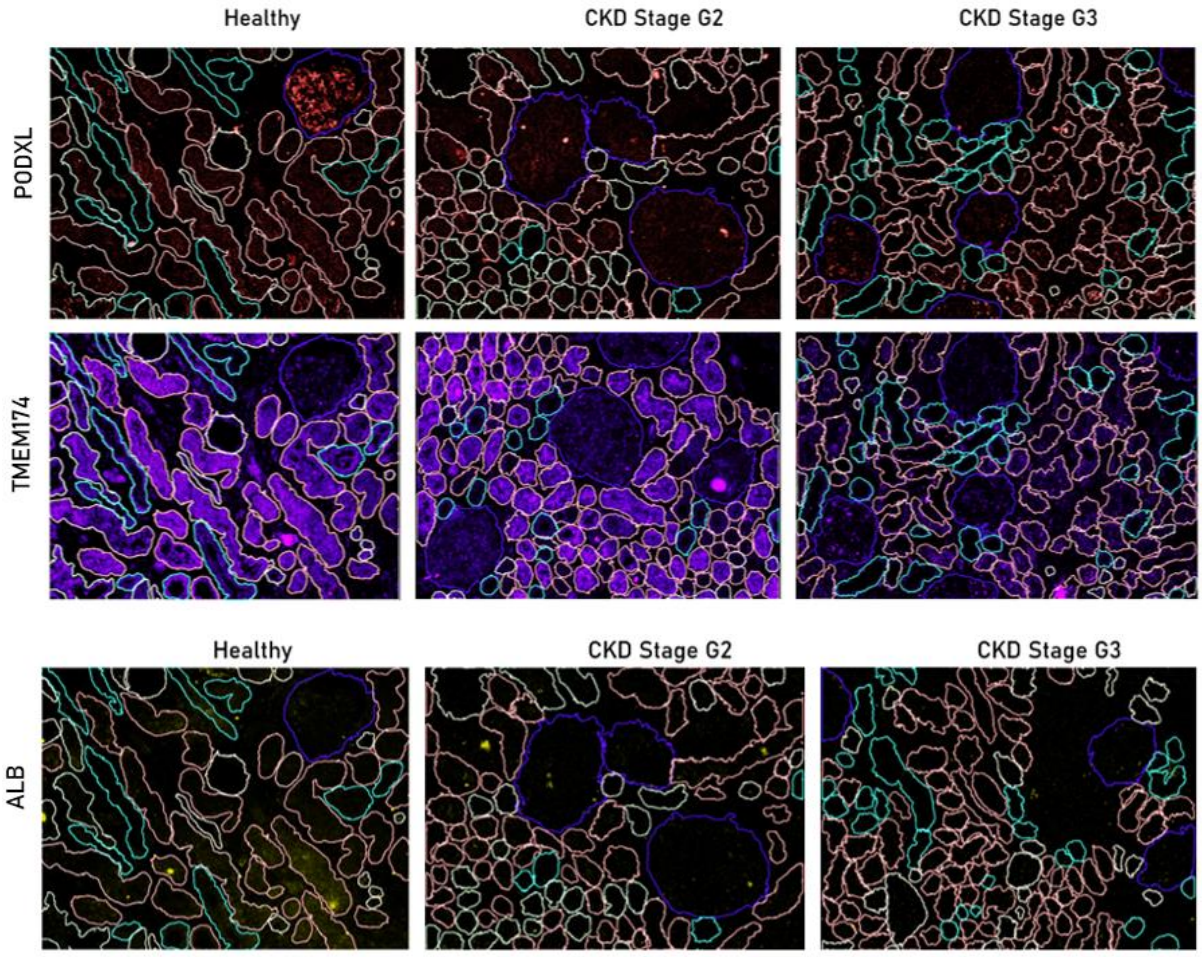
Healthy
CKD Stage G2
CKD Stage G3
PODXL
TMEM174
Healthy
CKD Stage G2
CKD Stage G3
ALB

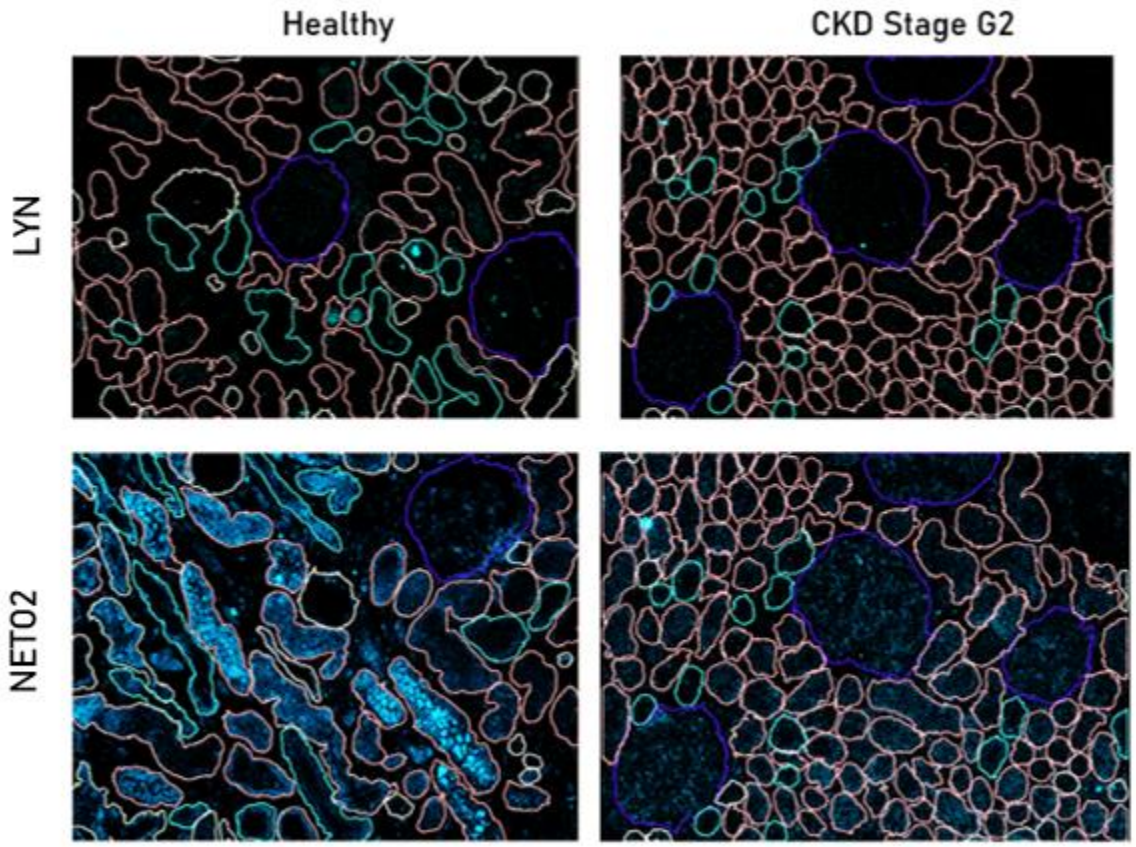

Figure 16 Antibodies staining in healthy and CKD Stage G2, G3.

ii) Statistical Analysis

a) GAPDH expression as a positive control of the method

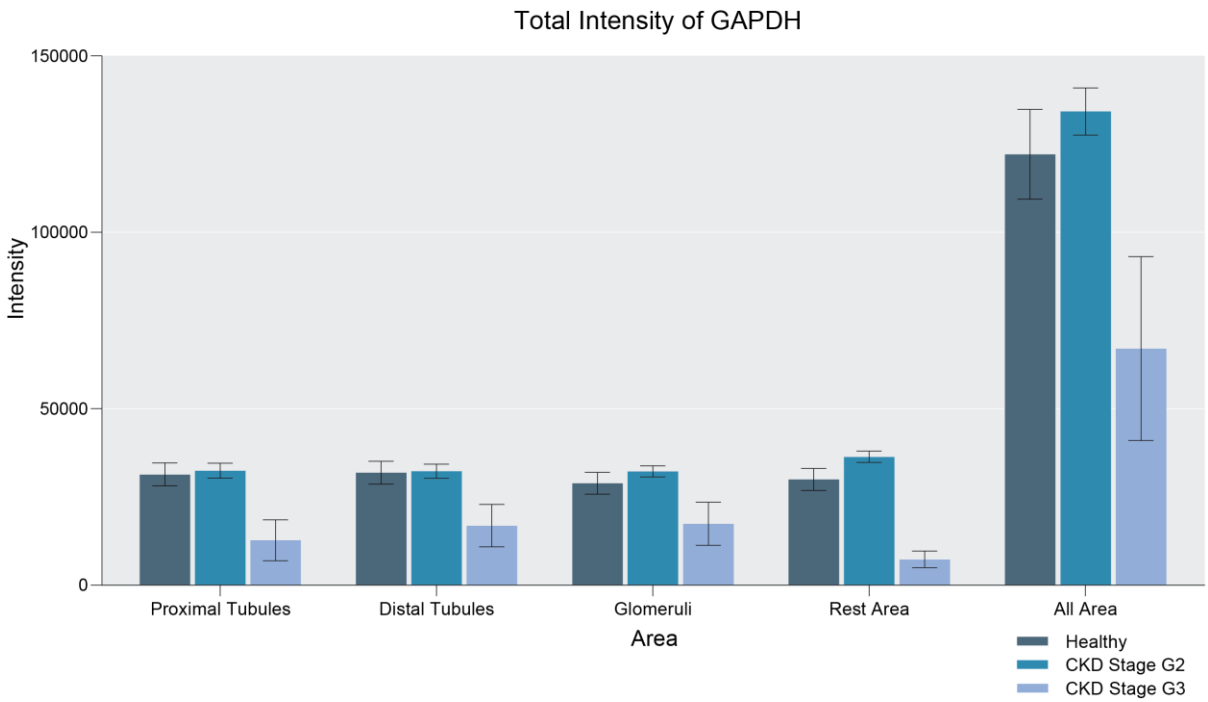

Figure 17 Total intensity of GAPDH staining. GAPDH was used as a positive control of the method. Data presented as median±SEM of at least three biological replicates.

GAPDH was chosen as a positive control of the method. GAPDH staining was performed in the first rounds of every experiment to ensure tissue integrity and sufficient antigen retrieval. GAPDH intensity levels presented low variability between the different samples, with the exception of CKD Stage G3 samples. This can be attributed to the general histological differences present as CKD advances, and especially to the lower metabolic rhythms and loss of the renal cells. Nonetheless, GAPDH's high-intensity values were proved its sufficiency as a positive control, and slides with low GAPDH intensity level were discarded from further analysis.

b) Protein expression in Healthy and CKD tissues

Healthy Samples:

The median intensity of every marker was calculated for the proximal/distal tubules and the glomeruli (Fig. 18).

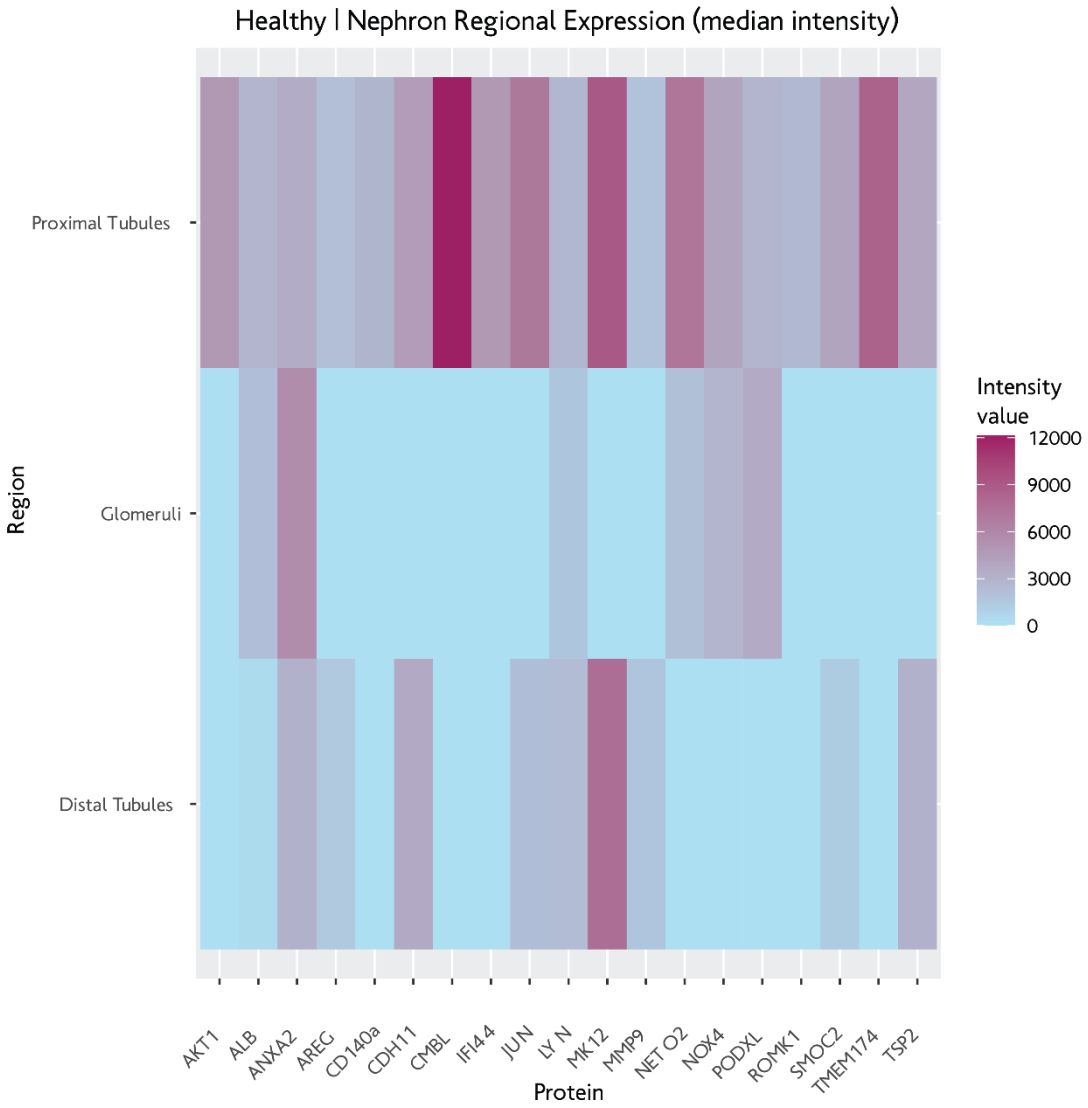

Figure 18 Heatmap of the antibodies median intensity per tissue area in Healthy samples.

The proteins tested are mostly expressed in the proximal tubules. Among them, the highest intensity value corresponds to CMBL, which is followed by MK12, TMEM174, NETO2, and JUN. The rest antibodies exhibit significant but lower intensity. In the distal tubules of healthy tissue, MK12 is mainly expressed. CDH11, TSP2, and ANXA2 display intermediate intensity values and AREG, JUN, LYN, NETO2, SMOC2 follow with the lowest intensity. In the healthy glomeruli, ANXA2 and PODXL display the highest expression. ALB, NOX4, LYN, and NETO2 are expressed in the glomeruli, as well.

CKD Samples:

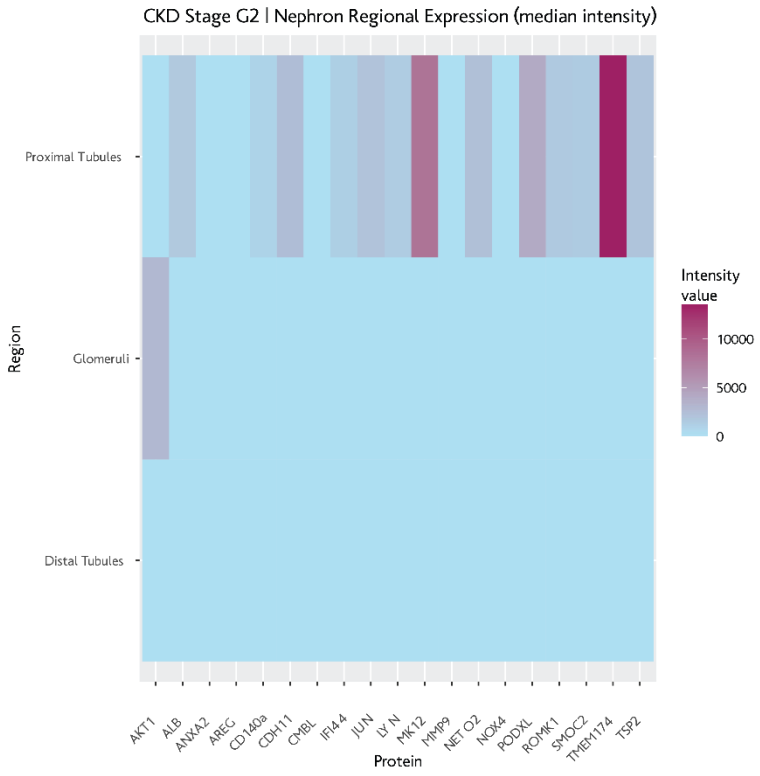

Figure 19 Heatmap of antibodies median intensity in CKD Stage G2 tissue samples.

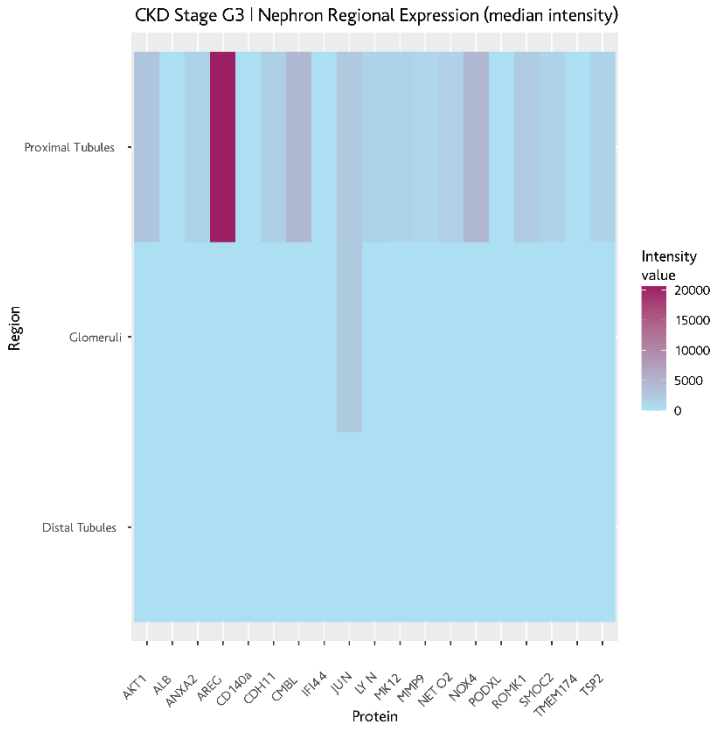

Figure 20 Heatmap of antibodies median intensity in CKD Stage G3 tissue samples

In the CKD samples the antibodies' presence is significantly decreased (Fig. 19-20). In the proximal tubules of CKD G2 Stage, TMEM174 and MK12 maintain a high median intensity, and in CKD Stage G3 AREG is highly elevated compared to the other samples. In the glomeruli of CKD stage G2, AKT1 is observed as the protein with the highest expression and in CKD Stage G3 this position belongs to JUN. The rest antibodies have a much lower median intensity in the glomeruli. In the distal tubules, the intensity value of all antibodies is importantly decreased in comparison to that of proximal tubules.

c) Comparison of Protein expression between the Healthy and CKD samples in the whole tissue area

Whole tissue area:

The relative expression of proteins between the Healthy and CKD stages G2, G3 was evaluated using two-way ANOVA with Tukey's multiple comparisons test.

The total median intensity was measured in the whole tissue area of the healthy and both CKD stages and the statistical significance of the differences between them was estimated (Fig. 21).

Between the healthy and both the CKD samples, 12 proteins showed a statistically significant difference, including ALB, SMOC2, NETO2, IFI44, JUN, AKT1, ROMK1, CMBL, and TMEM174. The median intensity of most of them was increased in the healthy condition except for NETO2 that was increased in CKD Stage 2 and TMEM174 that was increased in CKD Stage 2.

The difference between healthy and CKD Stage 2 samples was statistically significant in the proteins LYN, TSP2, and AREG, as well. LYN and TSP2 exhibited higher intensity in the healthy condition, whereas AREG was increased in the CKD Stage 2 samples. In addition, there is a statistically significant difference of ANXA2 and MK12 between healthy and CKD samples of stage G3. Both of them showed decreased intensity in CKD stage 3. Finally, AREG, NETO2, MK12 are differentially expressed between the two stages of CKD. TMEM174 and NETO2 are increased in CKD Stage 3 with a great difference from CKD Stage G2.

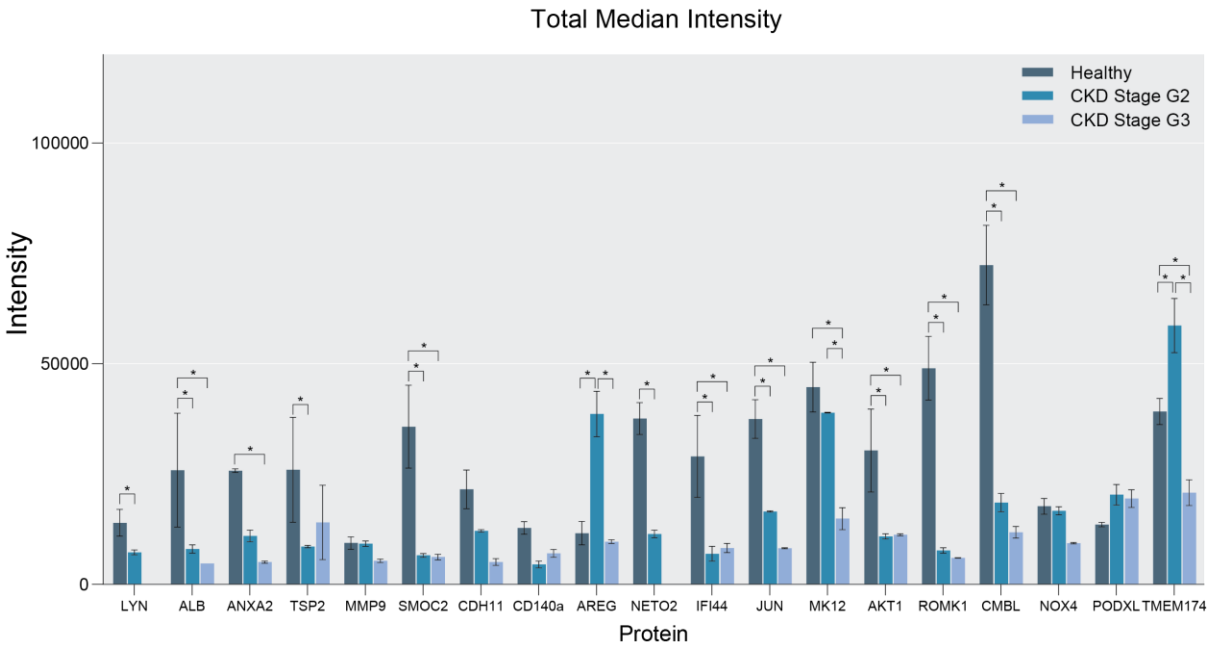

Figure 21 Evaluation of intensity differences between the Healthy and the two CKD conditions in the whole tissue area. The statistical importance of the difference was evaluated by ANOVA and is represented by (*) in the plot.

In specific tissue areas:

In the proximal tubules, the protein expression appears similar to that of the whole tissue with a few exceptions. TSP2 and CDH11, but not AKT1, were found different between the healthy and both CKD stages, with increased intensity in the healthy samples. AKT1 is significantly lower on healthy samples compared to CKD stage G2 along with AREG, which is increased in CKD samples. Another exception concern the ANXA2 staining between healthy and CKD 3 samples and the absence of difference in MK12 intensity between the two CKD stages (Fig. 22a).

In the distal tubules, the protein expression appears similar to that of proximal tubules. The main exceptions involve the different expression levels of CDH11, JUN, and TMEM174 which appear only between healthy and CKD Stage G3, the MK12 intensity levels between the two CKD Stages, and the non-significant difference of AKT1 between healthy and CKD Stage G2 samples (Fig. 22b).

In the glomeruli, the antibodies stained the area similarly to the whole tissue staining. However, a non-significant difference is observed in IFI44, AKT1, and TMEM174 between the healthy and CKD stages and in LYN and TSP2 between healthy and CKD stage G2 samples. Contrary, TSP2 is significantly higher in the healthy state compared to CKD stage 3 (Figure 22c).

In the tissue areas that were not easily identifiable and labelled as “Others”, the protein expression pattern is similar to that of the whole tissue. An exception appears for AKT1, which was only significantly different between healthy and CKD stage 2, and for LYN and TSP2, whose difference wan not found significant between these conditions (Fig. 22d).

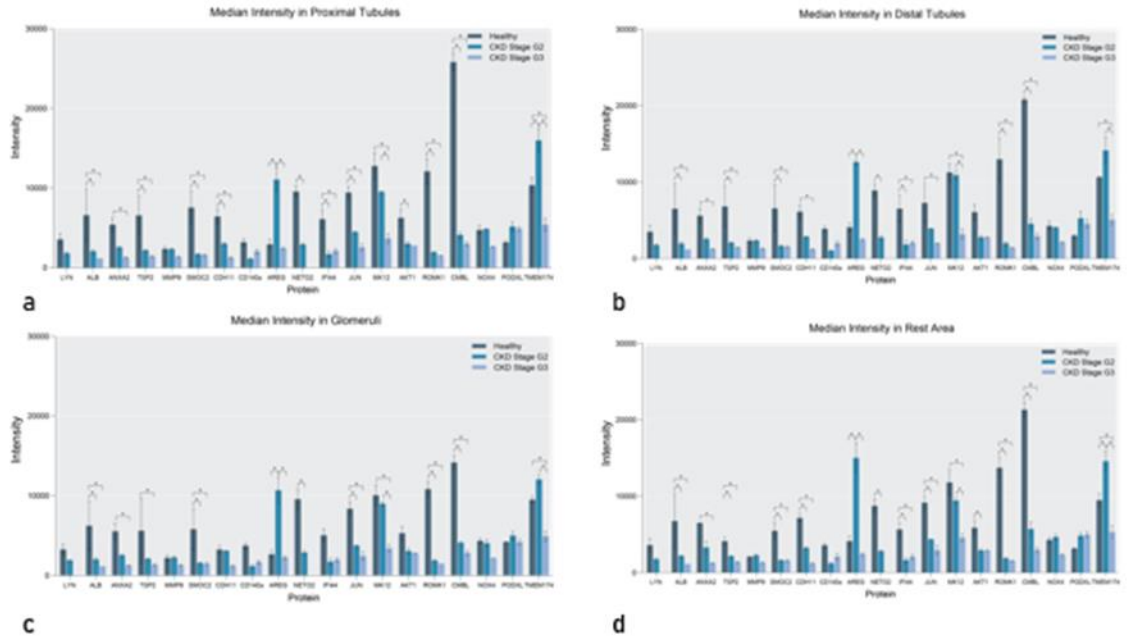

Figure 22 Evaluation of intensity differences between healthy and CKD stages G2, G2 in specific areas of the tissue. The evaluation of the statistical significance was calculated using two-way ANOVA with Tukey's multiple comparisons test and is represented with (*) in the plot.

d) Spatial distribution of every marker

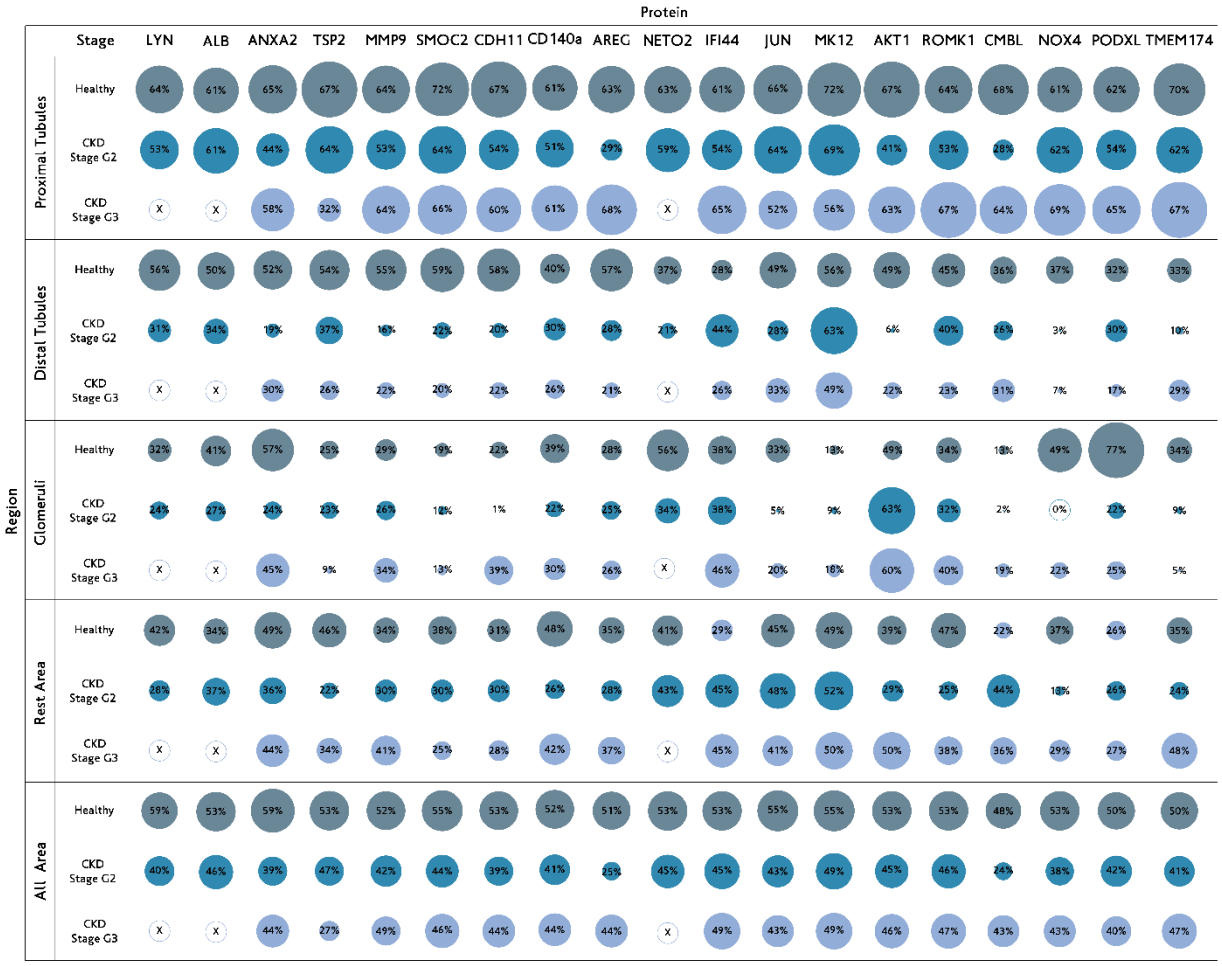

Figure 23 Spatial distribution of every marker. The percentage of cells per tissue are in which every marker was present was calculated for the healthy and CKD samples.

The spatial distribution of every marker was estimated by the percentage of cells per tissue area, in which the markers were expressed (Fig. 23).

In the healthy proximal tubules, all the markers exhibited broad spatial distribution with a presence in 60-70% of cells. In the distal tubules, the markers were expressed in a lower percentage with some of them covering around 50% of distal tubule cells such as LYN, ALB, ANXA2, TSP2, MMP9, SMOC2, CDH11, AREG, and MK12 or less. In the glomeruli, PODXL, NETO2, ANXA2, and NOX4 are expressed in more than half of the glomerular cells. The rest markers do not surpass the 40% of cells and MK12 along with CMBL display a very restricted distribution around 10% of the total glomerular cells.

Regarding the CKD proximal tubules, in stage 2, all the markers are found in fewer cells than that of healthy tissue. In stage 3, there are markers whose distribution is further decreased such as LYN, TSP2, ALB, NETO2, JUN, and MK12. The distribution of the rest of the markers is augmented comparing to that of stage 2, and it is noteworthy that the distribution of AREG, IFI44, ROMK1, NOX4, and PODXL is wider than that of the healthy proximal tubules.

In the distal tubules of CKD stage G2 samples, there is a significant increase in the distribution of MK12 and IFI44 and the rest are expressed in fewer cells. In CKD stage G3, half of them are further decreased and the rest increase but do not surpass the distribution of healthy distal tubules.

In the glomeruli, in CKD Stage G2, cells of AKT1 expression found to be above the level of healthy glomeruli cells and the rest proteins are expressed in a smaller number of cells. In Stage G3, the distribution of NET02, TMEM174, LYN, ALB, and TSP2 covers an even smaller percentage of cells than that of stage 2. The rest proteins cover a larger portion of cells, notably CDH11, IFI44, MK12, AKT1, and CMBL.

e) T-Distributed Stochastic neighbour embedded (t-SNE) Cellular Clustering

The data of protein expression in all cells of healthy and CKD samples were analyzed further by the t-SNE analysis in the R programming language. This analysis used the molecular characteristics of cells and showed that they constitute 9 clusters that are in accordance with the presence of 9 different cell types that occur in the kidney.

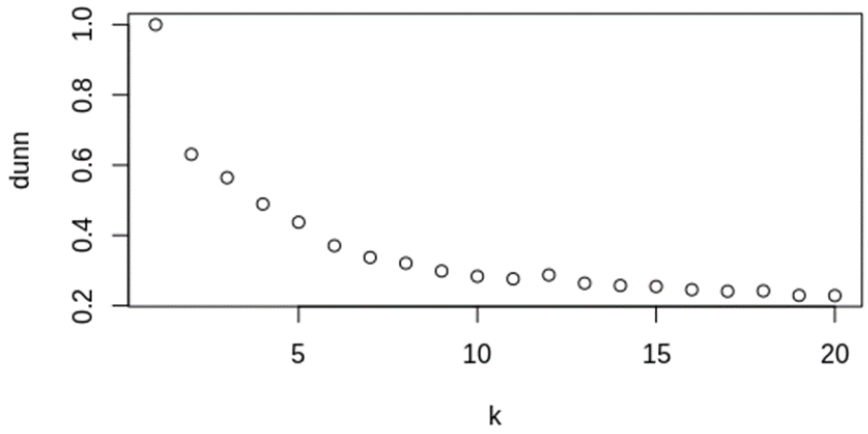

Figure 24 Elbow method για την επιλογή του βέλτιστου αριθμού ομάδων (clusters).

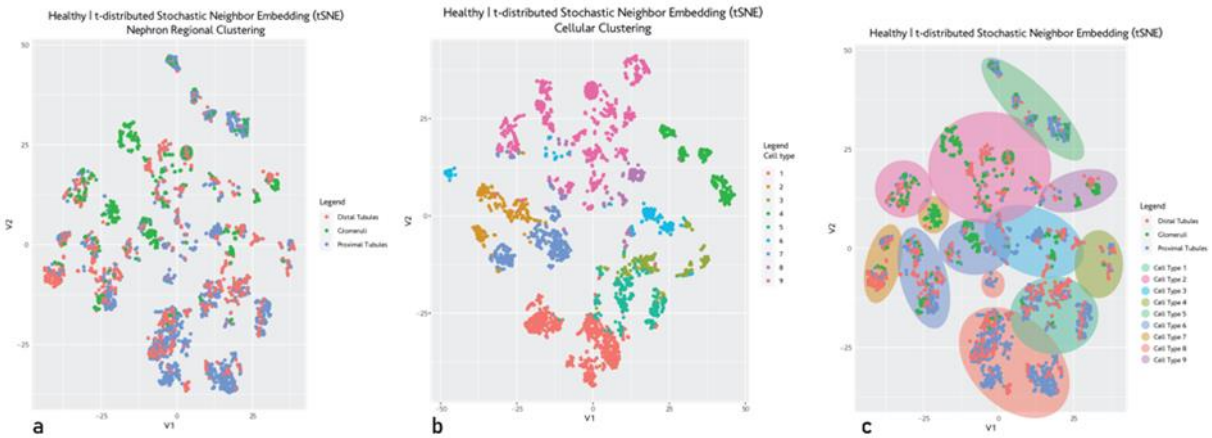

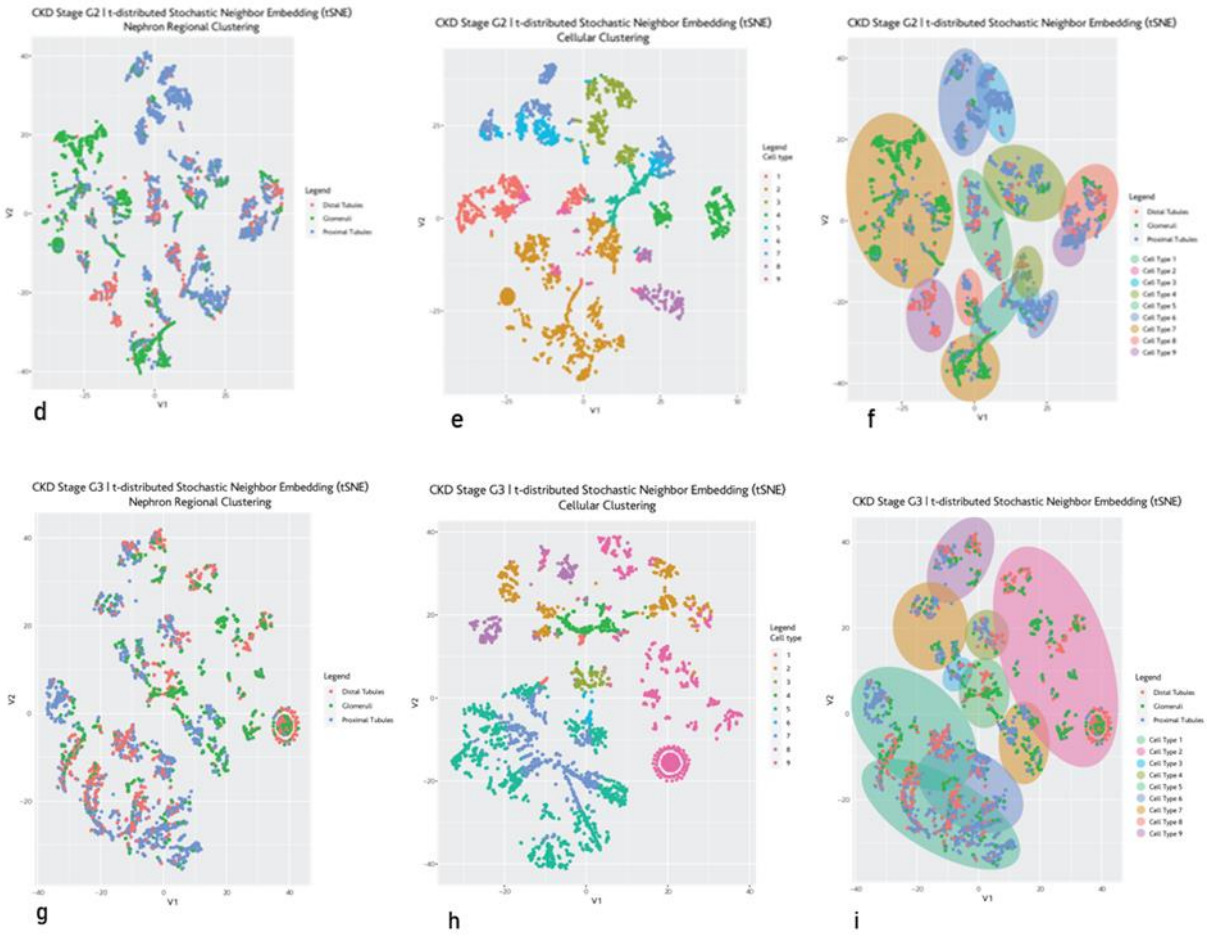

Figure 25 tSNE analysis for cellular clustering in healthy and CKD samples.

Figure 25 shows the 9 clusters, in which the cells were divided. These clusters are following the presence of e 9 different cell types present in the kidney. The colours in (Fig. 25a, d, g) indicate the tissue area in which every cell belongs to (proximal tubules, distal tubules, or glomeruli). In Fig. 25 (b, e, h) the colours indicate the different clusters. In Fig. 25 (c, f, i) the two initial clusters are combined to indicate the spatial localization and the cell types resulting from the molecular information of the cells tested.

V. Discussion

MILAN is a multiplex immunofluorescence protocol. The assay was optimized for the kidney tissue and applied to healthy and CKD FFPE tissue samples for the investigation of molecular mechanisms that contribute to the development of the disease. During the standardization process, the fact that the antibody staining occurs only due to the specific binding of primary and secondary antibodies was validated. The chemicals of the antibody diluent do not contribute to this increase and there is not irrelevant binding of the secondary antibody upon the tissue. Moreover, the assay optimization revealed that a minimum of 15 sequential rounds of staining and stripping can be applied to FFPE tissue samples with low tissue loss.

In addition, the existence of renal autofluorescence (AF) is confirmed through several studies. Natural autofluorescence is observed in the tubules, the blood vessels, the glomeruli, and other areas of the renal tissue. It is also verified that renal AF is augmented in cases of renal injuries such as cell carcinoma or ischemic pathologies. In these cases, the levels of AF have been proposed to indicate the degree of renal damage (Bellini et al., 2008, Patil et al., 2016, Schuh et al., 2016, Tirapelli et al., 2009). In this study, it was also shown that AF is higher in Chronic Kidney Disease than healthy samples. Given that, AF constitutes a major obstacle in the application of immunofluorescence protocols, though several ways have been proposed for its reduction mainly through chemicals. During assay development, it was observed that AF is lower after every stripping, so an additional stripping step was performed between the antigen retrieval and the first staining round.

The choice of proteins relied on a previous bioinformatic analysis performed in the Biomedical Systems laboratory regarding CKD. It was required, though to cover a broad range of molecules and molecular paths related to CKD, as there was no available information for the CKD patients' clinical background. The CKD tissue samples included 2 CKD stages: Stage G2 and Stage G3. Therefore, a set of 20 proteins related to CKD was tested including ALB, AREG, ANXA2, AKT1, NETO2, TMEM174, SMOC2, NOX4, LYN, TSP2, MMP9, CDH11, CD140a, JUN, PODXL, ROMK1, CMBL, IFI44, GAPDH, MK12. Afterwards, the images were computationally analyzed.

For that purpose, open-source image analysis software was used such as FIJI (Schindelin et al., 2012) and QuPath (Bankhead et al., 2017). In detail, a pipeline was written in Jython programming language in the FIJI software editor for the combination of the information acquired by the antibodies tested and the sequential analysis of numerous sets of images. Further, QuPath was used for the annotation of specific renal areas such as tubules and glomeruli, cell detection, and the cell classification according to the antibodies staining in each one of them. The results obtained by the image analysis process were statistically evaluated via ANOVA and t-SNE statistical methods. The statistical analysis revealed important information about the proteins' expression in the kidney and contributed to the investigation of their involvement in chronic kidney disease.

The intensity of the proteins tested was notably increased in the proximal tubules of healthy samples. Among them, CMBL indicated the highest intensity value followed by MK12, TMEM174, NETO2, and JUN. In the CKD G2 Stage, TMEM174 and MK12 are characterized by a high median intensity in proximal tubules, whereas in CKD Stage G3, AREG intensity is highly elevated. In the proximal tubules, the proteins ALB, SMOC2, NETO2, IFI44, JUN, ROMK1, CMBL, TSP2, CDH11, and TMEM174 showed a statistically significant difference between the healthy and both the CKD samples. The median intensity of these proteins was higher in the healthy condition except for NETO2 that was increased in CKD Stage G3 and TMEM174 that was increased in CKD Stage G2. The difference between healthy and CKD Stage 2 samples was statistically significant in the proteins LYN, TSP2, AKT1, and AREG, as well. LYN and TSP2 exhibited higher intensity in the healthy condition, whereas AKT1 and AREG were increased in the CKD Stage 2 samples. The only protein with different expression in proximal tubules between healthy and CKD samples of stage G3 is ANXA2, which was decreased in CKD samples.

Finally, AREG, MK12, TMEM174, and NETO2 are differentially expressed in this area between the two stages of CKD.

In the distal tubules of healthy tissue, MK12 had the most intense staining, while CDH11, TSP2, and ANXA2 displayed intermediate intensity values. In the distal tubules, the antibody staining is similar to that of proximal tubules. There is also a differentiated expression of CDH11, JUN, and TMEM174 between healthy and CKD Stage G3. MK12 intensity differs between the two CKD Stages, and the AKT1 difference is non-significant between healthy and CKD Stage G2 samples.

In the healthy glomeruli, ANXA2 and PODXL had the most intense and characteristic staining. On the other hand, in the CKD samples, the antibodies' intensity was significantly decreased. Also, AKT1 had increased intensity in the glomeruli of CKD stage G2 and JUN in the glomeruli of CKD stage 3 samples. In the glomeruli, a significant difference was noticed in the proteins: ALB, SMOC2, NETO2, JUN, ROMK1, and CMBL between the healthy and CKD stages. AREG is the only protein differentiated between healthy and CKD stage G2 samples. ANXA2, MK12, and TSP2 are differentiated between healthy and CKD stage 3. Finally, AREG, NETO2, MK12, and TMEM174 are differentially expressed between the two stages of CKD.

The spatial distribution of every marker, as estimated by the percentage of cells per area expressing the protein, enriched the expression profile of each one of them in the healthy and CKD state. In the healthy proximal tubules, all the markers exhibited broad spatial distribution with a presence in 60-70% of cells, whereas in the distal tubules, their expression was observed in a lower percentage with some of them covering around 50% of distal tubule cells such as LYN, ALB, ANXA2, TSP2, MMP9, SMOC2, CDH11, AREG, and MK12. In the glomeruli, PODXL, NETO2, ANXA2, and NOX4 are expressed in more than half of the glomerular cells.

Regarding the CKD proximal tubules, in stage 2, all the markers are found in fewer cells than that of healthy tissue. In stage 3, there are markers whose distribution is further decreased such as LYN, TSP2, ALB, NETO2, JUN, and MK12. The distribution of the rest markers is augmented comparing to that of stage 2 and it is noteworthy that the distribution of AREG, IFI44, ROMK1, NOX4, and PODXL is wider than that of the healthy proximal tubules.

In the distal tubules of CKD stage G2 samples, there is a significant increase in the distribution of MK12 and IFI44 and the rest are expressed in fewer cells. In CKD stage G3, half of them are further decreased and the rest increase but do not surpass the distribution of healthy distal tubules.

In the glomeruli, in CKD Stage G2, cells of AKT1 expression found to be above the level of healthy glomeruli cells and the rest of the proteins are expressed in a smaller number of cells. In Stage G3, the distribution of NETO2, TMEM174, LYN, ALB, and TSP2 covers an even smaller percentage of cells than that of stage 2. The remaining proteins cover a larger portion of cells, notably the proteins CDH11, IFI44, MK12, AKT1, and CMBL.

The protein expression profiles were further processed by the tSNE algorithm which divided them into 9 clusters. These clusters coincide with the 9 different types of cells that occur in the kidney. As a result, the molecular profile of this 20-protein-set of the cells can distinguish the different renal cell types. With the appropriate marker-based labelling of these clusters, this process can be used for the cell-type classification of the markers to proceed to the next level of single-cell analysis.

Albumin (ALB)

Albumin (ALB) is a predominant plasma protein, synthesized in the liver and distributed in all tissues by the vascular system (Gatta et al., 2012). Its role is important in the maintenance of homeostasis and the pressure within vessels (Nicholson et al., 2000). Within serum, albumin binds to hormones, ions, and drugs showing anti-inflammation and antioxidant properties (Arques and Ambrosi, 2011, Fanali et al., 2012).

The reduced levels of albumin in the organism, called hypoalbuminemia can occur due to many causes including inadequate energy or protein intake, impaired liver synthesis, decreased intestinal absorption, increased tissue catabolism, and is frequently found in CKD and DN patients (Franch-Arcas, 2001, Menon et al., 2003, Navarro et al., 2003, Stuveling et al., 2003). Moreover, several bioinformatic analysis revealed that ALB is a downregulated gene in several CKD pathologies, including tubulointerstitial fibrosis and pathologies of diseased glomeruli (Tajti et al., 2020, Wang et al., 2020, L.-T. Zhou et al., 2018). Regarding the typical symptoms of CKD, the albumin level is negatively correlated with proteinuria, cholesterol, and histopathological damage, including glomerular lesions, interstitial inflammation, and arteriolar hyalinosis. On the other hand, serum ALB levels are positively correlated with renal function and haemoglobin (Zhang et al., 2019).

ALB low levels during inflammation have been associated with the effect of IL-1, IL-6, and TNF-α on the hepatic synthesis (Moshage et al., 1987). In normal concentration, ALB inhibits TNF-a-induced expression of vascular cell adhesion molecule-1 (VCAM-1) to attenuate the inflammation (Zhang and Frei, 2002). On the other hand, oxidized ALB molecules appear to be important in the oxidative stress acceleration, inflammation, and neutrophil-mediated endothelial injury (Magzal et al., 2017, Michelis et al., 2013, 2010). So, hypoalbuminemia showing a chronic inflammatory state may accelerate the process of kidney malfunction by inducing oxidative stress and endothelial inflammatory injury (Kim et al., 1999, Wada and Makino, 2016).

Moreover, hypoalbuminemia influences lipid metabolism and evokes dyslipidemia resulting in an additional kidney injury induced by the lipids. Finally, the patients with hypoalbuminemia are also prone to anaemia, which might result in anaemia-induced hypoxia that accelerates kidney injury (He et al., 2015). Low levels of serum albumin might help in DN prognosis, as patients with lower levels of serum albumin seem prone to progress to ESRD.

In this analysis, ALB was expressed mostly in the proximal tubules and slightly in the glomeruli of the kidney. In CKD, its general expression is remarkably reduced in parallel with the CKD progression. The relative intensity was also gradually reduced from the healthy condition to CKD following the progression of the disease. The deviation between the healthy and both CKD stages was estimated as statistically significant. The spatial distribution followed the same gradually decreasing trend in the distal tubules and the glomeruli, whereas in the proximal tubules, the cellular expression was maintained up to the early CKD (Stage G2) and it abruptly dropped in the advanced CKD stage 3. In addition, in the cells of the rest area, the ALB expression was unexpectedly observed in more cells of the CKD stage 2 than the healthy cells and then it dropped again in the CKD Stage 3. Taking into consideration the general expression pattern of ALB, it is accepted that these findings coincide with the previous findings of the ALB downregulation during CKD.

Annexin A2 (ANXA2)

Annexin A2 (AnxA2) is a multifunctional protein that binds to phospholipids mainly regulated by the Ca^{2+} concentration. It participates in cell adhesion and transport across ion channels that constitute fundamental properties of a normal kidney (Alvares et al., 2013, Gassié et al., 2015, Markoff and Gerke, 2005, Xu et al., 2015). AnxA2 can also act as a heterotetramer. The heterotetramer interacts with the cytoskeleton, the membrane, and the extracellularmatrix (ECM) regulating various biological processes such as tissue remodelling, ECM degradation, angiogenesis, actin cytoskeletal dynamics, endocytosis, exocytosis, cell-cell adhesion and cell polarity (Hitchcock et al., 2014, Xu et al., 2015). Wang et al., (2020), performed a weighted gene correlation network analysis regarding the CKD tubulointerstitial fibrosis and found that AnxA2 is one of the upregulated genes and negatively correlated with the eGFR measurement and the CKD Stage.

Regarding the kidney, AnxA2 is expressed mainly in the ureteric bud and its derivatives, such as the collecting tubules and is rarely present in the proximal convoluted tubules of the

normal adult kidney. It is also expressed in the endothelial cells of arterioles and blood capillaries and the mesangial cells, podocytes and parietal cells of glomeruli. AnxA2 has specific roles in the kidney. In the collecting duct, it mediates cAMP-induced trafficking of aquaporin 2. Also, it participates in the Na+–K+–2Cl–recruitment and activation of NKCC2 cotransporter, which is responsible for the urine concentration and the systemic salt homeostasis in the thick ascending limb of Henle's loop (Dathe et al., 2014).

Interestingly, AnxA2 expression was observed in renal tubules and the glomeruli. In the CKD condition, its expression was downregulated in all renal areas mostly in CKD stage 2 and then it seems to increase in CKD stage 3. Its relative intensity was reduced accordingly to the CKD progression but only the difference between the healthy and CKD stage 3 was found of statistical significance. The AnxA2 areal distribution revealed that besides the increased intensity levels, AnxA2 is expressed in fewer cells of the proximal/distal tubules in the onset of CKD and then it increases its expression levels approaching the spatial distribution of the healthy condition. It is noteworthy though that the early decrease in the distal tubules is interestingly steep and the re-increase hardly approaches the half distribution of the healthy condition. The importance of this observation contradicts the literature data about its main presence in the collecting tubules and its specific role in these structures. The general pattern of AnxA2, revealed in this analysis, could coincide with the upregulation of AnxA2 in CKD, as there is an increasing direction in CKD stages. Future research in gradually advanced CKD samples could enlighten this observation.

Secreted modular calcium-binding protein 2 (SMOC2)

Secreted modular calcium-binding protein 2 (SMOC2) is a member of the secreted protein acidic and rich in cysteine (SPARC) family of matricellular proteins. SPARC family proteins are secreted into the extracellular space to regulate cell-matrix interactions and cell function by interaction with structural matrix proteins and cell surface receptors, growth factors, proteases, and other bioactive effectors (Wong and Rustgi, 2013). SPARC protein has been associated with various types including kidney fibrosis through binding to collagen and mediating its gathering into aggregates (Bradshaw et al., 2009, McCurdy et al., 2010, Sasaki et al., 1998). SMOC2 has low expression in normal kidneys, mainly in the tubules and the glomeruli except for the glomeruli basement membrane, but it is highly overexpressed in the injured kidneys participating in the fibrotic process (Craciun et al., 2016, Maier et al., 2008). SMOC2 activates matrix assembly signalling in the fibroblasts for their transition into myofibroblasts (Fibroblast-to-myofibroblast transition- FMT), such as stimulation of stress fibre formation, proliferation, migration, and ECM production. Myofibroblasts regulate the production of collagen and fibronectin, so FMT is a crucial event in the development of renal fibrosis.

Herein, SMOC2 was found to be expressed in all tissue areas with higher distribution in the renal tubules and weaker expression in the glomeruli. In the CKD samples, SMOC2 expression was reduced. The relative intensity is significantly reduced from the healthy to CKD but then it maintains at the same levels along with the CKD progression. SMOC2 is expressed in a smaller number of cells in CKD Stage 2 compared to the healthy condition with a severe decrease in the distal tubules. There is no significant change in its spatial distribution from CKD stage 2 to CKD stage 3. These findings are opposed to the expected upregulation of SMOC2 in CKD, but it can be explained by the CKD stages examined. SMOC2 plays a crucial role in the fibrotic process that has not been developed in stages G2, G3 but appears in more advanced CKD stages close to ESRD.

SMOC2 is activated by the TGFβ pathway, a major pathway in fibroblast-myofibroblast transition (FMT) inducement and the mechanism is different from that of its cognate SPARC protein, as SMOC2 does not have a collagen-binding site but it possibly mediates intercellular signalling and cell type-specific differentiation (Pazin and Albrecht, 2009). Firstly, it stimulates migration and adhesion of keratinocytes through integrin (αvβ1 and αvβ6) interaction (Maier et

al., 2008). Also, SMOC2 regulates the VEGF and FGF-induced mitogenesis and angiogenesis on endothelial cells (Rocnik et al., 2006), as well as cell cycle progression via integrin-linked kinase activity and cyclin D1 expression of fibroblasts (Liu et al., 2008).

Finally, SMOC2 activates FAK-P, MLC-P, and Pax-P pathway through which matricellular proteins are implicated in regulating integrin αβ heterodimers to promote changes in ECM signals into the fibroblast to form myofibroblasts (Bornstein and Sage, 2002, Grinnell, 2003, Mitra et al., 2005, Tomasek et al., 2002). Integrin acts as an upstream activator of SMOC2, as well (Gerarduzzi et al., 2017).

Neuropilin And Tolloid Like 2 (NETO2)

NETO2 is a transmembrane protein that belongs to a unique subfamily of CUB- and LDL-containing proteins. NETO2 isoform 1 is highly expressed in renal cell carcinoma regulated by the SAP30 transcription factor (Snezhkina et al., 2018). NETO2 specific function is unknown but it is highly expressed in the nerve tissue and participates in the formation of regulatory complexes with KARs and NMDA receptors (Michishita et al., 2003, Oparina et al., 2012, Stöhr et al., 2002). NMDA (N-methyl-d-aspartate acid) and kainate (KA) receptors constitute ionotropic glutamate-gated receptors (GLuRs) (Hansen et al., 2018, Hollmann et al., 1989, Mayer, 2017, Monaghan et al., 1989, Vyklicky et al., 2014).

The N-methyl-d-aspartate receptor (NMDAR) is a non-selective cation channel and its activation followed by an influx of calcium ions, stimulates numerous calcium-mediated intracellular cascades affecting many physiological processes of the organism (Blanke and VanDongen, 2009, Haddad, 2005). NMDAR is widely expressed all over the kidney (Anderson et al., 2010, Bozic et al., 2011, Deng et al., 2002, Leung et al., 2002, Parisi et al., 2010). Its role is important in renal hemodynamics and glomerular filtration when expressed in normal levels. However, an increased activation affects negatively its downstream signalling pathways with numerous pathophysiological changes. In CKD, NMDARs participate in renal fibrosis, Secondary Hyperparathyroidism, Acute Kidney Injury, Glomerular Disorders, Nephrotoxic Renal Failure (Valdivielso et al., 2020).

Zhou et al., (2018) found that NETO2 is an upregulated gene in the diseased glomeruli and Tajti et al., (2020) found that it is a differentially expressed gene across numerous CKD pathological conditions.

NETO2 expression was observed in the proximal tubules of a healthy kidney. It was also observed in the glomeruli but at a lower level. In the CKD samples, NETO2 expression was reduced in the whole area. NETO2 relative intensity was decreased in CKD stage 2 and the difference is statistically significant. This pattern coincides with its distribution in the different renal areas. In the tubules and the glomeruli, it is expressed on fewer cells in CKD stage 2 than the healthy condition. NETO2 is expected to be downregulated in renal injuries, as it participates in the general maintenance of kidney function and the results support this approach.

Mitogen-Activated Protein Kinase 12 (MAPK12/p38γ)

P38γ is an isoform of p38 protein of the p38 MAPK family of kinases, encoded by the MAPK12 gene (Grossi et al., 2014). P38 family proteins are upstream activators that regulate several cellular processes such as apoptosis, inflammation, proliferation differentiation, and are activated by cytokines, cell death receptors, mitogens. They are also activated by many stressors: oxidative stress, hypoxia, thermal shock, and ultraviolet radiation, and this is the reason why they are also known as stress-activated protein kinases (SAPK) (Sabio and Davis, 2014, Yamazaki et al., 2018). P38γ is expressed in specific tissues with the highest expression in the skeletal muscles (Barros et al., 2019, Escós et al., 2016, Lee and Kim, 2017).

P38γ regulates cardiomyocyte formation and promotes cardiac hypertrophy through the mTOR pathway (González-Terán et al., 2016, Ramachandra et al., 2016). It also participates in cell migration, metalloproteinase-2 secretion, cell proliferation through K-Ras-transformed fibroblasts (Cerezo-Guisado et al., 2011). Its role is crucial in the inflammatory response, as well, as it regulates the production cytokines and chemokines in different cells including IL-1β, IL-10, TNFα, IL-6 and CXCL1 (González-Terán et al., 2016, Risco et al., 2012, Zur et al., 2015). It also controls T-cell activation for the interferon (IFN) and IL-17 production (Criado et al., 2014).

In CKD, there is evidence that p38γ is induced by TGFβ1 in the autophagy process along with the activation of the TAB1/TAK1 (TGFB-activated kinase 1/MAP3K7 binding protein 1)-MAP2K3/MKK3 (mitogen-activated protein kinase kinase 3)-MAPK11/p38β-MAPK12/p38γ-MAPK13/p38δ-MAPK14/p38α signalling (Kim et al., 2012, Livingston et al., 2016).

MK12 was found mainly expressed in the renal tubules, whereas it exhibited a scarce expression in the glomerular cells. In CKD, its tubular expression dropped according to the severeness of each CKD stage and the glomerular expression increased. The relative intensity was reduced gradually across the CKD stages. MK12 was slightly reduced in the proximal tubular cells in parallel with CKD progression. In the distal tubules, MK12 indicated an increased distribution in the early CKD and then it dropped. The opposite was observed in the glomerular cells, in which its expression is very restricted. This variety in MK12 expression is reasonable, as it is an upstream activator that regulates numerous different cellular processes and its role in CKD has to be further investigated.

Potassium Inwardly Rectifying Channel Subfamily J Member 1 (KCNJ1/ROMK1)

KCNJ1 (Potassium Inwardly Rectifying Channel Subfamily J Member 1 or ROMK1) is an integral membrane protein and inward-rectifier type potassium channel. In the kidney, ROMK channels are located on the apical membrane of the distal tubules and play an important role in the maintenance of K^+ homeostasis. Their abundance changes according to the dietary intake by endocytosis and degradation of the channel protein (Lazrak et al., 2006). Its role is important in potassium recycling in the thick ascending limb of Henle's loop and potassium secretion in the collecting duct. ROMK1 activity is regulated by the lectin activity of the aKlotho protein (Kuro-O, 2019).

ROMK1 was expressed in all renal areas. In the healthy tissue, it exhibits intense staining in the distal tubules, whereas in the proximal it is widely diffused with intermediate intensity levels. Also, it is scarcely expressed in the glomeruli. In the CKD stage 2, the pattern of expression changes, showing characteristically intense staining in the apical membrane of tubules. In CKD stage 3, there is weak staining in the tubules and increased staining in the glomeruli.

Its relative intensity has been found significantly higher in the healthy tissue compared to the CKD stages. However, in its spatial distribution, this intense decrease is mirrored only to the distal tubules. In the other renal areas, ROMK1 is expressed in a smaller range of cells in the early stage of CKD, and then in the most severe CKD stage 3, it is spread in a larger number of cells reaching levels above the healthy distribution. The difference of ROMK1 expression observed between the distal tubules and the other renal areas is connected to its main role in the distal tubules for the maintenance of K^+ homeostasis.

Carboxymethylenebutenolidase (CMBL)

Carboxymethylenebutenolidase (CMBL) is a cysteine hydrolase of the dienelactone hydrolase family that has high cytosolic expression in several tissues such as the liver, intestine, and kidney. CMBL has been characterized as the bioactivating enzyme that hydrolyzes the ester bond of the many prodrugs such as Olmesartan medoxomil (OM), faropenem medoxomil, and lenampicillin and converts to their pharmacologically active metabolitein human liver and

intestine via an active Cys^{132} residue (Ishizuka et al., 2010). It is possible though that ALB and other plasma esterases contribute to this process, as well (Laeis et al., 2001, Ma et al., 2005). In particular, OM is a prodrug type angiotensin II type 1 receptor antagonist widely prescribed as an antihypertensive agent (Redon and Fabia, 2009, Scott and McCormack, 2008). The role of CMBL in CKD has not been investigated, yet.

CMBL was found expressed mainly in the healthy proximal tubules of the kidney. Weak expression was observed in the rest renal area as well. In CKD, the glomerular expression appeared increased whereas the tubular expression was importantly decreased in parallel with the CKD progression. The difference between the healthy and the CKD conditions was evaluated as statistically significant. However, the spatial distribution does not coincide with the changes in the relative intensity. CMBL distribution is restricted to a smaller number of cells in the CKD stage 2 and then it increases approaching the levels of the healthy distribution. Finally, in the rest area, the pattern of distribution follows the opposite direction with an increase in the CKD stage 2 and a decrease in the advanced CKD stage 3.

Trans-membrane 174 (TMEM174)

TMEM174 (Trans-membrane 174) is a kidney-specific protein located in the endoplasmic reticulum. It may act as an ion channel of the ER due to its similarities with other ion channel proteins such as the mitochondrial magnesium ion channel MSR2 (Goytain and Quamme, 2008, Zsurka et al., 2001).

TMEM174 participates in the renal cell proliferation process through the MAPK/ERK-AP1-cJUN activity. The possible mechanism involves the increased activity of ERK kinases by TMEM174 overexpression. ERKs phosphorylate ELK1, which is an important TCF component and further promotes cfos induction through binding to the SRE site in the promoter of c-fos. The increased c-Fos binds to endogenous c-Jun to form a dimer complex. The increased AP-1 (activator protein 1) further promotes the transcription of genes involved in cell proliferation, such as cyclin D1 (Wang et al., 2010).

The expression profile of TMEM174 in the healthy kidney indicated enhanced expression in the proximal tubules and weaker but observable expression in the distal tubules and the glomeruli. In CKD stage 2, there is a concentrated expression in the apical membrane of tubules and lower expression in the glomerular cells. In advanced CKD, the expression drops in low levels in the whole renal area.

The intensity alterations agree with the expression pattern described above. There is a significant difference between the healthy and both CKD samples and between the two CKD stages in the proximal tubules. On the other hand, the intensity variation in the glomeruli and distal tubules has been evaluated as statistically significant only between the healthy and CKD stage 3 and between the two CKD stages. TMEM174 spatial distribution indicates the same trend in the renal tubules between the healthy and CKD stage 2, whereas in CKD stage 3 the expression is observed in a larger number of cells with lower median intensity. In the glomeruli, the number of cells with TMEM174 expression is gradually reduced in parallel with CKD progression, which is following the expression pattern and the intensity differences. The general pattern of TMEM174 expression and distribution is reasonable given that in the injured kidney there is an imbalance in ions concentration and a hindered cell proliferation.

Interferon-inducible protein 44 (IFI44 or p44)

IFI44 (interferon-inducible protein 44 or p44) is a member of the type I interferon-inducible gene family. It plays a negative role in cell proliferation via its upstream PDGFR-b activator and promotes cell apoptosis. It is also involved in the autoimmune response and participates in the process of microtubule formation (Buhl et al., 2020, Hallen et al., 2007, Hu et al., 2017). In CKD

and mainly in the AKI, IFI44 has been observed activated in the proximal, distal, and collecting tubules participating in the inflammatory process (Rudman-Melnick et al., 2019). Zhou et al., (2018) found that IFI44 is an upregulated gene in the diseased glomeruli, whereas Wang et al., (2020), found its upregulation in the tubulointerstitial fibrosis, as well.

In the healthy tissue, IFI44 was mostly expressed in the proximal tubules. The expression in the distal tubules and the glomeruli was observable but at low levels. In the CKD stage 2 tissue, the expression was remarkably reduced in the tubules and unaltered in the glomeruli, whereas in CKD stage 3, IFI44 expression was increased in the tubules and slightly decreased in the glomerular space.

The intensity values represent the same pattern and the deviation between the healthy and CKD stages is statistically significant in the whole area except for the glomeruli. In addition, the intensity levels of CKD stage 3 is greater than stage 2 but do not surpass the healthy levels. Regarding the spatial distribution of IFI44 in the different renal areas in the proximal tubules and the glomeruli, there is a restriction in CKD stage 2 and an increase in the progressed CKD. The opposite trends are observed in the distal tubules. These results agree with the upregulation of IFI44 in kidney injuries and its role in cell apoptosis and inflammation.

Amphiregulin (AREG)

AREG (amphiregulin) is a low-affinity EGFR ligand that is highly overexpressed in CKD. AREG has a crucial role in kidney fibrosis as integrates signals by other EGFR ligands to maintain the EGFR sustained activation that is considered a fundamental effector of fibrosis (Kefaloyianni et al., 2016, Overstreet et al., 2017, Tang et al., 2016). AREG is regulated by the YAP1 (yes associated protein 1) that augments the AREG transcripts when the Hippo pathway is inactive and the ADAM17 enzyme that releases its soluble form (Kefaloyianni et al., 2019, 2016, Meng et al., 2016, Zhang et al., 2009). The interaction between AREG-YAP1 is a positive feedback loop, indicating that AREG acts as an amplifier of its action. Moreover, AREG induce the production of profibrotic and proinflammatory cytokines including MCP1, MIP1a, RANTES, and TGFa, which mediate the macrophage accumulation that further contributes to renal fibrosis (Cao et al., 2015, Zaiss et al., 2015). Finally, AREG triggers the Th2 and ILC2 type 2 immunity cells that have been associated with the progression of fibrosis (Kefaloyianni et al., 2019). In a bioinformatic analysis, performed by Tajti et al., (2020), AREG is found differentially expressed across numerous CKD pathological conditions.

AREG was scarcely expressed in the renal tubules and glomeruli of the healthy tissue. However, there is an observable reduction in the CKD samples. This deviation of its relative intensity was estimated significant between the healthy and CKD stage 2 and between the CKD stages. Besides its relative intensity was higher in CKD stage 2 and AREG was expressed in a smaller number of cells in this condition. A higher reduction was noticed in the distal tubules across the CKD stages, whereas in the glomeruli its expression remained low and steady. AREG plays a crucial role in the development of fibrosis. Therefore its vast upregulation is expected in more advanced CKD stages.

Thrombospondin 2 (TSP2)

TSP2 (thrombospondin 2) is a protein produced by fibroblasts and smooth muscle cells that regulates the ECM organization by modulating the activity of growth factors in the pericellular environment and by favouring matricellular angiogenesis (Bornstein et al., 2000). TSP2 is regulated by many cytokines, receptors, and proteases. In the normal kidney, TSP2 has low expression but its expression increases in renal injury (Hugo, 2003). In CKD, TSP2 regulates matrix remodelling along with other matrix molecules and increases thrombogenesis (Daniel

et al., 2007, Hugo and Daniel, 2009). It also inhibits inflammation and TGF-b activation (Ponticelli and Anders, 2017).

The expression of TSP2 in the healthy kidney was higher in the proximal tubules and low in the glomeruli. During the progression of CKD, TSP2 expression was significantly reduced. The same pattern occurs in TSP2 spatial distribution in the different renal areas. Regarding its relative intensity variation, it was found statistically significant between the healthy and both CKD stages in all areas apart from glomeruli in which it is significant only between the healthy and advanced CKD. The role of TSP2 in the kidney is considered protective and in cases of renal damage is expected to be reduced.

Cadherin 11 (CDH11)

CDH11 (cadherin 11) is a transmembrane glycoprotein that mediates cell-cell adherens junctions. In CKD, CDH11 participates in profibrotic intracellular signalling pathways. It mediates the fibroblasts migration and myofibroblasts formation and differentiation through the action of Rho GTPases and TGF-b activation (Nagatoya et al., 2002, Schneider et al., 2012, Xiao et al., 2008).

CDH11 expression in the normal kidney appeared with an intermediate expression in the tubules and low expression in the glomeruli. As CKD progresses, the tubular expression was initially reduced and then increased, and in the glomeruli, CDH11 expression was increased according to the CKD stage. The intensity values were higher in the healthy condition and the difference from the CKD samples were found statistically significant. In the glomeruli, there was a slight reduction but it was not significant. The spatial distribution followed the expression pattern with a steep decrease in the distal tubules.

JUN proto-oncogene (JUN)

JUN is a subunit of the AP-1 (activator protein-1). In CKD, AP-1 upregulates TGFB1 to promote gradual kidney dysfunction. In the nucleus, AP1 specifically binds to the promoter of *TGFB1* and recruits histone acetyltransferase and CtBP2 to form a complex. This complex activates the expression of *TGFB1* and promotes the production of mature TGF-β. The mature TGF-β is secreted to the extracellular space to initiate TGF-β signalling and phosphorylation of Smad2 and Smad3 (Zhou et al., 2020). c-Jun along with TGFB1 also participates in the fibrotic process (Hewitson et al., 2017, Wernig et al., 2017, Williams et al., 2020). Wang et al., (2020) and Zhou et al., (2018) found that JUN constitutes a downregulated hub gene in the tubulointerstitial fibrosis and is strongly negatively correlated with the eGFR levels.

JUN was highly expressed in the healthy renal tubules and scarcely in the glomeruli. During CKD progression, JUN expression was reduced in all renal areas. There was a significant intensity difference between the healthy and both CKD stages in all areas except for the distal tubules, in which the difference was considered significant only between the healthy and the advanced CKD. In its spatial distribution, a continuous drop is noticed in the early CKD, which is reversed in the distal tubules and the glomeruli. JUN is expected to be downregulated in cases of renal dysfunction. Its high drop in the distal tubules and the gradual reduction in the proximal may be indicative of this downregulation in CKD.

AKT Serine/Threonine Kinase 1 (AKT1)

AKT1 is widely expressed in most tissues and has been implicated in cell growth and survival. Regarding CKD, AKT1 participates in the CVD-related-CKD. In CVD-CKD, AKT1 levels decrease and FoxO is activated to cause increased insulin resistance and mediate ischemia-reperfusion

injury (Rota Marcello et al., 2005, Sindhu et al., 2004, Wang et al., 2019). Also, AKT1 regulates the Nrf2 and HMOX1 expression levels in the hypoxia-reoxygenation process in the renal epithelial cells (Potteti et al., 2016). Moreover, AKT1 regulates the expression of the ROMK potassium channel and influences the potassium homeostasis and secretion in the collecting duct. This regulation occurs via the PI3K-activating ligands like insulin or IGF-1 (Cheng and Huang, 2011, Satoh et al., 2015). Another role of AKT1 in CKD constitutes its coactivation with the P110θ to induce RUNX1 (runt-related transcription factor 1) expression in the renal tubules, contributing to the renal fibrosis (Galichon, 2018, T. Zhou et al., 2018). Finally, PAR2 inhibits autophagy via the PI3K/Akt/mTOR signalling pathway resulting in impairment of the inflammation in the tubular epithelial cells (Du et al., 2017).

In the normal kidney, AKT1 was observed in the whole tissue area, with higher expression in the tubules. In CKD, its expression was increased in the glomeruli and decreased in the tubules. The results of its cellular distribution in these areas showed the same tendency with a small shift in the tubules of advanced CKD. However, the difference in its relative intensity was found statistically significant only in the proximal tubules between the healthy and CKD stage 2 conditions. The role of AKT1 in CKD is considered protective as it contributes to cell growth and survival but it requires further research as it may regulate other cellular processes via the Akt signalling pathway.

Matrix metallopeptidase 9 (MMP9)

MMP9 (matrix metallopeptidase 9) is a member of the MMPs family, which participates in many cellular processes, including inflammation, epithelial-mesenchymal transition, cell proliferation, angiogenesis, and apoptosis. In the kidney, MMP9 is produced from mesangial, glomerular, epithelial, and endothelial cells, fibroblasts, and macrophages (Tan and Liu, 2012). In the normal condition, there is low MMP-9 expression in the kidney, whereas, in various pathological states of CKD, MMP-9 expression is importantly increased (Urushihara et al., 2002). MMP9 is important in the ECM transition as it process collagen, elastin, fibronectin, and other ECM substrates. Consequently, MMP9 participates in the fibrotic process, as well (Ntrinias et al., 2019). Its upregulation in the tubulointerstitial fibrosis was also shown by a bioinformatics analysis by Wang et al., (2020), which indicated its strong negative correlation with the eGFR levels.

In this analysis, MMP9 showed very low expression in the healthy renal tissue, with a small increase in the glomerular space during CKD. The intensity discrepancy between the different conditions was not statistically significant. In all areas, its diffusion in the space was restricted in the early stage of CKD and it was increased later in advanced CKD stage 3. In general, MMP9 is expected to be upregulated during CKD and mostly when the fibrotic process has started in the tissue. So, it is reasonable the statistical difference not to be significant between the healthy and early CKD stages.

NADPH oxidase 4 (NOX4)

NOX4 (NADPH oxidase 4) is an NADPH oxidase that catalyzes the formation of H202 (Takac et al., 2011). In the normal kidney, NOX4 is widely expressed. In the proximal tubules, NOX4 is expressed in the basolateral side of the proximal tubules and the cytoplasm, whereas its expression in the distal tubules is lower. In glomeruli, NOX4 is only expressed in the parietal epithelial cells. There is not NOX4 expression in the podocytes, the endothelial and mesangial cells. NOX4 is also found in the endothelial cells of middle size arteries but not at all in the peritubular capillaries.

In CKD, NOX4 expression decreases in the renal tubules in parallel with TGFb1, NOX2, and GSTA1. Therefore, its role is protective indicating an anti-apoptotic effect mediated by the NRF2,

BCL-2 and elF2 stress signalling pathways and loss of tubular cell differentiation (Babelova et al., 2012, Khodo et al., 2012, Nlandu-Khodo et al., 2016, Santos et al., 2016). It seems that represents a defence in oxidative stress during a renal injury. Besides, NOX4 expression increases in the glomeruli during CKD and shows up in the podocytes and mesangial cells. This increase promotes podocyte apoptosis and mesangial cell proliferation. It may enhance ROS formation and activate the profibrotic pathways for ECM deposition or decrease apoptosis and promote mesangial cell proliferation (Rajaram et al., 2019).

In this analysis, NOX4 expression was similar to the expression profile of Rajaram et al., (2019). In the normal kidney, it was expressed in the whole area, while in CKD its expression was significantly reduced in the tubules and increased in the glomerular cells. The difference between the intensity values of healthy and CKD samples was not found of statistical significance. However, the spatial distribution revealed a severe decrease in the distal tubules, whereas in the proximal there was an almost even distribution. In the glomeruli, though the initial decrease in the early CKD stage, changed while the disease progressed. These findings agree with the role of NOX4 in CKD. In the glomeruli, NOX4 is expected upregulated due to the late expression in podocytes and mesangial cells. Finally, NOX4 seems to protect tubular cells against apoptosis and verifies the downregulation observed in these results.

Podocalyxin (PODXL)

PODXL (Podocalyxin) belongs to the CD34 family of stem cell sialomucins and constitutes a single-pass transmembrane protein. In the kidney, PODXL is expressed exclusively on the surface of podocytes and vascular endothelial cells and regulates the morphogenesis and differentiation of podocytes (Debruin et al., 2014). It contributes to the disintegration of the adherens junctions to form the microvilli, the foot processes, and slit diaphragms. Therefore, it plays a crucial role in the glomerular filtration process (Doyonnas et al., 2001, Freedman et al., 2015, Freedman and Steinman, 2015, Kim et al., 2017).

PODXL mutations drive kidney disease (Barua et al., 2014, Kang et al., 2017, Lin et al., 2019, Refaeli et al., 2019). Homozygous mutations evoke congenital anuria and progressive disease (Doyonnas et al., 2001, Kang et al., 2017). On the other hand, heterozygous mutations have been linked with the development of proteinuria over a longer period (Lin et al., 2019). PODXL is necessary to immature podocytes, as it regulates the formation of the filtration slits. In mature podocytes, the role of PODXL is similarly indispensable in the maintenance of foot processes architecture, the localization of foot process and slit diaphragm proteins to the right membrane domains, and the structural integrity required for the ultrafiltration (Refaeli et al., 2020).

PODXL was observed mainly in the glomerular cells and indicated a weak expression in the renal tubules. In the CKD samples, PODXL glomerular expression was significantly reduced even though the relative intensity did not reveal a significant difference between the healthy and CKD stages. These findings coincide with the role of PODXL in the normal glomerular filtration and its imbalance during CKD.

Tyrosine-protein kinase Lyn (LYN)

Tyrosine-protein kinase Lyn, a member of the Src family of protein tyrosine kinases that was found upregulated in the diseased glomeruli during CKD (Zhou et al., 2018). In this analysis, LYN was weakly expressed in the different renal areas and decreased in the CKD samples.

Platelet-derived growth factor receptor a (PDGFRA/CD140a)

PDGFRa (Platelet-derived growth factor receptor a) is expressed in the interstitium and small areas of endothelial cells and the mesangial cells (Boor et al., 2015, Ruiz-Ortega et al., 2020). In the normal kidney, PDGFRa regulates connective tissue development and homeostasis (Olson and Soriano, 2009). In CKD, PDGFRa is upregulated and participates in the fibrotic process (Boor et al., 2014, Floege et al., 1998, 1997, Taneda et al., 2003). PDGFRa is the receptor of the PDGF-CC, that is upregulated in renal fibrosis and has been observed in the proximal tubule epithelial cells (PTESs), as well (Boor et al., 2014, Chen et al., 2011, Eitner et al., 2008, 2003, 2002). The absence of PDGFR in the PTCECs indicates that the PDGF-CC pro-angiogenic effect is indirect. The possible mechanisms include the direct effects on the renal vasculature and microvascular endothelium, effects on stroma and, in particular, fibroblasts indirectly influencing angiogenesis and via a switch of inflammatory macrophages toward a pro-angiogenic phenotype (Boor et al., 2015, 2010, Li et al., 2010).

PDGFRa (CD140a) revealed a weak expression in the normal kidney in this analysis and was further reduced in the CKD samples. The differences in intensity variation between the healthy and the CKD stages was not found of statistical significance. The most severe decrease though was observed in the distal tubules. PDGFRa is a major contributor to kidney fibrosis. So, its upregulation is expected to occur in later CKD stages along with the development of fibrosis.

In the first stages of CKD, patients present with low serum 25-hydroxyvitamin D and 1,25-dihydroxyvitamin D3 and high levels of serum parathyroid hormone (PTH) and fibroblast growth factor 23 (FGF23). These hormones are fundamental in mineral homeostasis and bone integrity, so CKD patients are prone to develop mineral bone disorder (Portale et al., 2014).

The AGE-RAGE signalling pathway plays a crucial role in the development of CKD as it regulates molecular cascades leading to vascular dysfunction and remodelling, cell proliferation and apoptosis, inflammation, and ECM production. Directly downstream of the RAGE receptor, NOX4 is located, influencing fundamental cellular processes. The mesangial matrix expansion and cell hypertrophy via the RAS system and the TGFb-TGFB1/Smad2-3 signalling pathway and the apoptotic process via the PI3K/AKT pathway constitute some of them. NOX4 also regulates cell proliferation through the Bcl-2, NRF2, elF stress pathways, and inflammation through the CA^{2+} signalling cascade, the MAPK/AP1 pathways, and the production of pro-inflammatory factors such as IL1, IL6, TNFa, MCP1, VCAM1 etc. In the regulation of cell proliferation, the transmembrane protein TMEM174 is also involved, via the MAPK/AP1 pathway (Wang et al., 2010).

In previous research of Rajaram et al., (2019), NOX4 was found downregulated along with TGFb1, NOX2, and GSTA1 in the renal tubules indicating an anti-apoptotic effect through the Bcl-2, NRF2, elF stress pathways. NOX4 was also increased in the glomerular podocytes and mesangial cells promoting ECM production and other profibrotic processes. The findings of the current research coincide with the previous data supporting the roles mentioned above of NOX4 in CKD. TMEM174 was also found downregulated in the CKD samples indicating a hindered cell proliferation process deriving from an imbalance in the Ca^{2+} homeostasis that further influences the MAPK/AP1 pathway.

Further validation of the MAPK/AP1 pathway downregulation comes from the fact that JUN, one of the two subunits of the AP1, is found significantly downregulated in CKD and is considered a central molecule of various CKD pathologies (Wang et al., 2020, Zhou et al., 2018). The role of AP1 is the activation of TGFB1 that promotes the production of mature TGF-β. TGF-β is secreted in the extracellular space to initiate the TGF-β signalling and phosphorylation of Smad2 and Smad3 (Zhou et al., 2020). Therefore, JUN and NOX4 downregulation at least in the CKD onset restricts the TGFb/Smad2/3 activation indicating a protective role against cell hypertrophy, ECM deposition, and inflammation in the renal tubules. However, the current results show a significant turnover in JUN expression in the glomeruli in advanced CKD, and NOX4 is upregulated in the diseased glomeruli. So, NOX4 and JUN acting through the TGFb pathway may promote glomerular hypertrophy and profibrotic processes in the diseased glomeruli.

Another important effector of AP1 activation is the alteration in Ca^{2+} homeostasis and signalling cascades. Ca^{2+}-mediated cascades are influenced by the NMDA receptors, among other factors (Blanke and VanDongen, 2009, Haddad, 2005), which form a complex with NETO2 protein (Michishita et al., 2003, Oparina et al., 2012, Stöhr et al., 2002). NETO2 protein is significantly decreased in all renal areas in CKD samples, implying a restricted Ca^{2+} content and the intracellular signalling that it entails leading to reduced AP1 activation, as well. The Ca^{2+} content regulates the expression of ANXA2, that regulates cell adhesion and transport across ion channels influencing salt homeostasis (Dathe et al., 2014, Alvares et al., 2013, Gassié et al., 2015, Markoff and Gerke, 2005, Xu et al., 2015). ANXA2 was found decreased in early CKD stage 2 that coincides with the Ca^{2+} imbalance and then its expression is inverted towards the CKD progression. Furthermore, CDH11 is a molecule regulated by the TGFb activation but is responsible for the calcium-dependant cell-cell adhesion and participates in the ECM transition. CDH11 exhibited a remarkable increase in the glomeruli in the stage CKD stage 3.

A major AGE is serum albumin (ALB) that undergoes glycation and produces the AGE glycoalbumin. In the normal kidney, ALB inhibits the TNFa-induced VCAM1 production and protects against inflammation. In CKD, though ALB is significantly reduced partly due to glycation. The ALB underexpression promotes the production of VCAM1 and other pro-inflammatory factors, that promote the inflammation process and further inhibit the hepatic synthesis of ALB.

Regarding the MAPK pathway, MK12 (p38γ) of the ERK MAPK kinases group is also very important in the progress of inflammation. P38γ also regulates the production of the major pro-inflammatory cytokines and chemokines mentioned above (González-Terán et al., 2016, Risco et al., 2012, Zur et al., 2015). It also controls T-cell activation for the interferon (IFN) and IL-17 production (Criado et al., 2014). MK12 exhibited different expression patterns in the renal areas. IL-17 production by the MK12 and the subsequent signalling pathway activates the production of the major pro-inflammatory factors that recruit the macrophages and T-cells that lead to tissue inflammation. IL17 also regulates the MMP9 that is responsible for the tissue remodelling and ECM transition via the MAPK/NFkB signalling pathway and influences the neutrophil recruitment and the auto-immune response. MMP9 was increased in CKD stage 3 compared to stage 2 but the difference was not found statistically significant. These results are expected, as MMP9 is overexpressed when the tissue is close to the fibrotic ESRD. Also, IFI44 a member of the type I interferon-inducible gene family a negative role in cell proliferation via its upstream PDGFR-b activator and promotes cell apoptosis. It is also involved in the autoimmune response and participates in the process of microtubule formation (Buhl et al., 2020, Hallen et al., 2007, Hu et al., 2017).

AREG is a low-affinity EGFR ligand regulated by the Hippo pathway, that contributes to the renal inflammation and fibrosis by overexpression of the major pro-inflammatory factors and macrophages/T cells recruitment similarly to the MK12/IL17 contribution to inflammation. On top of that, AREG regulates the MEK/ERK/AP1 pathway and the PDGFRa activation regarding the cell proliferation and differentiation. AREG expression in the proximal tubules exhibited a gradually increasing tendency in parallel with the CKD progression. PDGFRa did not reveal a statistically significant difference between the healthy and CKD state. However, its upregulation is expected to occur in later CKD stages along with the development of fibrosis.

TGFβ is considered the major regulator of renal fibrosis development (Kalluri and Neilson, 2003, Liu, 2010, Loeffler and Wolf, 2014). The downstream signalling includes both SMAD-dependent and SMAD-independent pathways (Ding and Choi, 2014, Kalluri and Neilson, 2003, Loeffler and Wolf, 2014, Zavadil et al., 2004). In the SMAD-dependent signalling, TGF-β activates receptor-regulated SMADs (R-SMADs) and as a complex with SMAD4 can regulate genes encoding proteins involved in the fibrotic process (Kalluri and Neilson, 2003, Loeffler and Wolf, 2014, Zavadil et al., 2004). In the ECM transition and mainly the fibroblasts-myofibroblasts transition, TGFβ regulates SMOC2 protein and is being regulated by the TSP2 that is responsible for the matrix remodelling.

Moreover, fluid and electrolyte abnormalities, such as hypervolemia and hyperkalemia are common in CKD patients due to the imbalanced exchange of Na+ and K+ in the distal tubules. ROMK1 is important in the maintenance of K+ homeostasis and is regulated by the AKT1 protein via the PI3K ligands insulin or IGF-1. ROMK1 was found significantly reduced in the distal tubules in CKD stages and increased in the glomerular compartment.

In summary, in this research, the MILAN protocol was optimized for FFPE kidney tissue samples. A set of 20 CKD-related proteins was tested in samples from healthy and CKD renal tissue including G2 and G3 CKD stages. From the 20 proteins tested, 15 were found to have a statistically significant difference between the healthy and CKD condition. The results of their relative expression were in accord with previous findings. The image processing enlightened their distribution in different renal compartments allowing for a further spatial proteomic analysis. A number of the proteins tested are involved in the regulation of cell proliferation, tissue inflammation, glomerular filtration, and renal fibrosis. To that end, the important role of AGE-RAGE and the TGFβ pathway was highlighted. Another subset of the proteins tested was decreased in initial CKD stages and increased in the advanced CKD. The expression of several proteins was more rapidly inverted in the glomeruli than the renal tubules across the CKD stages. However, in CKD onset the glomerular podocytes and therefore the glomerular filtration are initially damaged. When the kidney is injured, there are also wound-healing responses activated that when fail, the tissue deals with the forthcoming fibrosis before ending up to the ESRD. So, this variation in the expression of proteins between the renal areas and the CKD stages appears to be in accordance with the literature. Further research will enlighten these differences observed.

VI. Future Research

The current research was an innovative proteomic approach in the investigation of system-wide diseases such as Chronic Kidney Disease. After the MILAN protocol optimization in kidney samples, it resulted in a novel and promising approach regarding the investigation of CKD underlying mechanisms. A significant number of proteins can be tested in the very same tissue allowing the examination of specific CKD-related pathways or a combination of them, in gradually advanced stages of the disease. The acquisition of whole-slide images instead of

specific tissue sections will multiply the data obtained for every marker and will reveal their expression throughout the tissue in every CKD stage. The image processing pipeline developed, allows for the examination of the spatial distribution of proteins, while the accurate identification of the different renal areas will occur by the use of proteins-markers which are uniquely expressed in each one of them.

Moreover, the molecular signature of this 20-protein-set was able to identify the 9 different cell-types of the kidney. Consequently, the use of cell-type-specific markers can lead to the classification of the tissue according to the different cell-types promoting a single-cell-level approach in CKD research.

VII. FIJI script

```
# Ask for the directory in a new window
# User chooses the file with the slides to be processed
#@ File(label="Choose a directory", style="directory") input_path


import os
from ij import IJ, ImageStack, CompositeImage, ImagePlus, WindowManager as wm
from ij.process import ImageProcessor, LUT, ColorProcessor
from ij.plugin import ImagesToStack, HyperStackConverter, RGBStackConverter, ZProjector, ImageCalculator, Colors, \
                                                        ChannelArranger, StackEditor
from ij.gui import WaitForUserDialog, Toolbar, ImageWindow
from ij.measure import ResultsTable
from java.awt import Color
from java.awt import Image as img


def walk_main_path(path):

    """Create a list with the paths of all images contained in the initial directory

       This method acccepts the path of the initial directory as input parameter. Each iteration of the for loop
       processes a different directory: value1: represents the current directory -> value2: the list of included
       directories -> value3: the list of included files. Then it creates and returns a list with the the paths of all
       images."""

    print("Running through the directory given by the user")
    all_images = []
    for root, dirs, files in os.walk(path):
        for name in files:
            single_image_path = os.path.join(root, name)  # image_path contains the path that corresponds to every image
            all_images.append(single_image_path)  # List of the paths of all images included in the directory given
    print("A list of the paths of images of the directory given is created.")
    return all_images

def crop_left(stack):

    """ Check if there is need of cropping in the left side of the stack and crop one column per time until there are
       no zero pixels in this side.

       This method accepts as input the stack that will be cropped, then crops it in the left side
       using TransformJ Crop and returns the stack cropped in this side """

    print("Inside crop_left()")
    while True:
        ip = stack.getProcessor()

        # Check if there is need of cropping this side
        if check_crop_left_side(stack):
            break

        # Cropping borders refer to the first and last value to be included in the final image
        # We subtract one column each time, until there are no zero value pixels in the left border of the image
        # TransformJ Crop requires as last x/y borders, 1 value less than the width/height of the image.

        cmd = ("x-range=1," + str(ip.getWidth() - 1) +
               " y-range=0," + str(ip.getHeight() - 1) +
               " z-range=1," + str(stack.getNSlices()))
        IJ.run(stack, "TransformJ Crop", cmd)
        stack.close()
        stack = wm.getImage(stack.getTitle() + " cropped")
        ip = stack.getProcessor()

        # Check if this needs further cropping
        if check_crop_left_side(stack):
            break

    return stack
```

```
def crop_bottom(stack):

    """ Similar to def crop_left, for the bottom side. """

    print("Inside crop_bottom()")
    while True:
        ip = stack.getProcessor()

        # Check if there is need of cropping this side
        if check_crop_bottom(stack):
            break

        cmd = ("x-range=0," + str(ip.getWidth() - 1) +
            " y-range=0," + str(ip.getHeight() - 2) +
            " z-range=1," + str(stack.getNSlices()))
        IJ.run(stack, "TransformJ Crop", cmd)
        stack.close()
        stack = wm.getImage(stack.getTitle() + " cropped")
        ip = stack.getProcessor()

        # Check if we should continue cropping this side
        if check_crop_bottom(stack):
            break

    return stack

def crop_right(stack):

    """ Similar to def crop_left, for the right side. """

    print("Inside crop_right()")
    while True:
        ip = stack.getProcessor()

        x_last_line_zero_counter = int(0)
        x_previous_line_zero_counter = int(0)

        # Check if there is need of cropping this side
        if check_crop_right_side(stack):
            break

        cmd = ("x-range=0," + str(ip.getWidth() -2) +
              " y-range=0," + str(ip.getHeight() - 1) +
              " z-range=1," + str(stack.getNSlices()))
        IJ.run(stack, "TransformJ Crop", cmd)
        stack.close()
        stack = wm.getImage(stack.getTitle() + " cropped")
        ip = stack.getProcessor()

        # Check if we should continue cropping this side
        if check_crop_right_side(stack):
            break

    return stack

def crop_top(stack):

    """ Similar to def crop_left, for the top side. """

    print("Inside crop_top()")
    while True:
        ip = stack.getProcessor()

        x_last_line_zero_counter = int(0)
        x_previous_line_zero_counter = int(0)

        # Check if there is need of cropping this side
```

```
        if check_crop_top(stack):
            break

        cmd = ("x-range=0," + str(ip.getWidth() - 1) +
               " y-range=1," + str(ip.getHeight() - 1) +
               " z-range=1," + str(stack.getNSlices()))
        IJ.run(stack, "TransformJ Crop", cmd)
        stack.close()
        stack = wm.getImage(stack.getTitle() + " cropped")
        ip = stack.getProcessor()

        # Check if we should continue cropping this side
        if check_crop_top(stack):
            break

    return stack

def check_crop_left_side(stack):

    ''' Calculate the number of black pixels in the first and second column and check if there is need of further
        cropping in the left side. Cropping should continue as long as the first column has more zero pixels than the
        second one.

        This method accepts as input the stack to be cropped, calculates the number of black pixels in the first and
        second column. Returns true if the number of black pixels in the first column is smaller than or equal to that
        of the second column and if these columns are not full of black pixels. '''

    x0_zero_counter = int(0)
    x1_zero_counter = int(0)
    ip = stack.getProcessor()
    for i in range(1, stack.getNSlices() + 1):
        stack.setSlice(i)
        for y in range(0, ip.getHeight()):
            x=0
            if ip.getPixel(x,y)==0:
                x0_zero_counter +=1
            x=1
            if ip.getPixel(x,y)==0:
                x1_zero_counter +=1

    return (x0_zero_counter <= x1_zero_counter and
            x0_zero_counter / ip.getHeight() == 0)

def check_crop_bottom(stack):

    ''' The same as def check_crop_left_side for the bottom side.'''

    y_last_line_zero_counter = int(0)
    y_previous_line_zero_counter = int(0)
    ip = stack.getProcessor()
    for i in range(1, stack.getNSlices() + 1):
      stack.setSlice(i)
      for x in range(1, ip.getWidth()):
          y = ip.getHeight() -1
          if ip.getPixel(x,y)==0:
              y_last_line_zero_counter += 1
          y = ip.getHeight() - 2
          if ip.getPixel(x,y)==0:
              y_previous_line_zero_counter += 1

    return (y_last_line_zero_counter <= y_previous_line_zero_counter and
            y_last_line_zero_counter / ip.getWidth() == 0)

def check_crop_right_side(stack):

    ''' The same as def check_crop_left_side for the right side. '''
```

```
    x_last_line_zero_counter = int(0)
    x_previous_line_zero_counter = int(0)
    ip = stack.getProcessor()
    for i in range(1, stack.getNSlices() + 1):
      stack.setSlice(i)
      for y in range(0, ip.getHeight()):
          x = ip.getWidth() - 1
          if ip.getPixel(x,y) == 0:
              x_last_line_zero_counter += 1
          x = ip.getWidth() - 2
          if ip.getPixel(x,y) == 0:
              x_previous_line_zero_counter += 1

    return (x_last_line_zero_counter <= x_previous_line_zero_counter and
            x_last_line_zero_counter / ip.getHeight() == 0)

def check_crop_top(stack):

    ''' The same as def check_crop_left_side for the top side. '''

    y0_zero_counter = int(0)
    y1_zero_counter = int(0)
    ip = stack.getProcessor()
    for i in range(1, stack.getNSlices() + 1):
        stack.setSlice(i)
        for x in range(0, ip.getWidth()):
            y = 0
            if ip.getPixel(x,y) == 0:
                y0_zero_counter += 1
            y = 1
            if ip.getPixel(x,y) == 0:
                y1_zero_counter += 1

    return (y0_zero_counter <= y1_zero_counter and
            y0_zero_counter / ip.getWidth() == 0)

def crop_stack(title):

    ''' Crop stack in the four sides.

        This method accepts as input the title of stack to be cropped, crops it in all sides and returns the stack
        cropped. '''

    stack = wm.getImage(title)
    print "Cropping in the left side..."
    cropped = crop_left(stack)

    print "Cropping in bottom..."
    cropped = crop_bottom(cropped)

    print "Cropping in the right side..."
    cropped = crop_right(cropped)

    print "Cropping in top..."
    cropped = crop_top(cropped)

    return(cropped)

def close_window(title):

    """Close a window based on its title.

        This method accepts a title of a window as input parameter, gets the window and closes it, if it exists. """

   print("Closing window with title: " + title)
```

```
    w = wm.getWindow(title)
    if w is not None:
        w.close()
    print("Window with title: " + title + " is closed")

def correct_illumination(channel_list):

    """ Correct the illumination of images per channel.

    This method acccepts the list of images per channel as input parameter, creates a list with the opened images,
    converts the images to a stack and corrects the illumination via the BaSiC plugin.
    Then, returns the corrected channel. """

    print("Illumination correction in channel: " + str(channel_list))

    channel_list_open = []
    windows_open = []
    for i in range(0, len(channel_list)):
        img = IJ.openImage(str(channel_list[i]))
        channel_list_open.append(img)
    channel_stack = ImagesToStack.run(channel_list_open)
    channel_stack.show()
    IJ.run(channel_stack, "BaSiC ",
                          "processing_stack=Stack flat-field=None dark-field=None shading_estimation="
                          "[Estimate shading profiles] shading_model=[Estimate flat-field only "
                          "(ignore dark-field)] " "setting_regularisationparametes=Automatic temporal_drift="
                          "Ignore " "correction_options=" "[Compute shading and correct images] "
                          "lambda_flat=0.50" " lambda_dark=0.50")
    close_window("Flat-field:Stack")
    corrected_window = wm.getCurrentWindow()
    corrected_channel_stack = corrected_window.getImagePlus()

    channel_stack.close()
    return corrected_channel_stack

def equal_cropping(stacks_of_all_areas, list_of_widths, list_of_heights):
    ''' Cropping all stacks in equal dimensions.

        This methods accepts as imput the stacks of all areas and their widths and heights. It calculates the min
        value of widths and heights and crops each stack in these dimensions if necessary. '''

    equal_cropped_stacks_of_all_areas = {}
    min_width = int(0)
    min_height = int(0)
    min_width = min(list_of_widths)
    min_height = min(list_of_heights)

    for area, single_stack in  stacks_of_all_areas.items():
        if single_stack.getWidth() > min_width or single_stack.getHeight() > min_height:
            cmd = ("x-range=0," + str(min_width - 1) +
                   " y-range=0," + str(min_height - 1) +
                   " z-range=1," + str(single_stack.getNSlices()))
            IJ.run(single_stack, "TransformJ Crop", cmd)
            single_stack.setTitle("new_cropped_stack_in_area_" + area)
            equal_cropped_stacks_of_all_areas[area] = single_stack
            single_stack.show()
        else:
            equal_cropped_stacks_of_all_areas[area] = single_stack

    return equal_cropped_stacks_of_all_areas

def saving_images(equal_cropped_stacks_of_all_areas, images_per_area, channel):

    ''' Saving images in their initial directory as cropped.tiff.

        This method accepts as input the stacks cropped in equal dimensions, the lists of images paths per area and the
        channel of each one. It transforms each stack to single images and saves every image in its initial directory,
```

```
        as cropped.tiff. '"

    for area, single_stack in sorted(equal_cropped_stacks_of_all_areas.items()):

        wm.setTempCurrentImage(single_stack)
        n_slices_single_stack = single_stack.getNSlices()
        IJ.run("Stack to Images", "")
        single_stack.close()

        counter = int(1)
        while counter <= n_slices_single_stack:
            for process, images_groups in sorted(images_per_area[area].items()):
                for image_path in images_groups:
                    if area in image_path and process in image_path and channel in image_path:
                        new_path = '\\'.join(image_path.split('\\')[:-1]) + '\\'
                        k1 = str(counter).zfill(4)
                        imp = wm.getImage(area + "_" + process + "_" + channel)

                        print("Image: " + str(imp) + "is saved in path: " + new_path + "as cropped.tiff")

                        IJ.save(imp, new_path + channel + "_" + process + "_" + area + "_cropped.tiff")
                        if imp:
                            imp.close()
                print("In area : " + area + " and channel: " + channel + " the saving is completed!")
                counter += 1

def create_lists_per_area_of_corrected_slices(corrected_stack,images_per_area, corr_images_per_area):

    '"Create lists of the corrected images according to theis area from the corrected stacks.

        This method accepts as input the corrected stacks, the lists of images per area and empty lists for the
        corrected images per area. It transforms the stacks in single images and puts every image in another list
        according to its area. '"

    num_slices = corrected_stack.getNSlices()
    IJ.run("Stack to Images", "")
    for i in range (1, num_slices + 1):
        img = wm.getCurrentImage()
        for area in images_per_area.keys():
            if area in img.getTitle():
                corr_images_per_area[area].append(img)
                wm.putBehind()

    return corr_images_per_area

# Variable with the directory given as a string
main_path = input_path.getAbsolutePath()

print("Starting...")

# Create a list with the paths of all images included in the main path
images = walk_main_path(main_path)

# Lists with hex codes for specific colors

colour_codes =
["#ff77bf","#3f8c00","#c653ff","#ff7558","#0064ab","#f42100","#01d8c3","#6c7000","#c086ff","#db7f00",

"#009bff","#f30022","#02bec1","#e10076","#009678","#a60085","#c6ca92","#2b106a","#feb77c","#4a004a",

"#7ad2ee","#9f0033","#004c83","#7e4400","#ffa9e8","#223100","#ff95b6","#172543","#ffada6","#4a130c"]

# Create a list with groups of DAPI, GFP, RFP images per area, per process, per slide
slides = os.listdir(main_path)
for slide in slides:
    # List of processes per slide
    processes = os.listdir(main_path + "\\" + slide) # list.dir returns a list in arbitrary order.
```

```
d = {}
for process in processes:
    areas = os.listdir(main_path + "\\" + slide + "\\" + process)
    d[process] = {}
    for area in areas:
        d[process][area] = []
        images_to_process = []

        for i, image in enumerate(images):

            if process in image and area in image and "140_tiff" in image and "BRIGHT" in image:
                images_to_process.append(images[i + 1])
                images_to_process.append(images[i + 2])
                images_to_process.append(images[i + 3])

        # Calculate all images for <area><process>
        d[process][area] = images_to_process

# Here, the dict d is ready to use
# Create a new dict, indexed by area in the first level
images_per_area = {}
for process in d.keys():
    for area in d[process].keys():
        images_per_area[area] = {}

for area in images_per_area.keys():
    for process in d.keys():
        images_per_area[area][process]= []

for area in images_per_area.keys():
    for process in d.keys():
        images_per_area[area][process] = d[process][area]

RFP_stacks_of_all_areas = {}
GFP_stacks_of_all_areas = {}
DAPI_stacks_of_all_areas = {}
temp_width = int(0)
temp_height = int(0)
RFP_list_of_widths = []
RFP_list_of_heights = []
GFP_list_of_widths = []
GFP_list_of_heights = []
DAPI_list_of_widths = []
DAPI_list_of_heights = []

for area in sorted(images_per_area.keys()):
    print("The area is : " + area)

    dapi_list = []
    gfp_list = []
    rfp_list = []
    rfp_subtracted_images = []

    for process, images_groups in sorted(images_per_area[area].items()):
        opened_images_per_area = []
        print("In Process: " + process)
        for image_path in images_groups:

            # Create a list with the opened images per area
            img = IJ.openImage(image_path)
            opened_images_per_area.append(img)
        n_slices = len(opened_images_per_area)

        # Create a stack of the opened images and rename its slices
        image_stack = ImagesToStack.run(opened_images_per_area)
        stack = image_stack.getImageStack()
        for i in range (1, n_slices + 1):
```

```
            stack.setSliceLabel(process + "_" + area + " Slice " + str(i), i)
        image_stack.show()

        # Align all images per area via MultiStackReg plugin and save the transformation file
        IJ.run(image_stack, "MultiStackReg","stack_1=Stack action_1=Align file_1='" + main_path + "ImageStack" +
            process + area + ".txt' stack_2=None action_2=Ignore file_2=[] transformation=[Rigid Body] save")

        # Convert stack to images and rename the slices
        IJ.run("Stack to Images", "")
        DAPI_slice = wm.getImage(process + "_" + area + " Slice 1")
        GFP_slice = wm.getImage(process + "_" + area + " Slice 2")
        RFP_slice = wm.getImage(process + "_" + area + " Slice 3")

        # Separate the images in different lists according to their channel
        dapi_list.append(DAPI_slice)
        gfp_list.append(GFP_slice)
        rfp_list.append(RFP_slice)

    # Create a stack with the images per channel and rename the stack according to the channel
    dapi_stack = ImagesToStack.run(dapi_list)
    dapi_stack.setTitle(area + "_DAPI_Stack")

    gfp_stack = ImagesToStack.run(gfp_list)
    gfp_stack.setTitle(area + "_GFP_Stack")

    rfp_stack = ImagesToStack.run(rfp_list)
    rfp_stack.setTitle(area + "_RFP_Stack")
    dapi_stack.show()
    gfp_stack.show()
    rfp_stack.show()

    # Align the images in every stack via MultiStackReg. The rfp channel images are aligned based on the first image
    # of the channel. The other channels are aligned having the RFP stack as reference.

    IJ.run(rfp_stack, "MultiStackReg", "stack_1=" + area + "_RFP_Stack action_1=Align file_1='" + main_path +
        "_RFP_Stack" + "All_Processes" + area + ".txt' stack_2=None action_2=Ignore file_2=[] "
                                "transformation=[Rigid Body] save")
    IJ.run(gfp_stack, "MultiStackReg", "stack_1=" + area + "_GFP_Stack action_1=Align file_1='" + main_path +
        "_GFP_Stack" + "All_Processes" + area + ".txt' stack_2=None action_2=Ignore file_2=[] "
                                "transformation=[Rigid Body] save")
    IJ.run(dapi_stack,"MultiStackReg", "stack_1=" + area + "_DAPI_Stack action_1=[Load Transformation File]
file_1='"
        + main_path + "_RFP_Stack" + "All_Processes" + area + ".txt' +  stack_2=None action_2=Ignore file_2=[] "
                                "transformation=[Rigid Body]")

    # Crop black margins from the DAPI, RFP and GFP stack and append it in a list of channels per area
    # Calculate the dimensions of the cropped stacks and append them in the relevant lists
    cropped_DAPI_stack = crop_stack(area + "_DAPI_Stack")
    cropped_DAPI_stack_imgStack = cropped_DAPI_stack.getImageStack()
    i = int(1)
    for process in sorted(d.keys()):
        cropped_DAPI_stack_imgStack.setSliceLabel(area + "_" + process + "_" + "DAPI", i)
        i += 1
    DAPI_stacks_of_all_areas[area] = cropped_DAPI_stack
    temp_width = cropped_DAPI_stack.getWidth()
    DAPI_list_of_widths.append(temp_width)
    temp_height = cropped_DAPI_stack.getHeight()
    DAPI_list_of_heights.append(temp_height)

    cropped_RFP_stack = crop_stack(area + "_RFP_Stack") # cropped_RFP_stack is ImagePlus
    cropped_RFP_stack_imgStack = cropped_RFP_stack.getImageStack()
    i = int(1)
    for process in sorted(d.keys()):
        print(process)
        cropped_RFP_stack_imgStack.setSliceLabel(area + "_" + process + "_" + "RFP", i)
        i += 1
    RFP_stacks_of_all_areas[area] = cropped_RFP_stack
```

```
        temp_width = cropped_RFP_stack.getWidth()
        RFP_list_of_widths.append(temp_width)
        temp_height = cropped_RFP_stack.getHeight()
        RFP_list_of_heights.append(temp_height)

        cropped_GFP_stack = crop_stack(area + "_GFP_Stack")
        cropped_GFP_stack_imgStack = cropped_GFP_stack.getImageStack()
        i = int(1)
        for process in sorted(d.keys()):
            print(process)
            cropped_GFP_stack_imgStack.setSliceLabel(area + "_" + process + "_" + "GFP", i)
            i += 1
        GFP_stacks_of_all_areas[area] = cropped_GFP_stack
        temp_width = cropped_GFP_stack.getWidth()
        GFP_list_of_widths.append(temp_width)
        temp_height = cropped_GFP_stack.getHeight()
        GFP_list_of_heights.append(temp_height)

    # Crop all stacks in equal dimension and save the images in their initial directory as cropped.tiff.
    channel = "RFP"
    equal_cropped_stacks_of_all_areas = equal_cropping(RFP_stacks_of_all_areas, RFP_list_of_widths,
RFP_list_of_heights)
    saving_images(equal_cropped_stacks_of_all_areas, images_per_area, channel)

    channel = "GFP"
    equal_cropped_stacks_of_all_areas = equal_cropping(GFP_stacks_of_all_areas, GFP_list_of_widths,
GFP_list_of_heights)
    saving_images(equal_cropped_stacks_of_all_areas, images_per_area, channel)

    channel = "DAPI"
    equal_cropped_stacks_of_all_areas = equal_cropping(DAPI_stacks_of_all_areas, DAPI_list_of_widths,
DAPI_list_of_heights)
    saving_images(equal_cropped_stacks_of_all_areas, images_per_area, channel)

    DAPI_all_for_correction = []
    GFP_all_for_correction = []
    RFP_all_for_correction = []
# Close all open images
for i in range(1, wm.getWindowCount() + 1):
    image_to_close = wm.getCurrentImage()
    image_to_close.close()

# Create a list of paths of the cropped images
images_corrected = walk_main_path(main_path)
slides = os.listdir(main_path)
for slide in slides:
    processes = os.listdir(main_path + "\\" + slide)
    for process in processes:
        areas = os.listdir(main_path + "\\" + slide + "\\" + process)
        d[process] = {}
        for area in areas:
            for i, image in enumerate(images_corrected):
                if process in image and area in image and "140_tiff" in image and "BRIGHT" in image:

                    DAPI_all_for_correction.append(images_corrected[i + 2])
                    GFP_all_for_correction.append(images_corrected[i + 4])
                    RFP_all_for_correction.append(images_corrected[i + 6])

    corr_images_per_area = {}
    subtracted_images_per_area = {}
    heights_subtracted = {}
    widths_subtracted = {}
    stacks_of_subtracted_images = {}
    titles = {}
    for area in images_per_area.keys():
        corr_images_per_area[area] = []
        subtracted_images_per_area[area] = []
```

```
    heights_subtracted[area] = []
    widths_subtracted[area] = []
    titles[area] = []

ic = ImageCalculator()

 # Illumination correction in the cropped images per channel and creation of a list with the corrected images
RFP_corrected_stack = correct_illumination(RFP_all_for_correction)
corr_images_per_area = create_lists_per_area_of_corrected_slices(RFP_corrected_stack,images_per_area,
                                                 corr_images_per_area)

GFP_corrected_stack = correct_illumination(GFP_all_for_correction)
corr_images_per_area = create_lists_per_area_of_corrected_slices(GFP_corrected_stack,images_per_area,
                                                 corr_images_per_area)

DAPI_corrected_stack = correct_illumination(DAPI_all_for_correction)
corr_images_per_area = create_lists_per_area_of_corrected_slices(DAPI_corrected_stack,images_per_area,
                                                 corr_images_per_area)

 # Remove the DAPi imiges apart form the pair of Round 1
len_dapi_times_divide3 = len(corr_images_per_area["C09"]) / 3
len_dapi_times_divide3_2times = 2 * (len(corr_images_per_area["C09"]) / 3)

for area in corr_images_per_area.keys():
    len_DAPI_images = 2*(len(corr_images_per_area[area])/3)
    del(corr_images_per_area[area][len_DAPI_images:(len(corr_images_per_area[area])-2)])

 # Subtraction of stripping from staining image per area
for area in sorted(corr_images_per_area.keys()):
    print("In area: " + area)
    n1 = int(0)
    n2 = int(1)
    counter_subtr = int(0)

    while (n1 < len(corr_images_per_area[area])):
        counter_subtr += 1
        print("Stain_1: " + str(corr_images_per_area[area][n2]))
        print("Strip_1: " + str(corr_images_per_area[area][n1]))

        strip = corr_images_per_area[area][n1]
        stain = corr_images_per_area[area][n2]
        title = stain.getTitle()

        # Change the title of the subtracted image to contain the channel
        if "RFP" in title:
            title = title + "RFP_channel"
        if "GFP" in title:
            title = title + "GFP_channel"
        if "DAPI" in title:
            title = title + "DAPI_channel"
        titles[area].append(title)
        imp = ic.run("Subtract create", stain, strip)
        imp.setTitle(area + "_" + "Round_" + str(counter_subtr) + "_subtracted")
        imp.show()
        subtracted_images_per_area[area].append(imp)
        width = imp.width
        height = imp.height
        strip.close()
        stain.close()
        n1 += 2
        n2 += 2
        heights_subtracted[area].append(height)
        widths_subtracted[area].append(width)
width = int(0)
height = int(0)
```

```
# Create a stack of the subtracted images and convert it to HyperStack
for area in subtracted_images_per_area.keys():
    image_stack = ImagesToStack.run(subtracted_images_per_area[area]) # image_stack is ImagePlus
    min_height_of_area = min(heights_subtracted[area])
    min_width_of_area = min(widths_subtracted[area])

    if image_stack.getWidth() > min_width_of_area or image_stack.getHeight() > min_height_of_area:
        cmd = ("x-range=0," + str(min_width_of_area - 1) +
            " y-range=0," + str(min_height_of_area - 1) +
            " z-range=1," + str(image_stack.getNSlices()))
        IJ.run(image_stack, "TransformJ Crop", cmd)

    stack = image_stack.getImageStack()  # convert ImagePlus to ImageStack
    width = stack.getWidth()
    height = stack.getHeight()

    for i in range(1, wm.getWindowCount() + 1):
        image_to_close = wm.getCurrentImage()
        title = image_to_close.getTitle()
        if "cropped" in title:
            image_to_close.close()
        else:
            wm.putBehind()

    # A new stack to hold the data of the hyperstack
    stack2 = ImageStack(width, height)

    # Convert each color slice in the stack to two 32-bit FloatProcessor slices
    n_slices = image_stack.getNSlices()
    for i in xrange(1, n_slices + 1):

        # Get the ColorProcessor slice at index i
        cp = stack.getProcessor(i)              # requires ImageStack

#           # Extract the red and green channels as FloatProcessor
        fp = cp.toFloat(i - 1 , None)

        # Add to the new stack
        stack2.addSlice(None, fp)
    size = stack2.getSize()
    imp3 = ImagePlus('title', stack2)


    # Create a new ImagePlus with the new stack
    imp2 = ImagePlus("32-bit" + str(n_slices) +"-channel composite", stack2)
    imp2.setCalibration(image_stack.getCalibration().copy())

    # Tell the ImagePlus to represent the slices in its stack
    # in hyperstack form, and open it as a CompositeImage:
    nChannels = n_slices  # number of color channels equal to the number of slices
    nSlices = 1
    nFrames = 1
    imp2.setDimensions(nChannels, nSlices, nFrames)

    imp2.show()

    comp = CompositeImage(imp2, CompositeImage.COLOR)
    comp.show()
    my_lut = []

    # Apply a different LUT in every slice/channel
    for i in range(1, nChannels +1 ):  # requires ImagePlus
        my_color = Colors.decode(colour_codes[i-1], None)
        my_lut = LUT.createLutFromColor(my_color)

        print("Setting LUT to channel: " + str(i))
```

```
            comp.setChannelLut(my_lut, i)
        comp.updateAllChannelsAndDraw()
        comp.show()
        # Convert the stack to RGB stack and project it in a single image
        RGBStackConverter.convertToRGB(comp)
        z_projection = ZProjector.run(comp, "sum")
        IJ.save(z_projection, main_path + area + "zProjection_3.tiff")
        z_projection.show()

# Clean the initial directory from the images added during the pipeline
main_path = input_path.getAbsolutePath()
print("Deleting cropped images...")
for root, dirs, files in os.walk(main_path):
    for name in files:

        # image_path contains the path that corresponds to every image
        image_path = os.path.join(root, name)

        if "cropped" in image_path:
            print("Deleting image with path: " + image_path)
            os.remove(image_path)
```

VIII. References

Abbate, M., Zoja, C., Remuzzi, G., 2006. How Does Proteinuria Cause Progressive Renal Damage? J. Am. Soc. Nephrol. 17, 2974–2984. https://doi.org/10.1681/ASN.2006040377

Adams, D.L., Alpaugh, R.K., Tsai, S., Tang, C.-M., Stefansson, S., 2016. Multi-Phenotypic subtyping of circulating tumor cells using sequential fluorescent quenching and restaining. Sci. Rep. 6, 33488. https://doi.org/10.1038/srep33488

Alvares, K., Stern, P.H., Veis, A., 2013. Dentin Phosphoprotein Binds Annexin 2 and Is Involved in Calcium Transport in Rat Kidney Ureteric Bud Cells. J. Biol. Chem. 288, 13036–13045. https://doi.org/10.1074/jbc.M112.389627

Amdur, R.L., Feldman, H.I., Gupta, J., Yang, W., Kanetsky, P., Shlipak, M., Rahman, M., Lash, J.P., Townsend, R.R., Ojo, A., Roy-Chaudhury, A., Go, A.S., Joffe, M., He, J., Balakrishnan, V.S., Kimmel, P.L., Kusek, J.W., Raj, D.S., CRIC Study Investigators, 2016. Inflammation and Progression of CKD: The CRIC Study. Clin. J. Am. Soc. Nephrol. CJASN 11, 1546–1556. https://doi.org/10.2215/CJN.13121215

Anders, H.-J., Davis, J.M., Thurau, K., 2016. Nephron Protection in Diabetic Kidney Disease. N. Engl. J. Med. 375, 2096–2098. https://doi.org/10.1056/NEJMcibr1608564

Anderson, M., Suh, J.M., Kim, E.Y., Dryer, S.E., 2010. Functional NMDA receptors with atypical properties are expressed in podocytes. Am. J. Physiol.-Cell Physiol. 300, C22–C32. https://doi.org/10.1152/ajpcell.00268.2010

Andya, J.D., Maa, Y.F., Costantino, H.R., Nguyen, P.A., Dasovich, N., Sweeney, T.D., Hsu, C.C., Shire, S.J., 1999. The effect of formulation excipients on protein stability and aerosol performance of spray-dried powders of a recombinant humanized anti-IgE monoclonal antibody. Pharm. Res. 16, 350–358. https://doi.org/10.1023/a:1018805232453

Angers, S., Moon, R.T., 2009. Proximal events in Wnt signal transduction. Nat. Rev. Mol. Cell Biol. 10, 468–477. https://doi.org/10.1038/nrm2717

Arques, S., Ambrosi, P., 2011. Human Serum Albumin in the Clinical Syndrome of Heart Failure. J. Card. Fail. 17, 451–458. https://doi.org/10.1016/j.cardfail.2011.02.010

Asanuma, K., 2015. [The role of podocyte injury in chronic kidney disease]. Nihon Rinsho Meneki Gakkai Kaishi 38, 26–36. https://doi.org/10.2177/jsci.38.26

Asmar, A., Cramon, P.K., Simonsen, L., Asmar, M., Sorensen, C.M., Madsbad, S., Moro, C., Hartmann, B., Jensen, B.L., Holst, J.J., Bülow, J., 2019. Extracellular Fluid Volume Expansion Uncovers a Natriuretic Action of GLP-1: A Functional GLP-1-Renal Axis in Man. J. Clin. Endocrinol. Metab. 104, 2509–2519. https://doi.org/10.1210/jc.2019-00004

Attisano, L., Wrana, J.L., 2013. Signal integration in TGF-β, WNT, and Hippo pathways. F1000prime Rep. 5, 17. https://doi.org/10.12703/P5-17

Axelsson, A., Iversen, K., Vejlstrup, N., Ho, C., Norsk, J., Langhoff, L., Ahtarovski, K., Corell, P., Havndrup, O., Jensen, M., Bundgaard, H., 2015. Efficacy and safety of the angiotensin II receptor blocker losartan for hypertrophic cardiomyopathy: the INHERIT randomised, double-blind, placebo-controlled trial. Lancet Diabetes Endocrinol. 3, 123–131. https://doi.org/10.1016/S2213-8587(14)70241-4

Azzolin, L., Panciera, T., Soligo, S., Enzo, E., Bicciato, S., Dupont, S., Bresolin, S., Frasson, C., Basso, G., Guzzardo, V., Fassina, A., Cordenonsi, M., Piccolo, S., 2014. YAP/TAZ incorporation in the β-catenin destruction complex orchestrates the Wnt response. Cell 158, 157–170. https://doi.org/10.1016/j.cell.2014.06.013

Babelova, A., Avaniadi, D., Jung, O., Fork, C., Beckmann, J., Kosowski, J., Weissmann, N., Anilkumar, N., Shah, A.M., Schaefer, L., Schröder, K., Brandes, R.P., 2012. Role of Nox4 in murine models of kidney disease. Free Radic. Biol. Med. 53, 842–853. https://doi.org/10.1016/j.freeradbiomed.2012.06.027

Balbas, M.D., Burgess, M.R., Murali, R., Wongvipat, J., Skaggs, B.J., Mundel, P., Weins, A., Sawyers, C.L., 2014. MAGI-2 scaffold protein is critical for kidney barrier function. Proc. Natl. Acad. Sci. U. S. A. 111, 14876–14881. https://doi.org/10.1073/pnas.1417297111

Bankhead, P., Loughrey, M.B., Fernández, J.A., Dombrowski, Y., McArt, D.G., Dunne, P.D., McQuaid, S., Gray, R.T., Murray, L.J., Coleman, H.G., James, J.A., Salto-Tellez, M., Hamilton, P.W., 2017. QuPath: Open source software for digital pathology image analysis. Sci. Rep. 7, 16878. https://doi.org/10.1038/s41598-017-17204-5

Bär, L., Feger, M., Fajol, A., Klotz, L.-O., Zeng, S., Lang, F., Hocher, B., Föller, M., 2018. Insulin suppresses the production of fibroblast growth factor 23 (FGF23). Proc. Natl. Acad. Sci. U. S. A. 115, 5804–5809. https://doi.org/10.1073/pnas.1800160115

Barros, J.B. de S., Santos, R. da S., Ângela, Reis, A. da S., 2019. Implication of the MAPK Signalling Pathway in the Pathogenesis of Diabetic Nephropathy.

Barua, M., Shieh, E., Schlondorff, J., Genovese, G., Kaplan, B.S., Pollak, M.R., 2014. Exome sequencing and in vitro studies identified podocalyxin as a candidate gene for focal and segmental glomerulosclerosis. Kidney Int. 85, 124–133. https://doi.org/10.1038/ki.2013.354

Bellini, M., Coutinho, E., Courrol, L., Silva, F., Vieira, N., Schor, N., 2008. Correlation Between Autofluorescence Intensity and Tumor Area in Mice Bearing Renal Cell Carcinoma. J. Fluoresc. 18, 1163–8. https://doi.org/10.1007/s10895-008-0368-4

Bellomo, R., Kellum, J.A., Ronco, C., 2012. Acute kidney injury. The Lancet 380, 756–766. https://doi.org/10.1016/S0140-6736(11)61454-2

Benghanem Gharbi, M., Elseviers, M., Zamd, M., Belghiti Alaoui, A., Benahadi, N., Trabelssi, E.H., Bayahia, R., Ramdani, B., De Broe, M.E., 2016. Chronic kidney disease, hypertension, diabetes, and obesity in the adult population of Morocco: how to avoid "over"- and "under"-diagnosis of CKD. Kidney Int. 89, 1363–1371. https://doi.org/10.1016/j.kint.2016.02.019

Benigni, A., Gagliardini, E., Remuzzi, G., 2004. Changes in glomerular perm-selectivity induced by angiotensin II imply podocyte dysfunction and slit diaphragm protein rearrangement. Semin. Nephrol. 24, 131–140. https://doi.org/10.1016/j.semnephrol.2003.11.005

Berthier, C.C., Zhang, H., Schin, M., Henger, A., Nelson, R.G., Yee, B., Boucherot, A., Neusser, M.A., Cohen, C.D., Carter-Su, C., Argetsinger, L.S., Rastaldi, M.P., Brosius, F.C., Kretzler, M., 2009. Enhanced Expression of Janus Kinase–Signal Transducer and Activator of Transcription Pathway Members in Human Diabetic Nephropathy. Diabetes 58, 469–477. https://doi.org/10.2337/db08-1328

Bertram, J.F., Douglas-Denton, R.N., Diouf, B., Hughson, M.D., Hoy, W.E., 2011. Human nephron number: implications for health and disease. Pediatr. Nephrol. 26, 1529–1533. https://doi.org/10.1007/s00467-011-1843-8

Bienaimé, F., Muorah, M., Yammine, L., Burtin, M., Nguyen, C., Baron, W., Garbay, S., Viau, A., Broueilh, M., Blanc, T., Peters, D., Poli, V., Anglicheau, D., Friedlander, G., Pontoglio, M., Gallazzini, M., Terzi, F., 2016. Stat3 Controls Tubulointerstitial Communication during CKD. J. Am. Soc. Nephrol. JASN 27, 3690–3705. https://doi.org/10.1681/ASN.2015091014

Bikbov, B., Purcell, C.A., Levey, A.S., Smith, M., Abdoli, A., Abebe, M., Adebayo, O.M., Afarideh, M., Agarwal, S.K., Agudelo-Botero, M., Ahmadian, E., Al-Aly, Z., Alipour, V., Almasi-Hashiani, A., Al-Raddadi, R.M., Alvis-Guzman, N., Amini, S., Andrei, T., Andrei, C.L., Andualem, Z., Anjomshoa, M., Arabloo, J., Ashagre, A.F., Asmelash, D., Ataro, Z., Atout, M.M.W., Ayanore, M.A., Badawi, A., Bakhtiari, A., Ballew, S.H., Balouchi, A., Banach, M., Barquera, S., Basu, S., Bayih, M.T., Bedi, N., Bello, A.K., Bensenor, I.M., Bijani, A., Boloor, A., Borzì, A.M., Cámera, L.A., Carrero, J.J., Carvalho, F., Castro, F., Catalá-López, F., Chang, A.R., Chin, K.L., Chung, S.-C., Cirillo, M., Cousin, E., Dandona, L., Dandona, R., Daryani, A., Das Gupta, R., Demeke, F.M., Demoz, G.T., Desta, D.M., Do, H.P., Duncan, B.B., Eftekhari, A., Esteghamati, A., Fatima, S.S., Fernandes, J.C., Fernandes, E., Fischer, F., Freitas, M., Gad, M.M., Gebremeskel, G.G., Gebresillassie, B.M., Geta, B., Ghafourifard, M.,

Ghajar, A., Ghith, N., Gill, P.S., Ginawi, I.A., Gupta, R., Hafezi-Nejad, N., Haj-Mirzaian, Arvin, Haj-Mirzaian, Arya, Hariyani, N., Hasan, M., Hasankhani, M., Hasanzadeh, A., Hassen, H.Y., Hay, S.I., Heidari, B., Herteliu, C., Hoang, C.L., Hosseini, M., Hostiuc, M., Irvani, S.S.N., Islam, S.M.S., Jafari Balalami, N., James, S.L., Jassal, S.K., Jha, V., Jonas, J.B., Joukar, F., Jozwiak, J.J., Kabir, A., Kahsay, A., Kasaeian, A., Kassa, T.D., Kassaye, H.G., Khader, Y.S., Khalilov, R., Khan, E.A., Khan, M.S., Khang, Y.-H., Kisa, A., Kovesdy, C.P., Kuate Defo, B., Kumar, G.A., Larsson, A.O., Lim, L.-L., Lopez, A.D., Lotufo, P.A., Majeed, A., Malekzadeh, R., März, W., Masaka, A., Meheretu, H.A.A., Miazgowski, T., Mirica, A., Mirrakhimov, E.M., Mithra, P., Moazen, B., Mohammad, D.K., Mohammadpourhodki, R., Mohammed, S., Mokdad, A.H., Morales, L., Moreno Velasquez, I., Mousavi, S.M., Mukhopadhyay, S., Nachega, J.B., Nadkarni, G.N., Nansseu, J.R., Natarajan, G., Nazari, J., Neal, B., Negoi, R.I., Nguyen, C.T., Nikbakhsh, R., Noubiap, J.J., Nowak, C., Olagunju, A.T., Ortiz, A., Owolabi, M.O., Palladino, R., Pathak, M., Poustchi, H., Prakash, S., Prasad, N., Rafiei, A., Raju, S.B., Ramezanzadeh, K., Rawaf, S., Rawaf, D.L., Rawal, L., Reiner, R.C., Rezapour, A., Ribeiro, D.C., Roever, L., Rothenbacher, D., Rwegerera, G.M., Saadatagah, S., Safari, S., Sahle, B.W., Salem, H., Sanabria, J., Santos, I.S., Sarveazad, A., Sawhney, M., Schaeffner, E., Schmidt, M.I., Schutte, A.E., Sepanlou, S.G., Shaikh, M.A., Sharafi, Z., Sharif, M., Sharifi, A., Silva, D.A.S., Singh, J.A., Singh, N.P., Sisay, M.M.M., Soheili, A., Sutradhar, I., Teklehaimanot, B.F., Tesfay, B. etsay, Teshome, G.F., Thakur, J.S., Tonelli, M., Tran, K.B., Tran, B.X., Tran Ngoc, C., Ullah, I., Valdez, P.R., Varughese, S., Vos, T., Vu, L.G., Waheed, Y., Werdecker, A., Wolde, H.F., Wondmieneh, A.B., Wulf Hanson, S., Yamada, T., Yeshaw, Y., Yonemoto, N., Yusefzadeh, H., Zaidi, Z., Zaki, L., Zaman, S.B., Zamora, N., Zarghi, A., Zewdie, K.A., Ärnlöv, J., Coresh, J., Perico, N., Remuzzi, G., Murray, C.J.L., Vos, T., 2020. Global, regional, and national burden of chronic kidney disease, 1990–2017: a systematic analysis for the Global Burden of Disease Study 2017. The Lancet 395, 709–733. https://doi.org/10.1016/S0140-6736(20)30045-3

Blanke, M.L., VanDongen, A.M.J., 2009. Activation Mechanisms of the NMDA Receptor, in: Van Dongen, A.M. (Ed.), Biology of the NMDA Receptor, Frontiers in Neuroscience. CRC Press/Taylor & Francis, Boca Raton (FL).

Block, G.A., Klassen, P.S., Lazarus, J.M., Ofsthun, N., Lowrie, E.G., Chertow, G.M., 2004. Mineral metabolism, mortality, and morbidity in maintenance hemodialysis. J. Am. Soc. Nephrol. JASN 15, 2208–2218. https://doi.org/10.1097/01.ASN.0000133041.27682.A2

Boenisch, T., 2005. Effect of heat-induced antigen retrieval following inconsistent formalin fixation. Appl. Immunohistochem. Mol. Morphol. AIMM 13, 283–286. https://doi.org/10.1097/01.0000146524.74402.a4

Boes, E., Fliser, D., Ritz, E., König, P., Lhotta, K., Mann, J.F.E., Müller, G.A., Neyer, U., Riegel, W., Riegler, P., Kronenberg, F., 2006. Apolipoprotein A-IV Predicts Progression of Chronic Kidney Disease: The Mild to Moderate Kidney Disease Study. J. Am. Soc. Nephrol. 17, 528–536. https://doi.org/10.1681/ASN.2005070733

Boettner, B., Van Aelst, L., 2009. Control of cell adhesion dynamics by Rap1 signaling. Curr. Opin. Cell Biol. 21, 684–693. https://doi.org/10.1016/j.ceb.2009.06.004

Boi, G., Scalia, C.R., Gendusa, R., Ronchi, S., Cattoretti, G., 2016. Disaccharides Protect Antigens from Drying-Induced Damage in Routinely Processed Tissue Sections. J. Histochem. Cytochem. 64, 18–31. https://doi.org/10.1369/0022155415616162

Bolognesi, M.M., Manzoni, M., Scalia, C.R., Zannella, S., Bosisio, F.M., Faretta, M., Cattoretti, G., 2017. Multiplex Staining by Sequential Immunostaining and Antibody Removal on Routine Tissue Sections 14.

Bonegio, R.G.B., Fuhro, R., Wang, Z., Valeri, C.R., Andry, C., Salant, D.J., Lieberthal, W., 2005. Rapamycin ameliorates proteinuria-associated tubulointerstitial inflammation and fibrosis in experimental membranous nephropathy. J. Am. Soc. Nephrol. JASN 16, 2063–2072. https://doi.org/10.1681/ASN.2004030180

Boor, P., Bábíčková, J., Steegh, F., Hautvast, P., Martin, I.V., Djudjaj, S., Nakagawa, T., Ehling, J., Gremse, F., Bücher, E., Eriksson, U., van Roeyen, C.R.C., Eitner, F., Lammers, T., Floege, J., Peutz-Kootstra, C.J., Ostendorf, T., 2015. Role of Platelet-Derived Growth Factor-CC in Capillary Rarefaction in Renal Fibrosis. Am. J. Pathol. 185, 2132–2142. https://doi.org/10.1016/j.ajpath.2015.04.022

Boor, P., Ostendorf, T., Floege, J., 2014. PDGF and the progression of renal disease. Nephrol. Dial. Transplant. 29, i45–i54. https://doi.org/10.1093/ndt/gft273

Boor, P., van Roeyen, C.R.C., Kunter, U., Villa, L., Bücher, E., Hohenstein, B., Hugo, C.P.M., Eriksson, U., Satchell, S.C., Mathieson, P.W., Eitner, F., Floege, J., Ostendorf, T., 2010. PDGF-C Mediates Glomerular Capillary Repair. Am. J. Pathol. 177, 58–69. https://doi.org/10.2353/ajpath.2010.091008

Borbiev, T., Birukova, A., Liu, F., Nurmukhambetova, S., Gerthoffer, W.T., Garcia, J.G.N., Verin, A.D., 2004. p38 MAP kinase-dependent regulation of endothelial cell permeability. Am. J. Physiol.-Lung Cell. Mol. Physiol. 287, L911–L918. https://doi.org/10.1152/ajplung.00372.2003

Bornstein, P., Armstrong, L.C., Hankenson, K.D., Kyriakides, T.R., Yang, Z., 2000. Thrombospondin 2, a matricellular protein with diverse functions. Matrix Biol. J. Int. Soc. Matrix Biol. 19, 557–568. https://doi.org/10.1016/s0945-053x(00)00104-9

Bornstein, P., Sage, E.H., 2002. Matricellular proteins: extracellular modulators of cell function. Curr. Opin. Cell Biol. 14, 608–616. https://doi.org/10.1016/s0955-0674(02)00361-7

Boucherat, O., Nadeau, V., Bérubé-Simard, F.-A., Charron, J., Jeannotte, L., 2015. Crucial requirement of ERK/MAPK signaling in respiratory tract development. Dev. Camb. Engl. 142, 3801. https://doi.org/10.1242/dev.131821

Bozic, M., de Rooij, J., Parisi, E., Ortega, M.R., Fernandez, E., Valdivielso, J.M., 2011. Glutamatergic signaling maintains the epithelial phenotype of proximal tubular cells. J. Am. Soc. Nephrol. JASN 22, 1099–1111. https://doi.org/10.1681/ASN.2010070701

Bradshaw, A.D., Baicu, C.F., Rentz, T.J., Van Laer, A.O., Boggs, J., Lacy, J.M., Zile, M.R., 2009. Pressure overload-induced alterations in fibrillar collagen content and myocardial diastolic function: role of secreted protein acidic and rich in cysteine (SPARC) in post-synthetic procollagen processing. Circulation 119, 269–280. https://doi.org/10.1161/CIRCULATIONAHA.108.773424

Brenner, B.M., Garcia, D.L., Anderson, S., 1988. Glomeruli and Blood Pressure: Less of One, More the Other? Am. J. Hypertens. 1, 335–347. https://doi.org/10.1093/ajh/1.4.335

Brosius, F.C., He, J.C., 2015. JAK inhibition and progressive kidney disease. Curr. Opin. Nephrol. Hypertens. 24, 88–95. https://doi.org/10.1097/MNH.0000000000000079

Buhl, E.M., Djudjaj, S., Klinkhammer, B.M., Ermert, K., Puelles, V.G., Lindenmeyer, M.T., Cohen, C.D., He, C., Borkham-Kamphorst, E., Weiskirchen, R., Denecke, B., Trairatphisan, P., Saez-Rodriguez, J., Huber, T.B., Olson, L.E., Floege, J., Boor, P., 2020. Dysregulated mesenchymal PDGFR-β drives kidney fibrosis. EMBO Mol. Med. 12. https://doi.org/10.15252/emmm.201911021

Buscone, S., Argentieri, M.C., Pilla, D., Cattoretti, G., 2014. Whole-slide, quadruple immunofluorescence labeling of routinely processed paraffin sections. Appl. Immunohistochem. Mol. Morphol. AIMM 22, e1–7. https://doi.org/10.1097/PAI.0b013e31829928e7

Bussolati, G., Leonardo, E., 2008. Technical pitfalls potentially affecting diagnoses in immunohistochemistry. J. Clin. Pathol. 61, 1184–1192. https://doi.org/10.1136/jcp.2007.047720

Cachat, F., Combescure, C., Cauderay, M., Girardin, E., Chehade, H., 2015. A Systematic Review of Glomerular Hyperfiltration Assessment and Definition in the Medical Literature. Clin. J. Am. Soc. Nephrol. CJASN 10, 382–389. https://doi.org/10.2215/CJN.03080314

Cain, J.E., Di Giovanni, V., Smeeton, J., Rosenblum, N.D., 2010. Genetics of Renal Hypoplasia: Insights Into the Mechanisms Controlling Nephron Endowment. Pediatr. Res. 68, 91–98. https://doi.org/10.1203/PDR.0b013e3181e35a88

Cao, Q., Harris, D.C.H., Wang, Y., 2015. Macrophages in kidney injury, inflammation, and fibrosis. Physiol. Bethesda Md 30, 183–194. https://doi.org/10.1152/physiol.00046.2014

Cao, W., Li, A., Wang, L., Zhou, Z., Su, Z., Bin, W., Wilcox, C.S., Hou, F.F., 2015. A Salt-Induced Reno-Cerebral Reflex Activates Renin-Angiotensin Systems and Promotes CKD Progression. J. Am. Soc. Nephrol. 26, 1619–1633. https://doi.org/10.1681/ASN.2014050518

Cao, W., Xu, J., Zhou, Z.M., Wang, G.B., Hou, F.F., Nie, J., 2013. Advanced oxidation protein products activate intrarenal renin-angiotensin system via a CD36-mediated, redox-dependent pathway. Antioxid. Redox Signal. 18, 19–35. https://doi.org/10.1089/ars.2012.4603

Cao, W., Zhou, Q.G., Nie, J., Wang, G.B., Liu, Y., Zhou, Z.M., Hou, F.F., 2011. Albumin overload activates intrarenal renin-angiotensin system through protein kinase C and NADPH oxidase-dependent pathway. J. Hypertens. 29, 1411–1421. https://doi.org/10.1097/HJH.0b013e32834786f0

Cardoso, V., Gl, G., Jm, C.-P., K, T., Bb, L., Fam, C., Mc, de P., Nos, C., M, O.-S., 2018. Angiotensin II-induced podocyte apoptosis is mediated by endoplasmic reticulum stress/PKC-δ/p38 MAPK pathway activation and trough increased Na+/H+ exchanger isoform 1 activity. BMC Nephrol. 19, 179–179. https://doi.org/10.1186/s12882-018-0968-4

Carpenter, J.F., Crowe, J.H., 1989. An infrared spectroscopic study of the interactions of carbohydrates with dried proteins. Biochemistry 28, 3916–3922. https://doi.org/10.1021/bi00435a044

Cattoretti, G., Bosisio, F.M., Marcelis, L., Bolognesi, M.M., 2019. Multiple Iterative Labeling by Antibody Neodeposition (MILAN) (preprint). Protocol Exchange. https://doi.org/10.21203/rs.2.1646/v5

Cerezo-Guisado, M.I., Reino, P. del, Remy, G., Kuma, Y., Arthur, J.S.C., Gallego-Ortega, D., Cuenda, A., 2011. Evidence of p38 gamma and p38 delta involvement in cell transformation processes. Carcinogenesis 32, 1093–1099. https://doi.org/10.1093/carcin/bgr079

Charlton, J.R., Springsteen, C.H., Carmody, J.B., 2014. Nephron number and its determinants in early life: a primer. Pediatr. Nephrol. 29, 2299–2308. https://doi.org/10.1007/s00467-014-2758-y

Che, J., Okigaki, M., Takahashi, T., Katsume, A., Adachi, Y., Yamaguchi, S., Matsunaga, S., Takeda, M., Matsui, A., Kishita, E., Ikeda, K., Yamada, H., Matsubara, H., 2010. Endothelial FGF receptor signaling accelerates atherosclerosis. Am. J. Physiol.-Heart Circ. Physiol. 300, H154–H161. https://doi.org/10.1152/ajpheart.00075.2010

Chen, Y.T., Chang, F.C., Wu, C.F., Chou, Y.H., Hsu, H.L., Chiang, W.C., Shen, J., Chen, Y.M., Wu, K.D., Tsai, T.J., Duffield, J.S., Lin, S.L., 2011. Platelet-derived growth factor receptor signaling activates pericyte-myofibroblast transition in obstructive and post-ischemic kidney fibrosis. Kidney Int. 80, 1170–1181. https://doi.org/10.1038/ki.2011.208

Cheng, C.-J., Huang, C.-L., 2011. Activation of PI3-Kinase Stimulates Endocytosis of ROMK via Akt1/SGK1-Dependent Phosphorylation of WNK1. J. Am. Soc. Nephrol. 22, 460–471. https://doi.org/10.1681/ASN.2010060681

Chow, F.Y., Nikolic-Paterson, D.J., Ozols, E., Atkins, R.C., Rollin, B.J., Tesch, G.H., 2006. Monocyte chemoattractant protein-1 promotes the development of diabetic renal injury in streptozotocin-treated mice. Kidney Int. 69, 73–80. https://doi.org/10.1038/sj.ki.5000014

Chuang, P.Y., He, J.C., 2010. JAK/STAT signaling in renal diseases. Kidney Int. 78, 231–234. https://doi.org/10.1038/ki.2010.158

Clark, W.F., Macnab, J.J., Sontrop, J.M., Jain, A.K., Moist, L., Salvadori, M., Suri, R., Garg, A.X., 2011. Dipstick Proteinuria as a Screening Strategy to Identify Rapid Renal Decline. J. Am. Soc. Nephrol. 22, 1729–1736. https://doi.org/10.1681/ASN.2010111217

Clarke, G.M., Zubovits, J.T., Shaikh, K.A., Wang, D., Dinn, S.R., Corwin, A.D., Santamaria-Pang, A., Li, Q., Nofech-Mozes, S., Liu, K., Pang, Z., Filkins, R.J., Yaffe, M.J., 2014. A novel, automated technology for multiplex biomarker imaging and application to breast cancer. Histopathology 64, 242–255. https://doi.org/10.1111/his.12240

Clevers, H., Nusse, R., 2012. Wnt/β-catenin signaling and disease. Cell 149, 1192–1205. https://doi.org/10.1016/j.cell.2012.05.012

Clinkenbeard, E.L., Hanudel, M.R., Stayrook, K.R., Appaiah, H.N., Farrow, E.G., Cass, T.A., Summers, L.J., Ip, C.S., Hum, J.M., Thomas, J.C., Ivan, M., Richine, B.M., Chan, R.J., Clemens, T.L., Schipani, E., Sabbagh, Y., Xu, L., Srour, E.F., Alvarez, M.B., Kacena, M.A., Salusky, I.B., Ganz, T., Nemeth, E., White, K.E., 2017. Erythropoietin stimulates murine and human fibroblast growth factor-23, revealing novel roles for bone and bone marrow. Haematologica 102, e427–e430. https://doi.org/10.3324/haematol.2017.167882

Cortvrindt, C., Speeckaert, R., Moerman, A., Delanghe, J., Speeckaert, M., 2017. The role of interleukin-17A in the pathogenesis of kidney diseases. Pathology (Phila.) 49. https://doi.org/10.1016/j.pathol.2017.01.003

Costantini, F., 2010. GDNF/Ret signaling and renal branching morphogenesis. Organogenesis 6, 252–262. https://doi.org/10.4161/org.6.4.12680

Cox, S.N., Sallustio, F., Serino, G., Pontrelli, P., Verrienti, R., Pesce, F., Torres, D.D., Ancona, N., Stifanelli, P., Zaza, G., Schena, F.P., 2010. Altered modulation of WNT-beta-catenin and PI3K/Akt pathways in IgA nephropathy. Kidney Int. 78, 396–407. https://doi.org/10.1038/ki.2010.138

Craciun, F.L., Bijol, V., Ajay, A.K., Rao, P., Kumar, R.K., Hutchinson, J., Hofmann, O., Joshi, N., Luyendyk, J.P., Kusebauch, U., Moss, C.L., Srivastava, A., Himmelfarb, J., Waikar, S.S., Moritz, R.L., Vaidya, V.S., 2016. RNA Sequencing Identifies Novel Translational Biomarkers of Kidney Fibrosis. J. Am. Soc. Nephrol. JASN 27, 1702–1713. https://doi.org/10.1681/ASN.2015020225

Criado, G., Risco, A., Alsina-Beauchamp, D., Pérez-Lorenzo, M.J., Escós, A., Cuenda, A., 2014. Alternative p38 MAPKs are essential for collagen-induced arthritis. Arthritis Rheumatol. Hoboken NJ 66, 1208–1217. https://doi.org/10.1002/art.38327

Crowe, J.H., Carpenter, J.F., Crowe, L.M., Anchordoguy, T.J., 1990. Are freezing and dehydration similar stress vectors? A comparison of modes of interaction of stabilizing solutes with biomolecules. Cryobiology 27, 219–231. https://doi.org/10.1016/0011-2240(90)90023-W

Crowley, S.D., Coffman, T.M., 2012. Recent advances involving the renin–angiotensin system. Exp. Cell Res. 318, 1049–1056. https://doi.org/10.1016/j.yexcr.2012.02.023

Dabbs, 2013. Diagnostic Immunohistochemistry - 2nd Edition [WWW Document]. URL https://www.elsevier.com/books/diagnostic-immunohistochemistry/9780443066528 (accessed 7.21.20).

Dai, C., Stolz, D.B., Kiss, L.P., Monga, S.P., Holzman, L.B., Liu, Y., 2009. Wnt/beta-catenin signaling promotes podocyte dysfunction and albuminuria. J. Am. Soc. Nephrol. JASN 20, 1997–2008. https://doi.org/10.1681/ASN.2009010019

Daniel, C., Amann, K., Hohenstein, B., Bornstein, P., Hugo, C., 2007. Thrombospondin 2 Functions as an Endogenous Regulator of Angiogenesis and Inflammation in Experimental Glomerulonephritis in Mice. J. Am. Soc. Nephrol. 18, 788–798. https://doi.org/10.1681/ASN.2006080873

Daryadel, A., Bettoni, C., Haider, T., Imenez Silva, P.H., Schnitzbauer, U., Pastor-Arroyo, E.M., Wenger, R.H., Gassmann, M., Wagner, C.A., 2018. Erythropoietin stimulates fibroblast growth factor 23 (FGF23) in mice and men. Pflugers Arch. 470, 1569–1582. https://doi.org/10.1007/s00424-018-2171-7

Dathe, C., Daigeler, A.-L., Seifert, W., Jankowski, V., Mrowka, R., Kalis, R., Wanker, E., Mutig, K., Bachmann, S., Paliege, A., 2014. Annexin A2 mediates apical trafficking of renal Na^+-K^+-$2Cl^-$ cotransporter. J. Biol. Chem. 289, 9983–9997. https://doi.org/10.1074/jbc.M113.540948

David, V., Martin, A., Isakova, T., Spaulding, C., Qi, L., Ramirez, V., Zumbrennen-Bullough, K.B., Sun, C.C., Lin, H.Y., Babitt, J.L., Wolf, M., 2016. Inflammation and functional iron deficiency regulate fibroblast growth factor 23 production. Kidney Int. 89, 135–146. https://doi.org/10.1038/ki.2015.290

Debruin, E.J., Hughes, M.R., Sina, C., Liu, A., Cait, J., Jian, Z., Lopez, M., Lo, B., Abraham, T., McNagny, K.M., 2014. Podocalyxin Regulates Murine Lung Vascular Permeability by Altering Endothelial Cell Adhesion. PLOS ONE 9, e108881. https://doi.org/10.1371/journal.pone.0108881

Deng, A., Valdivielso, J.M., Munger, K.A., Blantz, R.C., Thomson, S.C., 2002. Vasodilatory n-Methyl-d-Aspartate Receptors Are Constitutively Expressed in Rat Kidney. J. Am. Soc. Nephrol. 13, 1381–1384. https://doi.org/10.1097/01.ASN.0000013293.11876.4E

Denic, A., Lieske, J.C., Chakkera, H.A., Poggio, E.D., Alexander, M.P., Singh, P., Kremers, W.K., Lerman, L.O., Rule, A.D., 2017. The Substantial Loss of Nephrons in Healthy Human Kidneys with Aging. J. Am. Soc. Nephrol. 28, 313–320. https://doi.org/10.1681/ASN.2016020154

Dikalov, S.I., Nazarewicz, R.R., 2013. Angiotensin II-induced production of mitochondrial reactive oxygen species: potential mechanisms and relevance for cardiovascular disease. Antioxid. Redox Signal. 19, 1085–1094. https://doi.org/10.1089/ars.2012.4604

Ding, Y., Choi, M.E., 2014. Regulation of autophagy by TGF-β: emerging role in kidney fibrosis. Semin. Nephrol. 34, 62–71. https://doi.org/10.1016/j.semnephrol.2013.11.009

Doyonnas, R., Kershaw, D.B., Duhme, C., Merkens, H., Chelliah, S., Graf, T., McNagny, K.M., 2001. Anuria, omphalocele, and perinatal lethality in mice lacking the CD34-related protein podocalyxin. J. Exp. Med. 194, 13–27. https://doi.org/10.1084/jem.194.1.13

Dráber, P., Dráberová, E., Nováková, M., 1995. Stability of monoclonal IgM antibodies freeze-dried in the presence of trehalose. J. Immunol. Methods 181, 37–43. https://doi.org/10.1016/0022-1759(94)00326-r

Druskovic, M., Suput, D., Milisav, I., 2006. Overexpression of caspase-9 triggers its activation and apoptosis in vitro. Croat. Med. J. 47, 832–840.

Du, C., Zhang, T., Xiao, X., Shi, Y., Duan, H., Ren, Y., 2017. Protease-activated receptor-2 promotes kidney tubular epithelial inflammation by inhibiting autophagy via the PI3K/Akt/mTOR signalling pathway. Biochem. J. 474, 2733–2747. https://doi.org/10.1042/BCJ20170272

Eckardt, K.-U., Alper, S.L., Antignac, C., Bleyer, A.J., Chauveau, D., Dahan, K., Deltas, C., Hosking, A., Kmoch, S., Rampoldi, L., Wiesener, M., Wolf, M.T., Devuyst, O., 2015. Autosomal dominant tubulointerstitial kidney disease: diagnosis, classification, and management—A KDIGO consensus report. Kidney Int. 88, 676–683. https://doi.org/10.1038/ki.2015.28

Egli-Spichtig, D., Silva, P.H.I., Glaudemans, B., Gehring, N., Bettoni, C., Zhang, M.Y.H., Pastor-Arroyo, E.M., Schönenberger, D., Rajski, M., Hoogewijs, D., Knauf, F., Misselwitz, B., Frey-Wagner, I., Rogler, G., Ackermann, D., Ponte, B., Pruijm, M., Leichtle, A., Fiedler, G.-M., Bochud, M., Ballotta, V., Hofmann, S., Perwad, F., Föller, M., Lang, F., Wenger, R.H., Frew, I., Wagner, C.A., 2019. Tumor necrosis factor stimulates fibroblast growth factor 23 levels in chronic kidney disease and non-renal inflammation. Kidney Int. 96, 890–905. https://doi.org/10.1016/j.kint.2019.04.009

Eitner, F., Bücher, E., van Roeyen, C., Kunter, U., Rong, S., Seikrit, C., Villa, L., Boor, P., Fredriksson, L., Bäckström, G., Eriksson, U., Östman, A., Floege, J., Ostendorf, T., 2008. PDGF-C Is a Proinflammatory Cytokine that Mediates Renal Interstitial Fibrosis. J. Am. Soc. Nephrol. JASN 19, 281–289. https://doi.org/10.1681/ASN.2007030290

Eitner, F., Ostendorf, T., Kretzler, M., Cohen, C.D., Eriksson, U., Gröne, H.-J., Floege, J., 2003. PDGF-C Expression in the Developing and Normal Adult Human Kidney and in Glomerular Diseases. J. Am. Soc. Nephrol. 14, 1145–1153. https://doi.org/10.1097/01.ASN.0000062964.75006.A8

Eitner, F., Ostendorf, T., van Roeyen, C., Kitahara, M., Li, X., Aase, K., Gröne, H.-J., Eriksson, U., Floege, J., 2002. Expression of a novel PDGF isoform, PDGF-C, in normal and diseased rat kidney. J. Am. Soc. Nephrol. JASN 13, 910–7.

Ellis, R.J., 2001. Macromolecular crowding: obvious but underappreciated. Trends Biochem. Sci. 26, 597–604. https://doi.org/10.1016/s0968-0004(01)01938-7

Escós, A., Risco, A., Alsina-Beauchamp, D., Cuenda, A., 2016. p38γ and p38δ Mitogen Activated Protein Kinases (MAPKs), New Stars in the MAPK Galaxy. Front. Cell Dev. Biol. 4. https://doi.org/10.3389/fcell.2016.00031

Fanali, G., Masi, A.D., Trezza, V., Marino, M., Fasano, M., Ascenzi, P., 2012. Human serum albumin: From bench to bedside. Mol. Aspects Med. 33, 209–290. https://doi.org/10.1016/j.mam.2011.12.002

Fantus, D., Rogers, N.M., Grahammer, F., Huber, T.B., Thomson, A.W., 2016. Roles of mTOR complexes in the kidney: implications for renal disease and transplantation. Nat. Rev. Nephrol. 12, 587–609. https://doi.org/10.1038/nrneph.2016.108

Fassett, R.G., Venuthurupalli, S.K., Gobe, G.C., Coombes, J.S., Cooper, M.A., Hoy, W.E., 2011. Biomarkers in chronic kidney disease: a review. Kidney Int. 80, 806–821. https://doi.org/10.1038/ki.2011.198

Feliers, D., Kasinath, B.S., 2011. Erk in Kidney Diseases [WWW Document]. J. Signal Transduct. https://doi.org/10.1155/2011/768512

Feng, Y.-M., Thijs, L., Zhang, Z.-Y., Yang, W.-Y., Huang, Q.-F., Wei, F.-F., Kuznetsova, T., Jennings, A.-M., Delles, C., Lennox, R., Verhamme, P., Dominiczak, A., Staessen, J.A., 2018. Glomerular function in relation to circulating adhesion molecules and inflammation markers in a general population. Nephrol. Dial. Transplant. Off. Publ. Eur. Dial. Transpl. Assoc. - Eur. Ren. Assoc. 33, 426–435. https://doi.org/10.1093/ndt/gfx256

Flamme, I., Ellinghaus, P., Urrego, D., Krüger, T., 2017. FGF23 expression in rodents is directly induced via erythropoietin after inhibition of hypoxia inducible factor proline hydroxylase. PLOS ONE 12, e0186979. https://doi.org/10.1371/journal.pone.0186979

Floege, J., Hudkins, K.L., Davis, C.L., Schwartz, S.M., Alpers, C.E., 1998. Expression of PDGF alpha-receptor in renal arteriosclerosis and rejecting renal transplants. J. Am. Soc. Nephrol. JASN 9, 211–223.

Floege, J., Hudkins, K.L., Seifert, R.A., Francki, A., Bowen-Pope, D.F., Alpers, C.E., 1997. Localization of PDGF α-receptor in the developing and mature human kidney. Kidney Int. 51, 1140–1150. https://doi.org/10.1038/ki.1997.157

Fowler, C.B., Cunningham, R.E., O'Leary, T.J., Mason, J.T., 2007. "Tissue surrogates" as a model for archival formalin-fixed paraffin-embedded tissues. Lab. Investig. J. Tech. Methods Pathol. 87, 836–846. https://doi.org/10.1038/labinvest.3700596

Fox, C.H., Johnson, F.B., Whiting, J., Roller, P.P., 1985. Formaldehyde fixation. J. Histochem. Cytochem. Off. J. Histochem. Soc. 33, 845–853. https://doi.org/10.1177/33.8.3894502

Franch-Arcas, G., 2001. The meaning of hypoalbuminaemia in clinical practice. Clin. Nutr. 20, 265–269. https://doi.org/10.1054/clnu.2001.0438

Freedman, B.S., Brooks, C.R., Lam, A.Q., Fu, H., Morizane, R., Agrawal, V., Saad, A.F., Li, M.K., Hughes, M.R., Werff, R.V., Peters, D.T., Lu, J., Baccei, A., Siedlecki, A.M., Valerius, M.T., Musunuru, K., McNagny, K.M., Steinman, T.I., Zhou, J., Lerou, P.H., Bonventre, J.V., 2015. Modelling kidney disease with CRISPR-mutant kidney organoids derived from human pluripotent epiblast spheroids. Nat. Commun. 6, 8715. https://doi.org/10.1038/ncomms9715

Freedman, B.S., Steinman, T.I., 2015. Stem cells represent a new area of kidney care. Nephrol. News Issues 29, 18–21.

Fu, Q., Colgan, S.P., Shelley, C.S., 2016. Hypoxia: The Force that Drives Chronic Kidney Disease. Clin. Med. Res. 14, 15–39. https://doi.org/10.3121/cmr.2015.1282

Gaffen, S.L., 2009. Structure and signalling in the IL-17 receptor family. Nat. Rev. Immunol. 9, 556–567. https://doi.org/10.1038/nri2586

Gaglia, G., Rashid, R., Yapp, C., Joshi, G.N., Li, C.G., Lindquist, S.L., Sarosiek, K.A., Whitesell, L., Sorger, P.K., Santagata, S., 2020. HSF1 phase transition mediates stress adaptation and cell fate decisions. Nat. Cell Biol. 22, 151–158. https://doi.org/10.1038/s41556-019-0458-3

Galichon, P., 2018. Epithelial Signaling through the RUNX1/AKT Pathway: A New Therapeutic Target in Kidney Fibrosis. EBioMedicine 32, 5. https://doi.org/10.1016/j.ebiom.2018.05.020

Gassié, L., Lombard, A., Moraldi, T., Bibonne, A., Leclerc, C., Moreau, M., Marlier, A., Gilbert, T., 2015. Hspa9 is Required for Pronephros Specification and Formation in Xenopus laevis. Dev. Dyn. 244. https://doi.org/10.1002/dvdy.24344

Gatta, A., Verardo, A., Bolognesi, M., 2012. Hypoalbuminemia. Intern. Emerg. Med. 7 Suppl 3, S193-199. https://doi.org/10.1007/s11739-012-0802-0

Gendusa, R., Scalia, C.R., Buscone, S., Cattoretti, G., 2014. Elution of High-affinity (>10-9 K) Antibodies from Tissue Sections: Clues to the MoleculaDr Mechanism and Use in Sequential Immunostaining 13.

Gerarduzzi, C., Kumar, R.K., Trivedi, P., Ajay, A.K., Iyer, A., Boswell, S., Hutchinson, J.N., Waikar, S.S., Vaidya, V.S., 2017. Silencing SMOC2 ameliorates kidney fibrosis by inhibiting fibroblast to myofibroblast transformation. JCI Insight 2, e90299. https://doi.org/10.1172/jci.insight.90299

Gerdes, M.J., Sevinsky, C.J., Sood, A., Adak, S., Bello, M.O., Bordwell, A., Can, A., Corwin, A., Dinn, S., Filkins, R.J., Hollman, D., Kamath, V., Kaanumalle, S., Kenny, K., Larsen, M., Lazare, M., Li, Q., Lowes, C., McCulloch, C.C., McDonough, E., Montalto, M.C., Pang, Z., Rittscher, J., Santamaria-Pang, A., Sarachan, B.D., Seel, M.L., Seppo, A., Shaikh, K., Sui, Y., Zhang, J., Ginty, F., 2013. Highly multiplexed single-cell analysis of formalin-fixed, paraffin-embedded cancer tissue. Proc. Natl. Acad. Sci. 110, 11982–11987. https://doi.org/10.1073/pnas.1300136110

Ghoreschi, K., Laurence, A., O'Shea, J.J., 2009. Janus kinases in immune cell signaling. Immunol. Rev. 228, 273–287. https://doi.org/10.1111/j.1600-065X.2008.00754.x

Giacco, F., Du, X., D'Agati, V.D., Milne, R., Sui, G., Geoffrion, M., Brownlee, M., 2014. Knockdown of Glyoxalase 1 Mimics Diabetic Nephropathy in Nondiabetic Mice. Diabetes 63, 291–299. https://doi.org/10.2337/db13-0316

Gifford, F.J., Gifford, R.M., Eddleston, M., Dhaun, N., 2017. Endemic Nephropathy Around the World. Kidney Int. Rep. 2, 282–292. https://doi.org/10.1016/j.ekir.2016.11.003

Glaser, J., Lemery, J., Rajagopalan, B., Diaz, H.F., García-Trabanino, R., Taduri, G., Madero, M., Amarasinghe, M., Abraham, G., Anutrakulchai, S., Jha, V., Stenvinkel, P., Roncal-Jimenez, C., Lanaspa, M.A., Correa-Rotter, R., Sheikh-Hamad, D., Burdmann, E.A., Andres-Hernando, A., Milagres, T., Weiss, I., Kanbay, M., Wesseling, C., Sánchez-Lozada, L.G., Johnson, R.J., 2016. Climate Change and the Emergent Epidemic of CKD from Heat Stress in Rural Communities: The Case for Heat Stress Nephropathy. Clin. J. Am. Soc. Nephrol. 11, 1472–1483. https://doi.org/10.2215/CJN.13841215

Glass, G., Papin, J.A., Mandell, J.W., 2009. SIMPLE: a sequential immunoperoxidase labeling and erasing method. J. Histochem. Cytochem. Off. J. Histochem. Soc. 57, 899–905. https://doi.org/10.1369/jhc.2009.953612

Glassock, R.J., Warnock, D.G., Delanaye, P., 2017. The global burden of chronic kidney disease: estimates, variability and pitfalls. Nat. Rev. Nephrol. 13, 104–114. https://doi.org/10.1038/nrneph.2016.163

González-Terán, B., López, J.A., Rodríguez, E., Leiva, L., Martínez-Martínez, S., Bernal, J.A., Jiménez-Borreguero, L.J., Redondo, J.M., Vazquez, J., Sabio, G., 2016. p38γ and δ promote heart hypertrophy by targeting the mTOR-inhibitory protein DEPTOR for degradation. Nat. Commun. 7, 10477. https://doi.org/10.1038/ncomms10477

Goytain, A., Quamme, G.A., 2008. Identification and characterization of a novel family of membrane magnesium transporters, MMgT1 and MMgT2. Am. J. Physiol.-Cell Physiol. 294, C495–C502. https://doi.org/10.1152/ajpcell.00238.2007

Graversen, J.H., Castro, G., Kandoussi, A., Nielsen, H., Christensen, E.I., Norden, A., Moestrup, S.K., 2008. A pivotal role of the human kidney in catabolism of HDL protein components apolipoprotein A-I and A-IV but not of A-II. Lipids 43, 467–470. https://doi.org/10.1007/s11745-008-3169-2

Grinnell, F., 2003. Fibroblast biology in three-dimensional collagen matrices. Trends Cell Biol. 13, 264–269. https://doi.org/10.1016/s0962-8924(03)00057-6

Grossi, V., Peserico, A., Tezil, T., Simone, C., 2014. p38α MAPK pathway: A key factor in colorectal cancer therapy and chemoresistance. World J. Gastroenterol. WJG 20, 9744–9758. https://doi.org/10.3748/wjg.v20.i29.9744

Gu, L., Hagiwara, S., Fan, Q., Tanimoto, M., Kobata, M., Yamashita, M., Nishitani, T., Gohda, T., Ni, Z., Qian, J., Horikoshi, S., Tomino, Y., 2006. Role of receptor for advanced glycation end-products and signalling events in advanced glycation end-product-induced monocyte chemoattractant protein-1 expression in differentiated mouse podocytes. Nephrol. Dial. Transplant. 21, 299–313. https://doi.org/10.1093/ndt/gfi210

Gupta, J., Hoque, M., Zaman, M., Khan, R.H., Saleemuddin, M., 2016. A detergent-based procedure for the preparation of IgG-like bispecific antibodies in high yield. Sci. Rep. 6. https://doi.org/10.1038/srep39198

Gutiérrez, O.M., 2010. Fibroblast growth factor 23 and disordered vitamin D metabolism in chronic kidney disease: updating the "trade-off" hypothesis. Clin. J. Am. Soc. Nephrol. CJASN 5, 1710–1716. https://doi.org/10.2215/CJN.02640310

Gutiérrez, O.M., Mannstadt, M., Isakova, T., Rauh-Hain, J.A., Tamez, H., Shah, A., Smith, K., Lee, H., Thadhani, R., Jüppner, H., Wolf, M., 2008. Fibroblast Growth Factor 23 and Mortality among Patients Undergoing Hemodialysis. N. Engl. J. Med. 359, 584–592. https://doi.org/10.1056/NEJMoa0706130

Haase, V.H., 2006. Hypoxia-inducible factors in the kidney. Am. J. Physiol. Renal Physiol. 291, F271-281. https://doi.org/10.1152/ajprenal.00071.2006

Haddad, J.J., 2005. N-methyl-D-aspartate (NMDA) and the regulation of mitogen-activated protein kinase (MAPK) signaling pathways: a revolving neurochemical axis for therapeutic intervention? Prog. Neurobiol. 77, 252–282. https://doi.org/10.1016/j.pneurobio.2005.10.008

Hallen, L.C., Burki, Y., Ebeling, M., Broger, C., Siegrist, F., Oroszlan-Szovik, K., Bohrmann, B., Certa, U., Foser, S., 2007. Antiproliferative activity of the human IFN-alpha-inducible protein IFI44. J. Interferon Cytokine Res. Off. J. Int. Soc. Interferon Cytokine Res. 27, 675–680. https://doi.org/10.1089/jir.2007.0021

Hansen, K.B., Yi, F., Perszyk, R.E., Furukawa, H., Wollmuth, L.P., Gibb, A.J., Traynelis, S.F., 2018. Structure, function, and allosteric modulation of NMDA receptors. J. Gen. Physiol. 150, 1081–1105. https://doi.org/10.1085/jgp.201812032

He, B.B., Xu, M., Wei, L., Gu, Y.J., Han, J.F., Liu, Y.X., Bao, Y.Q., Jia, W.P., 2015. Relationship between Anemia and Chronic Complications in Chinese Patients with Type 2 Diabetes Mellitus. Arch. Iran. Med. 18, 277–283. https://doi.org/0151805/AIM.005

Helal, I., Fick-Brosnahan, G.M., Reed-Gitomer, B., Schrier, R.W., 2012. Glomerular hyperfiltration: definitions, mechanisms and clinical implications. Nat. Rev. Nephrol. 8, 293–300. https://doi.org/10.1038/nrneph.2012.19

Hewitson, T.D., Holt, S.G., Smith, E.R., 2017. Progression of Tubulointerstitial Fibrosis and the Chronic Kidney Disease Phenotype – Role of Risk Factors and Epigenetics. Front. Pharmacol. 8. https://doi.org/10.3389/fphar.2017.00520

Higgins, D.F., Kimura, K., Bernhardt, W.M., Shrimanker, N., Akai, Y., Hohenstein, B., Saito, Y., Johnson, R.S., Kretzler, M., Cohen, C.D., Eckardt, K.-U., Iwano, M., Haase, V.H., 2007.

Hypoxia promotes fibrogenesis in vivo via HIF-1 stimulation of epithelial-to-mesenchymal transition. J. Clin. Invest. 117, 3810–3820. https://doi.org/10.1172/JCI30487
Hill, N.R., Fatoba, S.T., Oke, J.L., Hirst, J.A., O'Callaghan, C.A., Lasserson, D.S., Hobbs, F.D.R., 2016. Global Prevalence of Chronic Kidney Disease – A Systematic Review and Meta-Analysis. PLOS ONE 11, e0158765. https://doi.org/10.1371/journal.pone.0158765
Hirakawa, Y., Tanaka, T., Nangaku, M., 2017. Renal Hypoxia in CKD; Pathophysiology and Detecting Methods. Front. Physiol. 8. https://doi.org/10.3389/fphys.2017.00099
Hirano, D., Ishikura, K., Uemura, O., Ito, S., Wada, N., Hattori, M., Ohashi, Y., Hamasaki, Y., Tanaka, R., Nakanishi, K., Kaneko, T., Honda, M., 2016. Association between low birth weight and childhood-onset chronic kidney disease in Japan: a combined analysis of a nationwide survey for paediatric chronic kidney disease and the National Vital Statistics Report. Nephrol. Dial. Transplant. 31, 1895–1900. https://doi.org/10.1093/ndt/gfv425
Hitchcock, J.K., Katz, A.A., Schäfer, G., 2014. Dynamic reciprocity: the role of annexin A2 in tissue integrity. J. Cell Commun. Signal. 8, 125–133. https://doi.org/10.1007/s12079-014-0231-0
Hodgin, J.B., Bitzer, M., Wickman, L., Afshinnia, F., Wang, S.Q., O'Connor, C., Yang, Y., Meadowbrooke, C., Chowdhury, M., Kikuchi, M., Wiggins, J.E., Wiggins, R.C., 2015. Glomerular Aging and Focal Global Glomerulosclerosis: A Podometric Perspective. J. Am. Soc. Nephrol. 26, 3162–3178. https://doi.org/10.1681/ASN.2014080752
Hollmann, M., O'Shea-Greenfield, A., Rogers, S.W., Heinemann, S., 1989. Cloning by functional expression of a member of the glutamate receptor family. Nature 342, 643–648. https://doi.org/10.1038/342643a0
Hostetter, T.H., Olson, J.L., Rennke, H.G., Venkatachalam, M.A., Brenner, B.M., 1981. Hyperfiltration in remnant nephrons: a potentially adverse response to renal ablation. Am. J. Physiol.-Ren. Physiol. 241, F85–F93. https://doi.org/10.1152/ajprenal.1981.241.1.F85
Hsieh, T.-J., Zhang, S.-L., Filep, J.G., Tang, S.-S., Ingelfinger, J.R., Chan, J.S.D., 2002. High glucose stimulates angiotensinogen gene expression via reactive oxygen species generation in rat kidney proximal tubular cells. Endocrinology 143, 2975–2985. https://doi.org/10.1210/endo.143.8.8931
Hsu, H.-H., Hoffmann, S., Di Marco, G.S., Endlich, N., Peter-Katalinić, J., Weide, T., Pavenstädt, H., 2011. Downregulation of the antioxidant protein peroxiredoxin 2 contributes to angiotensin II-mediated podocyte apoptosis. Kidney Int. 80, 959–969. https://doi.org/10.1038/ki.2011.250
Hu, J.-G., Fu, Y., Xu, J.-J., Ding, X.-P., Xie, H.-Q., Li-Ling, J., 2017. Altered gene expression profile in a rat model of gentamicin-induced ototoxicity and nephrotoxicity, and the potential role of upregulated Ifi44 expression. Mol. Med. Rep. 16, 4650–4658. https://doi.org/10.3892/mmr.2017.7150
Hu, M.C., Shiizaki, K., Kuro-o, M., Moe, O.W., 2013. Fibroblast growth factor 23 and Klotho: physiology and pathophysiology of an endocrine network of mineral metabolism. Annu. Rev. Physiol. 75, 503–533. https://doi.org/10.1146/annurev-physiol-030212-183727
Huang, Y., Wongamorntham, S., Kasting, J., McQuillan, D., Owens, R.T., Yu, L., Noble, N.A., Border, W., 2006. Renin increases mesangial cell transforming growth factor-beta1 and matrix proteins through receptor-mediated, angiotensin II-independent mechanisms. Kidney Int. 69, 105–113. https://doi.org/10.1038/sj.ki.5000011
Huber, T.B., Kottgen, M., Schilling, B., Walz, G., Benzing, T., 2001. Interaction with podocin facilitates nephrin signaling. J. Biol. Chem. 276, 41543–41546. https://doi.org/10.1074/jbc.C100452200
Hugo, C., 2003. The thrombospondin 1-TGF- axis in fibrotic renal disease. Nephrol. Dial. Transplant. 18, 1241–1245. https://doi.org/10.1093/ndt/gfg159
Hugo, C., Daniel, C., 2009. Thrombospondin in renal disease. Nephron Exp. Nephrol. 111, e61-66. https://doi.org/10.1159/000198235

Humphreys, B.D., 2018. Mechanisms of Renal Fibrosis. Annu. Rev. Physiol. 80, 309–326. https://doi.org/10.1146/annurev-physiol-022516-034227
Hwang, I., Seo, E., Ha, H., 2009. Wnt/beta-catenin signaling: a novel target for therapeutic intervention of fibrotic kidney disease. Arch. Pharm. Res. 32, 1653–1662. https://doi.org/10.1007/s12272-009-2200-3
Ibrahim, H.N., Jackson, S., Connaire, J., Matas, A., Ney, A., Najafian, B., West, A., Lentsch, N., Ericksen, J., Bodner, J., Kasiske, B., Mauer, M., 2013. Angiotensin II blockade in kidney transplant recipients. J. Am. Soc. Nephrol. JASN 24, 320–327. https://doi.org/10.1681/ASN.2012080777
Ihara, K., Nishimura, T., Fukuda, T., Ookura, T., Nishimori, K., 2012. Generation of Venus reporter knock-in mice revealed MAGI-2 expression patterns in adult mice. Gene Expr. Patterns 12, 95–101. https://doi.org/10.1016/j.gep.2012.01.006
Ihara, K.-I., Asanuma, K., Fukuda, T., Ohwada, S., Yoshida, M., Nishimori, K., 2014. MAGI-2 is critical for the formation and maintenance of the glomerular filtration barrier in mouse kidney. Am. J. Pathol. 184, 2699–2708. https://doi.org/10.1016/j.ajpath.2014.06.019
Ihermann-Hella, A., T, H., J, K., K, K., H, L., Hn, K., C, C., A, S., A, D., I, M., Gr, D., M, M., S, K., 2018. Dynamic MAPK/ERK Activity Sustains Nephron Progenitors through Niche Regulation and Primes Precursors for Differentiation. Stem Cell Rep. 11, 912–928. https://doi.org/10.1016/j.stemcr.2018.08.012
Isakova, T., Wahl, P., Vargas, G.S., Gutiérrez, O.M., Scialla, J., Xie, H., Appleby, D., Nessel, L., Bellovich, K., Chen, J., Hamm, L., Gadegbeku, C., Horwitz, E., Townsend, R.R., Anderson, C.A.M., Lash, J.P., Hsu, C.-Y., Leonard, M.B., Wolf, M., 2011. Fibroblast growth factor 23 is elevated before parathyroid hormone and phosphate in chronic kidney disease. Kidney Int. 79, 1370–1378. https://doi.org/10.1038/ki.2011.47
Ishizuka, T., Fujimori, I., Kato, M., Noji-Sakikawa, C., Saito, M., Yoshigae, Y., Kubota, K., Kurihara, A., Izumi, T., Ikeda, T., Okazaki, O., 2010. Human Carboxymethylenebutenolidase as a Bioactivating Hydrolase of Olmesartan Medoxomil in Liver and Intestine. J. Biol. Chem. 285, 11892–11902. https://doi.org/10.1074/jbc.M109.072629
Jain, S., Bicknell, G.R., Whiting, P.H., Nicholson, M.L., 2001. Rapamycin reduces expression of fibrosis-associated genes in an experimental model of renal ischaemia reperfusion injury. Transplant. Proc. 33, 556–558. https://doi.org/10.1016/s0041-1345(00)02141-2
Jayasumana, C., Orantes, C., Herrera, R., Almaguer, M., Lopez, L., Silva, L.C., Ordunez, P., Siribaddana, S., Gunatilake, S., De Broe, M.E., 2016. Chronic interstitial nephritis in agricultural communities: a worldwide epidemic with social, occupational and environmental determinants. Nephrol. Dial. Transplant. gfw346. https://doi.org/10.1093/ndt/gfw346
Jha, V., Garcia-Garcia, G., Iseki, K., Li, Z., Naicker, S., Plattner, B., Saran, R., Wang, A.Y.-M., Yang, C.-W., 2013. Chronic kidney disease: global dimension and perspectives. The Lancet 382, 260–272. https://doi.org/10.1016/S0140-6736(13)60687-X
Johnson, D.W., Pat, B., Vesey, D.A., Guan, Z., Endre, Z., Gobe, G.C., 2006. Delayed administration of darbepoetin or erythropoietin protects against ischemic acute renal injury and failure. Kidney Int. 69, 1806–1813. https://doi.org/10.1038/sj.ki.5000356
Jolicoeur, E.M., Qi, S., Xu, D., Dumont, L., Daloze, P., Chen, H., 2003. Combination therapy of mycophenolate mofetil and rapamycin in prevention of chronic renal allograft rejection in the rat. Transplantation 75, 54–59. https://doi.org/10.1097/00007890-200301150-00010
Kaissling, B., LeHir, M., Kriz, W., 2013. Renal epithelial injury and fibrosis. Biochim. Biophys. Acta BBA - Mol. Basis Dis. 1832, 931–939. https://doi.org/10.1016/j.bbadis.2013.02.010
Kalluri, R., Neilson, E.G., 2003. Epithelial-mesenchymal transition and its implications for fibrosis. J. Clin. Invest. 112, 1776–1784. https://doi.org/10.1172/JCI20530
Kang, H.G., Lee, M., Lee, K.B., Hughes, M., Kwon, B.S., Lee, S., McNagny, K.M., Ahn, Y.H., Ko, J.M., Ha, I.-S., Choi, M., Cheong, H.I., 2017. Loss of podocalyxin causes a novel syndromic type

of congenital nephrotic syndrome. Exp. Mol. Med. 49, e414. https://doi.org/10.1038/emm.2017.227
Kanwar, Y.S., Wada, J., Sun, L., Xie, P., Wallner, E.I., Chen, S., Chugh, S., Danesh, F.R., 2008. Diabetic nephropathy: mechanisms of renal disease progression. Exp. Biol. Med. Maywood NJ 233, 4–11. https://doi.org/10.3181/0705-MR-134
Karbach, S., Croxford, A.L., Oelze, M., Schüler, R., Minwegen, D., Wegner, J., Koukes, L., Yogev, N., Nikolaev, A., Reißig, S., Ullmann, A., Knorr, M., Waldner, M., Neurath, M.F., Li, H., Wu, Z., Brochhausen, C., Scheller, J., Rose-John, S., Piotrowski, C., Bechmann, I., Radsak, M., Wild, P., Daiber, A., von Stebut, E., Wenzel, P., Waisman, A., Münzel, T., 2014. Interleukin 17 drives vascular inflammation, endothelial dysfunction, and arterial hypertension in psoriasis-like skin disease. Arterioscler. Thromb. Vasc. Biol. 34, 2658–2668. https://doi.org/10.1161/ATVBAHA.114.304108
Kaufman, D.P., Basit, H., Knohl, S.J., 2020. Physiology, Glomerular Filtration Rate (GFR), in: StatPearls. StatPearls Publishing, Treasure Island (FL).
KDIGO 2017 Clinical Practice Guideline Update for the Diagnosis, Evaluation, Prevention, and Treatment of Chronic Kidney Disease–Mineral and Bone Disorder (CKD-MBD), 2017. . Kidney Int. Suppl. 7, 1–59. https://doi.org/10.1016/j.kisu.2017.04.001
Kefaloyianni, E., Muthu, M.L., Kaeppler, J., Sun, X., Sabbisetti, V., Chalaris, A., Rose-John, S., Wong, E., Sagi, I., Waikar, S.S., Rennke, H., Humphreys, B.D., Bonventre, J.V., Herrlich, A., 2016. ADAM17 substrate release in proximal tubule drives kidney fibrosis. JCI Insight 1. https://doi.org/10.1172/jci.insight.87023
Kefaloyianni, E., Raja, M.R.K., Schumacher, J., Muthu, M.L., Krishnadoss, V., Waikar, S.S., Herrlich, A., 2019. Proximal Tubule–Derived Amphiregulin Amplifies and Integrates Profibrotic EGF Receptor Signals in Kidney Fibrosis. J. Am. Soc. Nephrol. 30, 2370–2383. https://doi.org/10.1681/ASN.2019030321
Kellum, J.A., Lameire, N., Aspelin, P., Barsoum, R.S., Burdmann, E.A., Goldstein, S.L., Herzog, C.A., Joannidis, M., Kribben, A., Levey, A.S., MacLeod, A.M., Mehta, R.L., Murray, P.T., Naicker, S., Opal, S.M., Schaefer, F., Schetz, M., Uchino, S., 2012. Kidney disease: Improving global outcomes (KDIGO) acute kidney injury work group. KDIGO clinical practice guideline for acute kidney injury. Kidney Int. Suppl. 2, 1–138. https://doi.org/10.1038/kisup.2012.1
Khalsa, D.D.K., Beydoun, H.A., Carmody, J.B., 2016. Prevalence of chronic kidney disease risk factors among low birth weight adolescents. Pediatr. Nephrol. 31, 1509–1516. https://doi.org/10.1007/s00467-016-3384-7
Khodo, S.N., Dizin, E., Sossauer, G., Szanto, I., Martin, P.-Y., Feraille, E., Krause, K.H., Seigneux, S. de, 2012. NADPH-Oxidase 4 Protects against Kidney Fibrosis during Chronic Renal Injury. J. Am. Soc. Nephrol. 23, 1967–1976. https://doi.org/10.1681/ASN.2012040373
Kim, M., Soontornniyomkij, V., Ji, B., Zhou, X., 2012. System-Wide Immunohistochemical Analysis of Protein Co-Localization. PLoS ONE 7, e32043. https://doi.org/10.1371/journal.pone.0032043
Kim, S.B., Yang, W.S., Park, J.S., 1999. Role of hypoalbuminemia in the genesis of cardiovascular disease in dialysis patients. Perit. Dial. Int. J. Int. Soc. Perit. Dial. 19 Suppl 2, S144-149.
Kim, S.I., Na, H.-J., Ding, Y., Wang, Z., Lee, S.J., Choi, M.E., 2012. Autophagy promotes intracellular degradation of type I collagen induced by transforming growth factor (TGF)-β1. J. Biol. Chem. 287, 11677–11688. https://doi.org/10.1074/jbc.M111.308460
Kim, Y.K., Refaeli, I., Brooks, C.R., Jing, P., Gulieva, R.E., Hughes, M.R., Cruz, N.M., Liu, Y., Churchill, A.J., Wang, Y., Fu, H., Pippin, J.W., Lin, L.Y., Shankland, S.J., Vogl, A.W., McNagny, K.M., Freedman, B.S., 2017. Gene-Edited Human Kidney Organoids Reveal Mechanisms of Disease in Podocyte Development. Stem Cells Dayt. Ohio 35, 2366–2378. https://doi.org/10.1002/stem.2707
Kiryluk, K., Bomback, A.S., Cheng, Y.-L., Xu, K., Camara, P.G., Rabadan, R., Sims, P.A., Barasch, J., 2018. Precision Medicine for Acute Kidney Injury (AKI): Redefining AKI by Agnostic

Kidney Tissue Interrogation and Genetics. Semin. Nephrol. 38, 40–51. https://doi.org/10.1016/j.semnephrol.2017.09.006
Klein, S., Staring, M., Murphy, K., Viergever, M.A., Pluim, J.P.W., 2010. elastix: a toolbox for intensity-based medical image registration. IEEE Trans. Med. Imaging 29, 196–205. https://doi.org/10.1109/TMI.2009.2035616
Komenda, P., Lavallee, B., Ferguson, T.W., Tangri, N., Chartrand, C., McLeod, L., Gordon, A., Dart, A., Rigatto, C., 2016. The Prevalence of CKD in Rural Canadian Indigenous Peoples: Results From the First Nations Community Based Screening to Improve Kidney Health and Prevent Dialysis (FINISHED) Screen, Triage, and Treat Program. Am. J. Kidney Dis. 68, 582–590. https://doi.org/10.1053/j.ajkd.2016.04.014
Kooistra, M.R.H., Dubé, N., Bos, J.L., 2007. Rap1: a key regulator in cell-cell junction formation. J. Cell Sci. 120, 17–22. https://doi.org/10.1242/jcs.03306
Köttgen, A., Glazer, N.L., Dehghan, A., Hwang, S.-J., Katz, R., Li, M., Yang, Q., Gudnason, V., Launer, L.J., Harris, T.B., Smith, A.V., Arking, D.E., Astor, B.C., Boerwinkle, E., Ehret, G.B., Ruczinski, I., Scharpf, R.B., Ida Chen, Y.-D., de Boer, I.H., Haritunians, T., Lumley, T., Sarnak, M., Siscovick, D., Benjamin, E.J., Levy, D., Upadhyay, A., Aulchenko, Y.S., Hofman, A., Rivadeneira, F., Uitterlinden, A.G., van Duijn, C.M., Chasman, D.I., Paré, G., Ridker, P.M., Kao, W.H.L., Witteman, J.C., Coresh, J., Shlipak, M.G., Fox, C.S., 2009. Multiple loci associated with indices of renal function and chronic kidney disease. Nat. Genet. 41, 712–717. https://doi.org/10.1038/ng.377
Krämer, S., Wang-Rosenke, Y., Scholl, V., Binder, E., Loof, T., Khadzhynov, D., Kawachi, H., Shimizu, F., Diekmann, F., Budde, K., Neumayer, H.-H., Peters, H., 2008. Low-dose mTOR inhibition by rapamycin attenuates progression in anti-thy1-induced chronic glomerulosclerosis of the rat. Am. J. Physiol. Renal Physiol. 294, F440–449. https://doi.org/10.1152/ajprenal.00379.2007
Kriz, W., Lemley, K., 1999. The role of the podocyte in glomerulosclerosis. Curr Opin Nephrol Hypertens 8, 489–97. https://doi.org/10.1097/00041552-199907000-00014
Kriz, W., Lemley, K.V., 2015. A Potential Role for Mechanical Forces in the Detachment of Podocytes and the Progression of CKD. J. Am. Soc. Nephrol. 26, 258–269. https://doi.org/10.1681/ASN.2014030278
Kruzel-Davila, E., Shemer, R., Ofir, A., Bavli-Kertselli, I., Darlyuk-Saadon, I., Oren-Giladi, P., Wasser, W.G., Magen, D., Zaknoun, E., Schuldiner, M., Salzberg, A., Kornitzer, D., Marelja, Z., Simons, M., Skorecki, K., 2017. APOL1-Mediated Cell Injury Involves Disruption of Conserved Trafficking Processes. J. Am. Soc. Nephrol. 28, 1117–1130. https://doi.org/10.1681/ASN.2016050546
Kuratsune, M., Masaki, T., Hirai, T., Kiribayashi, K., Yokoyama, Y., Arakawa, T., Yorioka, N., Kohno, N., 2007. Signal transducer and activator of transcription 3 involvement in the development of renal interstitial fibrosis after unilateral ureteral obstruction. Nephrol. Carlton Vic 12, 565–571. https://doi.org/10.1111/j.1440-1797.2007.00881.x
Kuro-O, M., 2019. The Klotho proteins in health and disease. Nat. Rev. Nephrol. 15, 27–44. https://doi.org/10.1038/s41581-018-0078-3
Kuro-O, M., Moe, O.W., 2017. FGF23-αKlotho as a paradigm for a kidney-bone network. Bone 100, 4–18. https://doi.org/10.1016/j.bone.2016.11.013
Laeis, P., Püchler, K., Kirch, W., 2001. The pharmacokinetic and metabolic profile of olmesartan medoxomil limits the risk of clinically relevant drug interaction. J. Hypertens. Suppl. Off. J. Int. Soc. Hypertens. 19, S21-32. https://doi.org/10.1097/00004872-200106001-00004
Laemmli, U.K., 1970. Cleavage of Structural Proteins during the Assembly of the Head of Bacteriophage T4. Nature 227, 680–685. https://doi.org/10.1038/227680a0
Lal, M.A., Patrakka, J., 2018. Understanding Podocyte Biology to Develop Novel Kidney Therapeutics. Front. Endocrinol. 9. https://doi.org/10.3389/fendo.2018.00409

Lanz, T.V., Ding, Z., Ho, P.P., Luo, J., Agrawal, A.N., Srinagesh, H., Axtell, R., Zhang, H., Platten, M., Wyss-Coray, T., Steinman, L., 2010. Angiotensin II sustains brain inflammation in mice via TGF-beta. J. Clin. Invest. 120, 2782–2794. https://doi.org/10.1172/JCI41709

Laouari, D., Burtin, M., Phelep, A., Martino, C., Pillebout, E., Montagutelli, X., Friedlander, G., Terzi, F., 2011. TGF-α Mediates Genetic Susceptibility to Chronic Kidney Disease. J. Am. Soc. Nephrol. 22, 327–335. https://doi.org/10.1681/ASN.2010040356

Lazrak, A., Liu, Z., Huang, C.-L., 2006. Antagonistic regulation of ROMK by long and kidney-specific WNK1 isoforms. Proc. Natl. Acad. Sci. U. S. A. 103, 1615–1620. https://doi.org/10.1073/pnas.0510609103

Lechago, J., Sun, N.C., Weinstein, W.M., 1979. Simultaneous visualization of two antigens in the same tissue section by combining immunoperoxidase with immunofluorescence techniques. J. Histochem. Cytochem. 27, 1221–1225. https://doi.org/10.1177/27.9.113453

Lee, H.H., Cho, Y.I., Kim, S.Y., Yoon, Y.E., Kim, K.S., Hong, S.J., Han, W.K., 2017. TNF-α-induced Inflammation Stimulates Apolipoprotein-A4 via Activation of TNFR2 and NF-κB Signaling in Kidney Tubular Cells. Sci. Rep. 7, 8856. https://doi.org/10.1038/s41598-017-08785-2

Lee, J., An, J.N., Hwang, J.H., Lee, H., Lee, J.P., Kim, S.G., 2019. p38 MAPK activity is associated with the histological degree of interstitial fibrosis in IgA nephropathy patients. PLoS ONE 14. https://doi.org/10.1371/journal.pone.0213981

Lee, J.K., Kim, N.-J., 2017. Recent Advances in the Inhibition of p38 MAPK as a Potential Strategy for the Treatment of Alzheimer's Disease. Mol. Basel Switz. 22. https://doi.org/10.3390/molecules22081287

Lefebvre, J., Clarkson, M., Massa, F., Bradford, S.T., Charlet, A., Buske, F., Lacas-Gervais, S., Schulz, H., Gimpel, C., Hata, Y., Schaefer, F., Schedl, A., 2015. Alternatively spliced isoforms of WT1 control podocyte-specific gene expression. Kidney Int. 88, 321–331. https://doi.org/10.1038/ki.2015.140

Lehtonen, S., Ryan, J.J., Kudlicka, K., Iino, N., Zhou, H., Farquhar, M.G., 2005. Cell junction-associated proteins IQGAP1, MAGI-2, CASK, spectrins, and alpha-actinin are components of the nephrin multiprotein complex. Proc. Natl. Acad. Sci. U. S. A. 102, 9814–9819. https://doi.org/10.1073/pnas.0504166102

Leung, J.C., Travis, B.R., Verlander, J.W., Sandhu, S.K., Yang, S.-G., Zea, A.H., Weiner, I.D., Silverstein, D.M., 2002. Expression and developmental regulation of the NMDA receptor subunits in the kidney and cardiovascular system. Am. J. Physiol. Regul. Integr. Comp. Physiol. 283, R964-971. https://doi.org/10.1152/ajpregu.00629.2001

Levin, A., Stevens, P.E., Bilous, R.W., Coresh, J., Francisco, A.L.M.D., Jong, P.E.D., Griffith, K.E., Hemmelgarn, B.R., Iseki, K., Lamb, E.J., Levey, A.S., Riella, M.C., Shlipak, M.G., Wang, H., White, C.T., Winearls, C.G., 2013. Kidney disease: Improving global outcomes (KDIGO) CKD work group. KDIGO 2012 clinical practice guideline for the evaluation and management of chronic kidney disease. Kidney Int. Suppl. 3, 1–150. https://doi.org/10.1038/kisup.2012.73

Li, X., Kumar, A., Zhang, F., Lee, C., Li, Y., Tang, Z., Arjunan, P., 2010. VEGF-independent angiogenic pathways induced by PDGF-C. Oncotarget 1, 309–314.

Liao, Y.-H., Brown, M.B., Nazir, T., Quader, A., Martin, G.P., 2002. Effects of Sucrose and Trehalose on the Preservation of the Native Structure of Spray-Dried Lysozyme. Pharm. Res. 19, 1847–1853. https://doi.org/10.1023/A:1021445608807

Lim, J.C.T., Yeong, J., Lim, C.J., Ong, C., Wong, S.-C., Chew, V., Ahmed, S., Tan, P., Iqbal, J., 2018. An automated staining protocol for 7-colour immunofluorescence of human tissue sections for diagnostic and prognostic use. Pathology (Phila.) 50. https://doi.org/10.1016/j.pathol.2017.11.087

Lima Santos, P.C.J., Krieger, J.E., Pereira, A.C., 2012. Renin–Angiotensin System, Hypertension, and Chronic Kidney Disease: Pharmacogenetic Implications. J. Pharmacol. Sci. 120, 77–88. https://doi.org/10.1254/jphs.12R03CR

L'Imperio, V., Smith, A., Chinello, C., Pagni, F., Magni, F., 2016. Proteomics and glomerulonephritis: A complementary approach in renal pathology for the identification of chronic kidney disease related markers. Proteomics Clin. Appl. 10, 371–383. https://doi.org/10.1002/prca.201500075

Lin, F., Prichard, J. (Eds.), 2015. Handbook of Practical Immunohistochemistry: Frequently Asked Questions, 2nd ed. Springer-Verlag, New York. https://doi.org/10.1007/978-1-4939-1578-1

Lin, F.-J., Yao, L., Hu, X.-Q., Bian, F., Ji, G., Jiang, G.-R., Gale, D.P., Ren, H.-Q., 2019. First identification of PODXL nonsense mutations in autosomal dominant focal segmental glomerulosclerosis. Clin. Sci. Lond. Engl. 1979 133, 9–21. https://doi.org/10.1042/CS20180676

Lin, J.H., Zhang, J.J., Lin, S.-L., Chertow, G.M., 2015. Design of a phase 2 clinical trial of an ASK1 inhibitor, GS-4997, in patients with diabetic kidney disease. Nephron 129, 29–33. https://doi.org/10.1159/000369152

Lin, J.-R., Fallahi-Sichani, M., Chen, J.-Y., Sorger, P.K., 2016. Cyclic Immunofluorescence (CycIF), A Highly Multiplexed Method for Single-cell Imaging. Curr. Protoc. Chem. Biol. 8, 251–264. https://doi.org/10.1002/cpch.14

Lin, J.-R., Fallahi-Sichani, M., Sorger, P.K., 2015. Highly multiplexed imaging of single cells using a high-throughput cyclic immunofluorescence method. Nat. Commun. 6, 8390. https://doi.org/10.1038/ncomms9390

Lin, J.-R., Izar, B., Wang, S., Yapp, C., Mei, S., Shah, P.M., Santagata, S., Sorger, P.K., 2018. Highly multiplexed immunofluorescence imaging of human tissues and tumors using t-CyCIF and conventional optical microscopes. eLife 7. https://doi.org/10.7554/eLife.31657

Lin, X., Jiang, C., Luo, Z., Qu, S., 2013. Protective effect of erythropoietin on renal injury induced in rats by four weeks of exhaustive exercise. BMC Nephrol. 14, 130. https://doi.org/10.1186/1471-2369-14-130

Liu, C.-J., Lo, J.-F., Kuo, C.-H., Chu, C.-H., Chen, L.-M., Tsai, F.-J., Tsai, C.-H., Tzang, B.-S., Kuo, W.-W., Huang, C.-Y., 2009. Akt mediates 17beta-estradiol and/or estrogen receptor-alpha inhibition of LPS-induced tumor necresis factor-alpha expression and myocardial cell apoptosis by suppressing the JNK1/2-NFkappaB pathway. J. Cell. Mol. Med. 13, 3655–3667. https://doi.org/10.1111/j.1582-4934.2009.00669.x

Liu, J., Wei, Q., Guo, C., Dong, G., Liu, Y., Tang, C., Dong, Z., 2017. Hypoxia, HIF, and Associated Signaling Networks in Chronic Kidney Disease. Int. J. Mol. Sci. 18. https://doi.org/10.3390/ijms18050950

Liu, J., Zhang, Y., Chen, X.-L., Zhu, X.-L., Chen, X., Wu, J.-H., Guo, N.-F., 2018. The protective effect of the EP2 receptor on TGF-β1 induced podocyte injury via the PI3K / Akt signaling pathway. PloS One 13, e0197158. https://doi.org/10.1371/journal.pone.0197158

Liu, P., Lu, J., Cardoso, W.V., Vaziri, C., 2008. The SPARC-related Factor SMOC-2 Promotes Growth Factor-induced Cyclin D1 Expression and DNA Synthesis via Integrin-linked Kinase. Mol. Biol. Cell 19, 248–261. https://doi.org/10.1091/mbc.E07-05-0510

Liu, Y., 2010. New Insights into Epithelial-Mesenchymal Transition in Kidney Fibrosis. J. Am. Soc. Nephrol. 21, 212–222. https://doi.org/10.1681/ASN.2008121226

Livingston, M.J., Ding, H.-F., Huang, S., Hill, J.A., Yin, X.-M., Dong, Z., 2016. Persistent activation of autophagy in kidney tubular cells promotes renal interstitial fibrosis during unilateral ureteral obstruction. Autophagy 12, 976–998. https://doi.org/10.1080/15548627.2016.1166317

Loeffler, I., Wolf, G., 2014. Transforming growth factor-β and the progression of renal disease. Nephrol. Dial. Transplant. Off. Publ. Eur. Dial. Transpl. Assoc. - Eur. Ren. Assoc. 29 Suppl 1, i37–i45. https://doi.org/10.1093/ndt/gft267

Lu, Q.L., Partridge, T.A., 1998. A New Blocking Method for Application of Murine Monoclonal Antibody to Mouse Tissue Sections. J. Histochem. Cytochem. 46, 977–983. https://doi.org/10.1177/002215549804600813

Ma, F.Y., Tesch, G.H., Nikolic-Paterson, D.J., 2014. ASK1/p38 signaling in renal tubular epithelial cells promotes renal fibrosis in the mouse obstructed kidney. Am. J. Physiol. Renal Physiol. 307, F1263-1273. https://doi.org/10.1152/ajprenal.00211.2014

Ma, S.-F., Anraku, M., Iwao, Y., Yamasaki, K., Kragh-Hansen, U., Yamaotsu, N., Hirono, S., Ikeda, T., Otagiri, M., 2005. Hydrolysis of angiotensin II receptor blocker prodrug olmesartan medoxomil by human serum albumin and identification of its catalytic active sites. Drug Metab. Dispos. Biol. Fate Chem. 33, 1911–1919. https://doi.org/10.1124/dmd.105.006163

MacDonald, B.T., Tamai, K., He, X., 2009. Wnt/beta-catenin signaling: components, mechanisms, and diseases. Dev. Cell 17, 9–26. https://doi.org/10.1016/j.devcel.2009.06.016

Magzal, F., Sela, S., Szuchman-Sapir, A., Tamir, S., Michelis, R., Kristal, B., 2017. In-vivo oxidized albumin– a pro-inflammatory agent in hypoalbuminemia. PLoS ONE 12. https://doi.org/10.1371/journal.pone.0177799

Maier, S., Paulsson, M., Hartmann, U., 2008. The widely expressed extracellular matrix protein SMOC-2 promotes keratinocyte attachment and migration. Exp. Cell Res. 314, 2477–2487. https://doi.org/10.1016/j.yexcr.2008.05.020

Mansfield, J.R., 2014. Multispectral imaging: a review of its technical aspects and applications in anatomic pathology. Vet. Pathol. 51, 185–210. https://doi.org/10.1177/0300985813506918

Markó, L., Vigolo, E., Hinze, C., Park, J.-K., Roël, G., Balogh, A., Choi, M., Wübken, A., Cording, J., Blasig, I.E., Luft, F.C., Scheidereit, C., Schmidt-Ott, K.M., Schmidt-Ullrich, R., Müller, D.N., 2016. Tubular Epithelial NF-κB Activity Regulates Ischemic AKI. J. Am. Soc. Nephrol. JASN 27, 2658–2669. https://doi.org/10.1681/ASN.2015070748

Markoff, A., Gerke, V., 2005. Expression and functions of annexins in the kidney. Am. J. Physiol. Renal Physiol. 289, F949-956. https://doi.org/10.1152/ajprenal.00089.2005

Marrero, M.B., Banes-Berceli, A.K., Stern, D.M., Eaton, D.C., 2006. Role of the JAK/STAT signaling pathway in diabetic nephropathy. Am. J. Physiol. Renal Physiol. 290, F762-768. https://doi.org/10.1152/ajprenal.00181.2005

Martin, C.E., Jones, N., 2018. Nephrin Signaling in the Podocyte: An Updated View of Signal Regulation at the Slit Diaphragm and Beyond. Front. Endocrinol. 9, 302. https://doi.org/10.3389/fendo.2018.00302

Mason, D.Y., Micklem, K., Jones, M., 2000. Double immunofluorescence labelling of routinely processed paraffin sections. J. Pathol. 191, 452–461. https://doi.org/10.1002/1096-9896(2000)9999:9999<::AID-PATH665>3.0.CO;2-O

Matsui, F., Meldrum, K.K., 2012. The role of the Janus kinase family/signal transducer and activator of transcription signaling pathway in fibrotic renal disease. J. Surg. Res. 178, 339–345. https://doi.org/10.1016/j.jss.2012.06.050

Matsumoto, M., Tanaka, T., Yamamoto, T., Noiri, E., Miyata, T., Inagi, R., Fujita, T., Nangaku, M., 2004. Hypoperfusion of Peritubular Capillaries Induces Chronic Hypoxia before Progression of Tubulointerstitial Injury in a Progressive Model of Rat Glomerulonephritis. J. Am. Soc. Nephrol. 15, 1574–1581. https://doi.org/10.1097/01.ASN.0000128047.13396.48

Mayer, M.L., 2017. The Challenge of Interpreting Glutamate-Receptor Ion-Channel Structures. Biophys. J. 113, 2143–2151. https://doi.org/10.1016/j.bpj.2017.07.028

McCullough, K.P., Morgenstern, H., Saran, R., Herman, W.H., Robinson, B.M., 2019. Projecting ESRD Incidence and Prevalence in the United States through 2030. J. Am. Soc. Nephrol. 30, 127–135. https://doi.org/10.1681/ASN.2018050531

McCurdy, S., Baicu, C.F., Heymans, S., Bradshaw, A.D., 2010. Cardiac extracellular matrix remodeling: fibrillar collagens and Secreted Protein Acidic and Rich in Cysteine (SPARC). J. Mol. Cell. Cardiol. 48, 544–549. https://doi.org/10.1016/j.yjmcc.2009.06.018

McMaster, W.G., Kirabo, A., Madhur, M.S., Harrison, D.G., 2015. Inflammation, immunity, and hypertensive end-organ damage. Circ. Res. 116, 1022–1033. https://doi.org/10.1161/CIRCRESAHA.116.303697

Mehta, R.L., Kellum, J.A., Shah, S.V., Molitoris, B.A., Ronco, C., Warnock, D.G., Levin, A., Acute Kidney Injury Network, 2007. Acute Kidney Injury Network: report of an initiative to improve outcomes in acute kidney injury. Crit. Care Lond. Engl. 11, R31. https://doi.org/10.1186/cc5713

Mendoza, J.M., Isakova, T., Ricardo, A.C., Xie, H., Navaneethan, S.D., Anderson, A.H., Bazzano, L.A., Xie, D., Kretzler, M., Nessel, L., Hamm, L.L., Negrea, L., Leonard, M.B., Raj, D., Wolf, M., Cohort, for the C.R.I., 2012. Fibroblast Growth Factor 23 and Inflammation in CKD. Clin. J. Am. Soc. Nephrol. 7, 1155–1162. https://doi.org/10.2215/CJN.13281211

Meng, Z., Moroishi, T., Guan, K.-L., 2016. Mechanisms of Hippo pathway regulation. Genes Dev. 30, 1–17. https://doi.org/10.1101/gad.274027.115

Menon, V., Wang, X., Greene, T., Beck, G.J., Kusek, J.W., Marcovina, S.M., Levey, A.S., Sarnak, M.J., 2003. Relationship between C-reactive protein, albumin, and cardiovascular disease in patients with chronic kidney disease. Am. J. Kidney Dis. 42, 44–52. https://doi.org/10.1016/S0272-6386(03)00407-4

Michelis, R., B, K., T, S., S, S., 2010. Oxidative modifications impair albumin quantification. Biochem. Biophys. Res. Commun. 401, 137–142.

Michelis, R., Kristal, B., Zeitun, T., Shapiro, G., Fridman, Y., Geron, R., Sela, S., 2013. Albumin oxidation leads to neutrophil activation in vitro and inaccurate measurement of serum albumin in patients with diabetic nephropathy. Free Radic. Biol. Med. 60, 49–55. https://doi.org/10.1016/j.freeradbiomed.2013.02.005

Michishita, M., Ikeda, T., Nakashiba, T., Ogawa, M., Tashiro, K., Honjo, T., Doi, K., Itohara, S., Endo, S., 2003. A novel gene, Btcl1, encoding CUB and LDLa domains is expressed in restricted areas of mouse brain. Biochem. Biophys. Res. Commun. 306, 680–686. https://doi.org/10.1016/s0006-291x(03)01035-0

Mitra, S.K., Hanson, D.A., Schlaepfer, D.D., 2005. Focal adhesion kinase: in command and control of cell motility. Nat. Rev. Mol. Cell Biol. 6, 56–68. https://doi.org/10.1038/nrm1549

Miura, K., 2019. miura/MultiStackRegistration.

Mizoguchi, E., Mizoguchi, A., Takedatsu, H., Cario, E., Jong, Y.P.D., Ooi, C.J., Xavier, R.J., Terhorst, C., Podolsky, D.K., Bhan, A.K., 2002. Role of tumor necrosis factor receptor 2 (TNFR2) in colonic epithelial hyperplasia and chronic intestinal inflammation in mice. Gastroenterology 122, 134–144. https://doi.org/10.1053/gast.2002.30347

Monaghan, D.T., Bridges, R.J., Cotman, C.W., 1989. The excitatory amino acid receptors: their classes, pharmacology, and distinct properties in the function of the central nervous system. Annu. Rev. Pharmacol. Toxicol. 29, 365–402. https://doi.org/10.1146/annurev.pa.29.040189.002053

Moshage, H.J., Janssen, J.A., Franssen, J.H., Hafkenscheid, J.C., Yap, S.H., 1987. Study of the molecular mechanism of decreased liver synthesis of albumin in inflammation. J. Clin. Invest. 79, 1635–1641. https://doi.org/10.1172/JCI113000

Murphy, R.F., 2006. Putting proteins on the map. Nat. Biotechnol. 24, 1223–1224. https://doi.org/10.1038/nbt1006-1223

Nagatoya, K., Moriyama, T., Kawada, N., Takeji, M., Oseto, S., Murozono, T., Ando, A., Imai, E., Hori, M., 2002. Y-27632 prevents tubulointerstitial fibrosis in mouse kidneys with unilateral ureteral obstruction. Kidney Int. 61, 1684–1695. https://doi.org/10.1046/j.1523-1755.2002.00328.x

Navarro, J.F., Mora, C., Macıéa, M., Garcıéa, J., 2003. Inflammatory parameters are independently associated with urinary albumin in type 2 diabetes mellitus. Am. J. Kidney Dis. 42, 53–61. https://doi.org/10.1016/S0272-6386(03)00408-6

Nechemia-Arbely, Y., Barkan, D., Pizov, G., Shriki, A., Rose-John, S., Galun, E., Axelrod, J.H., 2008. IL-6/IL-6R axis plays a critical role in acute kidney injury. J. Am. Soc. Nephrol. JASN 19, 1106–1115. https://doi.org/10.1681/ASN.2007070744

Negoescu, A., Labat-Moleur, F., Lorimier, P., Lamarcq, L., Guillermet, C., Chambaz, E., Brambilla, E., 1994. F(ab) secondary antibodies: a general method for double

immunolabeling with primary antisera from the same species. Efficiency control by chemiluminescence. J. Histochem. Cytochem. 42, 433–437. https://doi.org/10.1177/42.3.7508473

Newbern, J., Zhong, J., Wickramasinghe, R.S., Li, X., Wu, Y., Samuels, I., Cherosky, N., Karlo, J.C., O'Loughlin, B., Wikenheiser, J., Gargesha, M., Doughman, Y.Q., Charron, J., Ginty, D.D., Watanabe, M., Saitta, S.C., Snider, W.D., Landreth, G.E., 2008. Mouse and human phenotypes indicate a critical conserved role for ERK2 signaling in neural crest development. Proc. Natl. Acad. Sci. U. S. A. 105, 17115–17120. https://doi.org/10.1073/pnas.0805239105

Nicholson, J.P., Wolmarans, M.R., Park, G.R., 2000. The role of albumin in critical illness. BJA Br. J. Anaesth. 85, 599–610. https://doi.org/10.1093/bja/85.4.599

Nicolaou, N., Renkema, K.Y., Bongers, E.M.H.F., Giles, R.H., Knoers, N.V.A.M., 2015. Genetic, environmental, and epigenetic factors involved in CAKUT. Nat. Rev. Nephrol. 11, 720–731. https://doi.org/10.1038/nrneph.2015.140

Nielsen, B., Borup-Christensen, P., Erb, K., Jensenius, J.C., Husby, S., 1987. A Method for the Blocking of Endogenous Immunoglobulin on Frozen Tissue Sections in the Screening of Human Hybridoma Antibody in Culture Supernatants. Hybridoma 6, 103–109. https://doi.org/10.1089/hyb.1987.6.103

Nlandu-Khodo, S., Dissard, R., Hasler, U., Schäfer, M., Pircher, H., Jansen-Durr, P., Krause, K.H., Martin, P.-Y., de Seigneux, S., 2016. NADPH oxidase 4 deficiency increases tubular cell death during acute ischemic reperfusion injury. Sci. Rep. 6, 38598. https://doi.org/10.1038/srep38598

Norlander, A.E., Saleh, M.A., Kamat, N.V., Ko, B., Gnecco, J., Zhu, L., Dale, B.L., Iwakura, Y., Hoover, R.S., McDonough, A.A., Madhur, M.S., 2016. Interleukin-17A Regulates Renal Sodium Transporters and Renal Injury in Angiotensin II-Induced Hypertension. Hypertens. Dallas Tex 1979 68, 167–174. https://doi.org/10.1161/HYPERTENSIONAHA.116.07493

Ntrinias, T., Papasotiriou, M., Balta, L., Kalavrizioti, D., Vamvakas, S., Papachristou, E., Goumenos, D.S., 2019. Biomarkers in Progressive Chronic Kidney Disease. Still a Long Way to Go. PRILOZI 40, 27–39. https://doi.org/10.2478/prilozi-2020-0002

Oda, M., 2004. Review Antibody flexibility observed in antigen binding and its subsequent signaling.

Ohashi, R., Shimizu, A., Masuda, Y., Kitamura, H., Ishizaki, M., Sugisaki, Y., Yamanaka, N., 2002. Peritubular Capillary Regression during the Progression of Experimental Obstructive Nephropathy. J. Am. Soc. Nephrol. 13, 1795–1805. https://doi.org/10.1097/01.ASN.0000018408.51388.57

Oliveira, B., Kleta, R., Bockenhauer, D., Walsh, S.B., 2016. Genetic, pathophysiological, and clinical aspects of nephrocalcinosis. Am. J. Physiol.-Ren. Physiol. 311, F1243–F1252. https://doi.org/10.1152/ajprenal.00211.2016

Olson, L.E., Soriano, P., 2009. Increased PDGFRα Activation Disrupts Connective Tissue Development and Drives Systemic Fibrosis. Dev. Cell 16, 303–313. https://doi.org/10.1016/j.devcel.2008.12.003

Oparina, N.Yu., Sadritdinova, A.F., Snezhkina, A.V., Dmitriev, A.A., Krasnov, G.S., Senchenko, V.N., Melnikova, N.V., Belenikin, M.S., Lakunina, V.A., Veselovsky, V.A., Stepanov, O.A., Kudryavtseva, A.V., 2012. Increase in NETO2 gene expression is a potential molecular genetic marker in renal and lung cancers. Russ. J. Genet. 48, 506–512. https://doi.org/10.1134/S1022795412050171

Orejudo, M., Rodrigues-Diez, R.R., Rodrigues-Diez, R., Garcia-Redondo, A., Santos-Sánchez, L., Rández-Garbayo, J., Cannata-Ortiz, P., Ramos, A.M., Ortiz, A., Selgas, R., Mezzano, S., Lavoz, C., Ruiz-Ortega, M., 2019. Interleukin 17A Participates in Renal Inflammation Associated to Experimental and Human Hypertension. Front. Pharmacol. 10. https://doi.org/10.3389/fphar.2019.01015

Overstreet, J.M., Wang, Y., Wang, X., Niu, A., Gewin, L.S., Yao, B., Harris, R.C., Zhang, M.-Z., 2017. Selective activation of epidermal growth factor receptor in renal proximal tubule induces tubulointerstitial fibrosis. FASEB J. Off. Publ. Fed. Am. Soc. Exp. Biol. 31, 4407–4421. https://doi.org/10.1096/fj.201601359RR

Pan, D., 2010. The hippo signaling pathway in development and cancer. Dev. Cell 19, 491–505. https://doi.org/10.1016/j.devcel.2010.09.011

Pang, M., Ma, L., Gong, R., Tolbert, E., Mao, H., Ponnusamy, M., Chin, Y.E., Yan, H., Dworkin, L.D., Zhuang, S., 2010. A novel STAT3 inhibitor, S3I-201, attenuates renal interstitial fibroblast activation and interstitial fibrosis in obstructive nephropathy. Kidney Int. 78, 257–268. https://doi.org/10.1038/ki.2010.154

Parisi, E., Bozic, M., Ibarz, M., Panizo, S., Valcheva, P., Coll, B., Fernández, E., Valdivielso, J.M., 2010. Sustained activation of renal N-methyl-d-aspartate receptors decreases vitamin D synthesis: a possible role for glutamate on the onset of secondary HPT. Am. J. Physiol.-Endocrinol. Metab. 299, E825–E831. https://doi.org/10.1152/ajpendo.00428.2010

Patil, C.N., Wallace, K., LaMarca, B.D., Moulana, M., Lopez-Ruiz, A., Soljancic, A., Juncos, L.A., Grande, J.P., Reckelhoff, J.F., 2016. Low-dose testosterone protects against renal ischemia-reperfusion injury by increasing renal IL-10-to-TNF-α ratio and attenuating T-cell infiltration. Am. J. Physiol. Renal Physiol. 311, F395-403. https://doi.org/10.1152/ajprenal.00454.2015

Pazin, D.E., Albrecht, K.H., 2009. Developmental Expression of Smoc1 and Smoc2 Suggests Potential Roles in Fetal Gonad and Reproductive Tract Differentiation. Dev. Dyn. Off. Publ. Am. Assoc. Anat. 238, 2877–2890. https://doi.org/10.1002/dvdy.22124

Peired, A., Angelotti, M.L., Ronconi, E., la Marca, G., Mazzinghi, B., Sisti, A., Lombardi, D., Giocaliere, E., Della Bona, M., Villanelli, F., Parente, E., Ballerini, L., Sagrinati, C., Wanner, N., Huber, T.B., Liapis, H., Lazzeri, E., Lasagni, L., Romagnani, P., 2013. Proteinuria Impairs Podocyte Regeneration by Sequestering Retinoic Acid. J. Am. Soc. Nephrol. 24, 1756–1768. https://doi.org/10.1681/ASN.2012090950

Peng, T., Thorn, K., Schroeder, T., Wang, L., Theis, F.J., Marr, C., Navab, N., 2017. A BaSiC tool for background and shading correction of optical microscopy images. Nat. Commun. 8, 14836. https://doi.org/10.1038/ncomms14836

Pietrowski, E., Bender, B., Huppert, J., White, R., Luhmann, H.J., Kuhlmann, C.R.W., 2011. Pro-inflammatory effects of interleukin-17A on vascular smooth muscle cells involve NAD(P)H- oxidase derived reactive oxygen species. J. Vasc. Res. 48, 52–58. https://doi.org/10.1159/000317400

Pirici, D., Mogoanta, L., Kumar-Singh, S., Pirici, I., Margaritescu, C., Simionescu, C., Stanescu, R., 2009. Antibody Elution Method for Multiple Immunohistochemistry on Primary Antibodies Raised in the Same Species and of the Same Subtype. J. Histochem. Cytochem. 57, 567–575. https://doi.org/10.1369/jhc.2009.953240

Piva, R., Belardo, G., Santoro, M.G., 2006. NF-kappaB: a stress-regulated switch for cell survival. Antioxid. Redox Signal. 8, 478–486. https://doi.org/10.1089/ars.2006.8.478

Ponticelli, C., Anders, H.-J., 2017. Thrombospondin immune regulation and the kidney. Nephrol. Dial. Transplant. 32, 1084–1089. https://doi.org/10.1093/ndt/gfw431

Potla, U., Ni, J., Vadaparampil, J., Yang, G., Leventhal, J.S., Campbell, K.N., Chuang, P.Y., Morozov, A., He, J.C., D'Agati, V.D., Klotman, P.E., Kaufman, L., 2014. Podocyte-specific RAP1GAP expression contributes to focal segmental glomerulosclerosis–associated glomerular injury. J. Clin. Invest. 124, 1757–1769. https://doi.org/10.1172/JCI67846

Potteti, H.R., Tamatam, C.R., Marreddy, R., Reddy, N.M., Noel, S., Rabb, H., Reddy, S.P., 2016. Nrf2-AKT interactions regulate heme oxygenase 1 expression in kidney epithelia during hypoxia and hypoxia-reoxygenation. Am. J. Physiol. - Ren. Physiol. 311, F1025–F1034. https://doi.org/10.1152/ajprenal.00362.2016

Prikryl, P., Vojtova, L., Maixnerova, D., Vokurka, M., Neprasova, M., Zima, T., Tesar, V., 2017. Proteomic approach for identification of IgA nephropathy-related biomarkers in urine. Physiol. Res. 66, 621–632. https://doi.org/10.33549/physiolres.933380

Quarles, L.D., 2012. Skeletal secretion of FGF-23 regulates phosphate and vitamin D metabolism. Nat. Rev. Endocrinol. 8, 276–286. https://doi.org/10.1038/nrendo.2011.218

Rabbani, N., Thornalley, P.J., 2018. Advanced glycation end products in the pathogenesis of chronic kidney disease. Kidney Int. 93, 803–813. https://doi.org/10.1016/j.kint.2017.11.034

Rajaram, R.D., Dissard, R., Faivre, A., Ino, F., Delitsikou, V., Jaquet, V., Cagarelli, T., Lindenmeyer, M., Jansen-Duerr, P., Cohen, C., Moll, S., de Seigneux, S., 2019. Tubular NOX4 expression decreases in chronic kidney disease but does not modify fibrosis evolution. Redox Biol. 26, 101234. https://doi.org/10.1016/j.redox.2019.101234

Ramachandra, C.J.A., Mehta, A., Wong, P., Shim, W., 2016. ErbB4 Activated p38γ MAPK Isoform Mediates Early Cardiogenesis Through NKx2.5 in Human Pluripotent Stem Cells. STEM CELLS 34, 288–298. https://doi.org/10.1002/stem.2223

Ramani, K., Garg, A.V., Jawale, C.V., Conti, H.R., Whibley, N., Jackson, E.K., Shiva, S.S., Horne, W., Kolls, J.K., Gaffen, S.L., Biswas, P.S., 2016. The Kallikrein-Kinin System: A Novel Mediator of IL-17-Driven Anti-Candida Immunity in the Kidney. PLOS Pathog. 12, e1005952. https://doi.org/10.1371/journal.ppat.1005952

Ramesh, G., Reeves, W.B., 2002. TNF-alpha mediates chemokine and cytokine expression and renal injury in cisplatin nephrotoxicity. J. Clin. Invest. 110, 835–842. https://doi.org/10.1172/JCI15606

Rangan, G.K., Coombes, J.D., 2007. Renoprotective effects of sirolimus in non-immune initiated focal segmental glomerulosclerosis. Nephrol. Dial. Transplant. Off. Publ. Eur. Dial. Transpl. Assoc. - Eur. Ren. Assoc. 22, 2175–2182. https://doi.org/10.1093/ndt/gfm191

Rao, T.P., Kühl, M., 2010. An updated overview on Wnt signaling pathways: a prelude for more. Circ. Res. 106, 1798–1806. https://doi.org/10.1161/CIRCRESAHA.110.219840

Redon, J., Fabia, M.J., 2009. Efficacy in angiotensin receptor blockade: a comparative review of data with olmesartan. J. Renin-Angiotensin-Aldosterone Syst. JRAAS 10, 147–156. https://doi.org/10.1177/1470320309342735

Refaeli, I., Hughes, M.R., McNagny, K.M., 2019. The first identified heterozygous nonsense mutations in podocalyxin offer new perspectives on the biology of podocytopathies. Clin. Sci. 133, 443–447. https://doi.org/10.1042/CS20181067

Refaeli, I., Hughes, M.R., Wong, A.K.-W., Bissonnette, M.L.Z., Roskelley, C.D., Wayne Vogl, A., Barbour, S.J., Freedman, B.S., McNagny, K.M., 2020. Distinct Functional Requirements for Podocalyxin in Immature and Mature Podocytes Reveal Mechanisms of Human Kidney Disease. Sci. Rep. 10, 9419. https://doi.org/10.1038/s41598-020-64907-3

Reiser, J., Altintas, M.M., 2016. Podocytes. F1000Research 5. https://doi.org/10.12688/f1000research.7255.1

Reiser, J., Sever, S., 2013. Podocyte Biology and Pathogenesis of Kidney Disease. Annu. Rev. Med. 64, 357–366. https://doi.org/10.1146/annurev-med-050311-163340

Remark, R., Merghoub, T., Grabe, N., Litjens, G., Damotte, D., Wolchok, J.D., Merad, M., Gnjatic, S., 2016. In-depth tissue profiling using multiplexed immunohistochemical consecutive staining on single slide. Sci. Immunol. 1, aaf6925–aaf6925. https://doi.org/10.1126/sciimmunol.aaf6925

Ren, Q., You Yu, S., 2016. CD2-associated protein participates in podocyte apoptosis via PI3K/Akt signaling pathway. J. Recept. Signal Transduct. Res. 36, 288–291. https://doi.org/10.3109/10799893.2015.1101137

Risco, A., del Fresno, C., Mambol, A., Alsina-Beauchamp, D., MacKenzie, K.F., Yang, H.-T., Barber, D.F., Morcelle, C., Arthur, J.S.C., Ley, S.C., Ardavin, C., Cuenda, A., 2012. p38γ and p38δ kinases regulate the Toll-like receptor 4 (TLR4)-induced cytokine production by controlling ERK1/2 protein kinase pathway activation. Proc. Natl. Acad. Sci. U. S. A. 109, 11200–11205. https://doi.org/10.1073/pnas.1207290109

Rizzo, P., Perico, N., Gagliardini, E., Novelli, R., Alison, M.R., Remuzzi, G., Benigni, A., 2013. Nature and Mediators of Parietal Epithelial Cell Activation in Glomerulonephritides of Human and Rat. Am. J. Pathol. 183, 1769–1778. https://doi.org/10.1016/j.ajpath.2013.08.008

Rocnik, E.F., Liu, P., Sato, K., Walsh, K., Vaziri, C., 2006. The Novel SPARC Family Member SMOC-2 Potentiates Angiogenic Growth Factor Activity. J. Biol. Chem. 281, 22855–22864. https://doi.org/10.1074/jbc.M513463200

Romagnani, P., Remuzzi, G., Glassock, R., Levin, A., Jager, K.J., Tonelli, M., Massy, Z., Wanner, C., Anders, H.-J., 2017. Chronic kidney disease. Nat. Rev. Dis. Primer 3, 17088. https://doi.org/10.1038/nrdp.2017.88

Rota Marcello, Boni Alessandro, Urbanek Konrad, Padin-Iruegas Maria Elena, Kajstura Tymoteusz J., Fiore Giuseppe, Kubo Hajime, Sonnenblick Edmund H., Musso Ezio, Houser Steve R., Leri Annarosa, Sussman Mark A., Anversa Piero, 2005. Nuclear Targeting of Akt Enhances Ventricular Function and Myocyte Contractility. Circ. Res. 97, 1332–1341. https://doi.org/10.1161/01.RES.0000196568.11624.ae

Rudman-Melnick, V., Adam, M., Potter, A., Chokshi, S.M., Ma, Q., Drake, K.A., Schuh, M.P., Kofron, J.M., Devarajan, P., Potter, S.S., 2019. Single Cell Profiling of Acute Kidney Injury Reveals Novel Transcriptional Signatures, Mixed Identities and Epithelial-to-Stromal Crosstalk. bioRxiv 2019.12.30.890905. https://doi.org/10.1101/2019.12.30.890905

Ruggajo, P., Svarstad, E., Leh, S., Marti, H.-P., Reisæther, A.V., Vikse, B.E., 2016. Low Birth Weight and Risk of Progression to End Stage Renal Disease in IgA Nephropathy—A Retrospective Registry-Based Cohort Study. PLOS ONE 11, e0153819. https://doi.org/10.1371/journal.pone.0153819

Ruggenenti, P., Cravedi, P., Remuzzi, G., 2012. Mechanisms and Treatment of CKD. J. Am. Soc. Nephrol. 23, 1917–1928. https://doi.org/10.1681/ASN.2012040390

Ruiz-Ortega, M., Rayego-Mateos, S., Lamas, S., Ortiz, A., Rodrigues-Diez, R.R., 2020. Targeting the progression of chronic kidney disease. Nat. Rev. Nephrol. 16, 269–288. https://doi.org/10.1038/s41581-019-0248-y

Rüster, C., Wolf, G., 2011. Angiotensin II as a morphogenic cytokine stimulating renal fibrogenesis. J. Am. Soc. Nephrol. JASN 22, 1189–1199. https://doi.org/10.1681/ASN.2010040384

Sabio, G., Davis, R.J., 2014. TNF and MAP kinase signalling pathways. Semin. Immunol. 26, 237–245. https://doi.org/10.1016/j.smim.2014.02.009

Saito, S., Shimizu, H., Yisireyili, M., Nishijima, F., Enomoto, A., Niwa, T., 2014. Indoxyl sulfate-induced activation of (pro)renin receptor is involved in expression of TGF-β1 and α-smooth muscle actin in proximal tubular cells. Endocrinology 155, 1899–1907. https://doi.org/10.1210/en.2013-1937

Santos, C.X., Hafstad, A.D., Beretta, M., Zhang, M., Molenaar, C., Kopec, J., Fotinou, D., Murray, T.V., Cobb, A.M., Martin, D., Zeh Silva, M., Anilkumar, N., Schröder, K., Shanahan, C.M., Brewer, A.C., Brandes, R.P., Blanc, E., Parsons, M., Belousov, V., Cammack, R., Hider, R.C., Steiner, R.A., Shah, A.M., 2016. Targeted redox inhibition of protein phosphatase 1 by Nox4 regulates eIF2α-mediated stress signaling. EMBO J. 35, 319–334. https://doi.org/10.15252/embj.201592394

Saran, R., Robinson, B., Abbott, K.C., Agodoa, L.Y.C., Albertus, P., Ayanian, J., Balkrishnan, R., Bragg-Gresham, J., Cao, J., Chen, J.L.T., Cope, E., Dharmarajan, S., Dietrich, X., Eckard, A., Eggers, P.W., Gaber, C., Gillen, D., Gipson, D., Gu, H., Hailpern, S.M., Hall, Y.N., Han, Y., He, K., Hebert, P., Helmuth, M., Herman, W., Heung, M., Hutton, D., Jacobsen, S.J., Ji, N., Jin, Y., Kalantar-Zadeh, K., Kapke, A., Katz, R., Kovesdy, C.P., Kurtz, V., Lavallee, D., Li, Y., Lu, Y., McCullough, K., Molnar, M.Z., Montez-Rath, M., Morgenstern, H., Mu, Q., Mukhopadhyay, P., Nallamothu, B., Nguyen, D.V., Norris, K.C., O'Hare, A.M., Obi, Y., Pearson, J., Pisoni, R., Plattner, B., Port, F.K., Potukuchi, P., Rao, P., Ratkowiak, K., Ravel, V., Ray, D., Rhee, C.M., Schaubel, D.E., Selewski, D.T., Shaw, S., Shi, J., Shieu, M., Sim, J.J., Song, P., Soohoo, M., Steffick, D., Streja, E., Tamura, M.K., Tentori, F., Tilea, A., Tong, L.,

Turf, M., Wang, D., Wang, M., Woodside, K., Wyncott, A., Xin, X., Zeng, W., Zepel, L., Zhang, S., Zho, H., Hirth, R.A., Shahinian, V., 2017. US Renal Data System 2016 Annual Data Report: Epidemiology of Kidney Disease in the United States. Am. J. Kidney Dis. 69, A7–A8. https://doi.org/10.1053/j.ajkd.2016.12.004

Sasaki, T., Hohenester, E., Göhring, W., Timpl, R., 1998. Crystal structure and mapping by site-directed mutagenesis of the collagen-binding epitope of an activated form of BM-40/SPARC/osteonectin. EMBO J. 17, 1625–1634. https://doi.org/10.1093/emboj/17.6.1625

Satoh, N., Nakamura, M., Suzuki, M., Suzuki, A., Seki, G., Horita, S., 2015. Roles of Akt and SGK1 in the Regulation of Renal Tubular Transport [WWW Document]. BioMed Res. Int. https://doi.org/10.1155/2015/971697

Scalia, C.R., Gendusa, R., Cattoretti, G., 2016. A 2-Step Laemmli and Antigen Retrieval Method Improves Immunodetection. Appl. Immunohistochem. Mol. Morphol. AIMM 24, 436–446. https://doi.org/10.1097/PAI.0000000000000203

Schindelin, J., Arganda-Carreras, I., Frise, E., Kaynig, V., Longair, M., Pietzsch, T., Preibisch, S., Rueden, C., Saalfeld, S., Schmid, B., Tinevez, J.-Y., White, D.J., Hartenstein, V., Eliceiri, K., Tomancak, P., Cardona, A., 2012. Fiji: an open-source platform for biological-image analysis. Nat. Methods 9, 676–682. https://doi.org/10.1038/nmeth.2019

Schmidt, U., Weigert, M., Broaddus, C., Myers, G., 2018. Cell Detection with Star-convex Polygons. ArXiv180603535 Cs 11071, 265–273. https://doi.org/10.1007/978-3-030-00934-2_30

Schnaper, H.W., 2017. The Tubulointerstitial Pathophysiology of Progressive Kidney Disease. Adv. Chronic Kidney Dis. 24, 107–116. https://doi.org/10.1053/j.ackd.2016.11.011

Schneider, D.J., Wu, M., Le, T.T., Cho, S.-H., Brenner, M.B., Blackburn, M.R., Agarwal, S.K., 2012. Cadherin-11 contributes to pulmonary fibrosis: potential role in TGF-β production and epithelial to mesenchymal transition. FASEB J. 26, 503–512. https://doi.org/10.1096/fj.11-186098

Schubert, W., 2003. Topological proteomics, toponomics, MELK-technology. Adv. Biochem. Eng. Biotechnol. 83, 189–209. https://doi.org/10.1007/3-540-36459-5_8

Schubert, W., Bonnekoh, B., Pommer, A.J., Philipsen, L., Böckelmann, R., Malykh, Y., Gollnick, H., Friedenberger, M., Bode, M., Dress, A.W.M., 2006. Analyzing proteome topology and function by automated multidimensional fluorescence microscopy. Nat. Biotechnol. 24, 1270–1278. https://doi.org/10.1038/nbt1250

Schubert, W., Dress, A., Ruonala, M., Krusche, A., Hillert, R., Gieseler, A., Walden, P., 2014. Imaging cycler microscopy. Proc. Natl. Acad. Sci. 111, E215–E215. https://doi.org/10.1073/pnas.1319017111

Schuh, C.D., Haenni, D., Craigie, E., Ziegler, U., Weber, B., Devuyst, O., Hall, A.M., 2016. Long wavelength multiphoton excitation is advantageous for intravital kidney imaging. Kidney Int. 89, 712–719. https://doi.org/10.1038/ki.2015.323

Scott, L.J., McCormack, P.L., 2008. Olmesartan medoxomil: a review of its use in the management of hypertension. Drugs 68, 1239–1272. https://doi.org/10.2165/00003495-200868090-00005

Semenza, G.L., 2001. HIF-1, O(2), and the 3 PHDs: how animal cells signal hypoxia to the nucleus. Cell 107, 1–3. https://doi.org/10.1016/s0092-8674(01)00518-9

Sendoel, A., Hengartner, M.O., 2014. Apoptotic cell death under hypoxia. Physiol. Bethesda Md 29, 168–176. https://doi.org/10.1152/physiol.00016.2013

Seo, E., Kim, W.-Y., Hur, J., Kim, H., Nam, S.A., Choi, A., Kim, Y.-M., Park, S.H., Chung, C., Kim, J., Min, S., Myung, S.-J., Lim, D.-S., Kim, Y.K., 2016. The Hippo-Salvador signaling pathway regulates renal tubulointerstitial fibrosis. Sci. Rep. 6, 31931. https://doi.org/10.1038/srep31931

Shamonin, D.P., Bron, E.E., Lelieveldt, B.P.F., Smits, M., Klein, S., Staring, M., Alzheimer's Disease Neuroimaging Initiative, 2013. Fast parallel image registration on CPU and GPU

for diagnostic classification of Alzheimer's disease. Front. Neuroinformatics 7, 50. https://doi.org/10.3389/fninf.2013.00050

Shi, S.R., Key, M.E., Kalra, K.L., 1991. Antigen retrieval in formalin-fixed, paraffin-embedded tissues: an enhancement method for immunohistochemical staining based on microwave oven heating of tissue sections. J. Histochem. Cytochem. Off. J. Histochem. Soc. 39, 741–748. https://doi.org/10.1177/39.6.1709656

Shin, R.W., Iwaki, T., Kitamoto, T., Tateishi, J., 1991. Hydrated autoclave pretreatment enhances TAU immunoreactivity in formalin-fixed normal and Alzheimer's disease brain tissues. Lab. Invest. 64, 693–702.

Shirata, N., Ihara, K., Yamamoto-Nonaka, K., Seki, T., Makino, S., Trejo, J.A.O., Miyake, T., Yamada, H., Campbell, K.N., Nakagawa, T., Mori, K., Yanagita, M., Mundel, P., Nishimori, K., Asanuma, K., 2017. Glomerulosclerosis Induced by Deficiency of Membrane-Associated Guanylate Kinase Inverted 2 in Kidney Podocytes. J. Am. Soc. Nephrol. 28, 2654–2669. https://doi.org/10.1681/ASN.2016121356

Silva, G.E.B., Costa, R.S., Ravinal, R.C., Ramalho, L.Z., Dos Reis, M.A., Coimbra, T.M., Dantas, M., 2011. NF-kB expression in IgA nephropathy outcome. Dis. Markers 31, 9–15. https://doi.org/10.3233/DMA-2011-0795

Sindhu, R.K., Ehdaie, A., Vaziri, N.D., Roberts, C.K., 2004. Effects of chronic renal failure on caveolin-1, guanylate cyclase and AKT protein expression. Biochim. Biophys. Acta BBA - Mol. Basis Dis. 1690, 231–237. https://doi.org/10.1016/j.bbadis.2004.06.013

Snezhkina, A.V., Nyushko, K.M., Zaretsky, A.R., Shagin, D.A., Sadritdinova, A.F., Fedorova, M.S., Guvatova, Z.G., Abramov, I.S., Pudova, E.A., Alekseev, B.Y., Dmitriev, A.A., Kudryavtseva, A.V., 2018. Transcription Factor SAP30 Is Involved in the Activation of NETO2 Gene Expression in Clear Cell Renal Cell Carcinoma. Mol. Biol. 52, 385–392. https://doi.org/10.1134/S0026893318020152

Sparks, M.A., Crowley, S.D., Gurley, S.B., Mirotsou, M., Coffman, T.M., 2014. Classical Renin-Angiotensin System in Kidney Physiology. Compr. Physiol. 4, 1201–1228. https://doi.org/10.1002/cphy.c130040

Srinivasa, S., Fitch, K.V., Wong, K., Torriani, M., Mayhew, C., Stanley, T., Lo, J., Adler, G.K., Grinspoon, S.K., 2015. RAAS Activation Is Associated With Visceral Adiposity and Insulin Resistance Among HIV-infected Patients. J. Clin. Endocrinol. Metab. 100, 2873–2882. https://doi.org/10.1210/jc.2015-1461

Stack, E.C., Wang, C., Roman, K.A., Hoyt, C.C., 2014. Multiplexed immunohistochemistry, imaging, and quantitation: A review, with an assessment of Tyramide signal amplification, multispectral imaging and multiplex analysis. Methods, Advancing the boundaries of molecular cellular pathology 70, 46–58. https://doi.org/10.1016/j.ymeth.2014.08.016

Stambe, C., Atkins, R., Tesch, G., Masaki, T., Schreiner, G., Nikolic-Paterson, D., 2004. The role of p38alpha mitogen-activated protein kinase activation in renal fibrosis. J. Am. Soc. Nephrol. JASN 15, 370–9.

Stanifer, J.W., Kilonzo, K., Wang, D., Su, G., Mao, W., Zhang, Lei, Zhang, La, Nayak-Rao, S., Miranda, J.J., 2017. Traditional Medicines and Kidney Disease in Low- and Middle-Income Countries: Opportunities and Challenges. Semin. Nephrol. 37, 245–259. https://doi.org/10.1016/j.semnephrol.2017.02.005

Stanifer, J.W., Muiru, A., Jafar, T.H., Patel, U.D., 2016. Chronic kidney disease in low- and middle-income countries. Nephrol. Dial. Transplant. 31, 868–874. https://doi.org/10.1093/ndt/gfv466

Sternberger, L.A., Joseph, S.A., 2017. The unlabeled antibody method. Contrasting color staining of paired pituitary hormones without antibody removal.: J. Histochem. Cytochem. https://doi.org/10.1177/27.11.92498

Stöhr, H., Berger, C., Fröhlich, S., Weber, B.H.F., 2002. A novel gene encoding a putative transmembrane protein with two extracellular CUB domains and a low-density

lipoprotein class A module: isolation of alternatively spliced isoforms in retina and brain. Gene 286, 223–231. https://doi.org/10.1016/s0378-1119(02)00438-9
Stuveling, E.M., Hillege, H.L., Bakker, S.J.L., Gans, R.O.B., Jong, P. de, Zeeuw, D. de, 2003. C-reactive protein is associated with renal function abnormalities in a non-diabetic population. Kidney Int. 63, 654–661.
Sugiyama, N., Kohno, M., Yokoyama, T., 2012. Inhibition of the p38 MAPK pathway ameliorates renal fibrosis in an NPHP2 mouse model. Nephrol. Dial. Transplant. Off. Publ. Eur. Dial. Transpl. Assoc. - Eur. Ren. Assoc. 27, 1351–1358. https://doi.org/10.1093/ndt/gfr550
Sun, F., Teng, J., Yu, P., Li, W., Chang, J., Xu, H., 2018. Involvement of TWEAK and the NF-κB signaling pathway in lupus nephritis. Exp. Ther. Med. 15, 2611–2619. https://doi.org/10.3892/etm.2018.5711
Sun, H., Ding, J., Zheng, H., Lv, K., Hu, Y., Luo, Y., Wu, X., Pei, W., Wang, L., Wu, M., Zhang, Y., Gao, J., 2020. The Effects of Sidt2 on the Inflammatory Pathway in Mouse Mesangial Cells [WWW Document]. Mediators Inflamm. https://doi.org/10.1155/2020/3560793
Tajti, F., Kuppe, C., Antoranz, A., Ibrahim, M.M., Kim, H., Ceccarelli, F., Holland, C.H., Olauson, H., Floege, J., Alexopoulos, L.G., Kramann, R., Saez-Rodriguez, J., 2020. A Functional Landscape of CKD Entities From Public Transcriptomic Data. Kidney Int. Rep. 5, 211–224. https://doi.org/10.1016/j.ekir.2019.11.005
Takac, I., Schröder, K., Zhang, L., Lardy, B., Anilkumar, N., Lambeth, J.D., Shah, A.M., Morel, F., Brandes, R.P., 2011. The E-loop Is Involved in Hydrogen Peroxide Formation by the NADPH Oxidase Nox4. J. Biol. Chem. 286, 13304–13313. https://doi.org/10.1074/jbc.M110.192138
Tan, R.J., Liu, Y., 2012. Matrix metalloproteinases in kidney homeostasis and diseases. Am. J. Physiol. Renal Physiol. 302, F1351-1361. https://doi.org/10.1152/ajprenal.00037.2012
Taneda, S., Kl, H., S, T., Dg, G., V, O., L, T., Rj, J., Ce, A., 2003. Obstructive uropathy in mice and humans: potential role for PDGF-D in the progression of tubulointerstitial injury. J. Am. Soc. Nephrol. JASN 14, 2544–2555. https://doi.org/10.1097/01.asn.0000089828.73014.c8
Tang, B., Tang, F., Wang, Z., Qi, G., Liang, X., Li, B., Yuan, S., Liu, J., Yu, S., He, S., 2016. Upregulation of Akt/NF-κB-regulated inflammation and Akt/Bad-related apoptosis signaling pathway involved in hepatic carcinoma process: suppression by carnosic acid nanoparticle [WWW Document]. Int. J. Nanomedicine. https://doi.org/10.2147/IJN.S101285
Taylor, A.H., Colley, Stead, 2013. Education Guide Immunohistochemical Staining Methods Sixth Edition 218.
The Low Birth Weight and Nephron Number Working Group, 2017. The Impact of Kidney Development on the Life Course: A Consensus Document for Action. Nephron 136, 3–49. https://doi.org/10.1159/000457967
Thévenaz, P., Ruttimann, U.E., Unser, M., 1998. A pyramid approach to subpixel registration based on intensity. IEEE Trans. Image Process. Publ. IEEE Signal Process. Soc. 7, 27–41. https://doi.org/10.1109/83.650848
Tirapelli, L.F., Trazzi, B.F.M., Bagnato, V.S., Tirapelli, D.P.C., Kurachi, C., da Costa, M.M., Tucci, S., Cologna, A.J., Martins, A.C.P., 2009. Histopathology and laser autofluorescence of ischemic kidneys of rats. Lasers Med. Sci. 24, 397–404. https://doi.org/10.1007/s10103-008-0578-7
Tischer, 2019. ElastixWrapper: Fiji plugin for 3D image registration with elastix | Zenodo [WWW Document]. URL https://zenodo.org/record/2602549 (accessed 7.22.20).
Tomasek, J.J., Gabbiani, G., Hinz, B., Chaponnier, C., Brown, R.A., 2002. Myofibroblasts and mechano-regulation of connective tissue remodelling. Nat. Rev. Mol. Cell Biol. 3, 349–363. https://doi.org/10.1038/nrm809
Tornehave, D., Hougaard, D.M., Larsson, L., 2000. Microwaving for double indirect immunofluorescence with primary antibodies from the same species and for staining of

mouse tissues with mouse monoclonal antibodies. Histochem. Cell Biol. 113, 19–23. https://doi.org/10.1007/s004180050002
Tóth, Z.E., Mezey, E., 2007. Simultaneous visualization of multiple antigens with tyramide signal amplification using antibodies from the same species. J. Histochem. Cytochem. Off. J. Histochem. Soc. 55, 545–554. https://doi.org/10.1369/jhc.6A7134.2007
Tramu, G., Pillez, A., Leonardelli, J., 1978. An efficient method of antibody elution for the successive or simultaneous localization of two antigens by immunocytochemistry. J. Histochem. Cytochem. 26, 322–324. https://doi.org/10.1177/26.4.207771
Trautmann, A., Bodria, M., Ozaltin, F., Gheisari, A., Melk, A., Azocar, M., Anarat, A., Caliskan, S., Emma, F., Gellermann, J., Oh, J., Baskin, E., Ksiazek, J., Remuzzi, G., Erdogan, O., Akman, S., Dusek, J., Davitaia, T., Özkaya, O., Papachristou, F., Firszt-Adamczyk, A., Urasinski, T., Testa, S., Krmar, R.T., Hyla-Klekot, L., Pasini, A., Özcakar, Z.B., Sallay, P., Cakar, N., Galanti, M., Terzic, J., Aoun, B., Caldas Afonso, A., Szymanik-Grzelak, H., Lipska, B.S., Schnaidt, S., Schaefer, F., 2015. Spectrum of Steroid-Resistant and Congenital Nephrotic Syndrome in Children: The PodoNet Registry Cohort. Clin. J. Am. Soc. Nephrol. 10, 592–600. https://doi.org/10.2215/CJN.06260614
Urakawa, I., Yamazaki, Y., Shimada, T., Iijima, K., Hasegawa, H., Okawa, K., Fujita, T., Fukumoto, S., Yamashita, T., 2006. Klotho converts canonical FGF receptor into a specific receptor for FGF23. Nature 444, 770–774. https://doi.org/10.1038/nature05315
Urushihara, M., Kagami, S., Kuhara, T., Tamaki, T., Kuroda, Y., 2002. Glomerular distribution and gelatinolytic activity of matrix metalloproteinases in human glomerulonephritis. Nephrol. Dial. Transplant. 17, 1189–1196. https://doi.org/10.1093/ndt/17.7.1189
Uy, N., Reidy, K., 2015. Developmental Genetics and Congenital Anomalies of the Kidney and Urinary Tract. J. Pediatr. Genet. 05, 051–060. https://doi.org/10.1055/s-0035-1558423
Valdivielso, J., Eritja, À., Caus, M., Bozic Stanojevic, M., 2020. Glutamate-Gated NMDA Receptors: Insights into the Function and Signaling in the Kidney. Biomolecules 10, 1051. https://doi.org/10.3390/biom10071051
Vallon, V., 2015. The Mechanisms and Therapeutic Potential of SGLT2 Inhibitors in Diabetes Mellitus. Annu. Rev. Med. 66, 255–270. https://doi.org/10.1146/annurev-med-051013-110046
van Bommel, E.J.M., Muskiet, M.H.A., Tonneijck, L., Kramer, M.H.H., Nieuwdorp, M., van Raalte, D.H., 2017. SGLT2 Inhibition in the Diabetic Kidney—From Mechanisms to Clinical Outcome. Clin. J. Am. Soc. Nephrol. 12, 700–710. https://doi.org/10.2215/CJN.06080616
Van Kooten, C., Boonstra, J.G., Paape, M.E., Fossiez, F., Banchereau, J., Lebecque, S., Bruijn, J.A., De Fijter, J.W., Van Es, L.A., Daha, M.R., 1998. Interleukin-17 activates human renal epithelial cells in vitro and is expressed during renal allograft rejection. J. Am. Soc. Nephrol. JASN 9, 1526–1534.
Varelas, X., Miller, B.W., Sopko, R., Song, S., Gregorieff, A., Fellouse, F.A., Sakuma, R., Pawson, T., Hunziker, W., McNeill, H., Wrana, J.L., Attisano, L., 2010. The Hippo pathway regulates Wnt/beta-catenin signaling. Dev. Cell 18, 579–591. https://doi.org/10.1016/j.devcel.2010.03.007
Varelas, X., Sakuma, R., Samavarchi-Tehrani, P., Peerani, R., Rao, B.M., Dembowy, J., Yaffe, M.B., Zandstra, P.W., Wrana, J.L., 2008. TAZ controls Smad nucleocytoplasmic shuttling and regulates human embryonic stem-cell self-renewal. Nat. Cell Biol. 10, 837–848. https://doi.org/10.1038/ncb1748
Villarino, A.V., Kanno, Y., O'Shea, J.J., 2017. Mechanisms and consequences of Jak-STAT signaling in the immune system. Nat. Immunol. 18, 374–384. https://doi.org/10.1038/ni.3691
Vivarelli, M., Massella, L., Ruggiero, B., Emma, F., 2017. Minimal Change Disease. Clin. J. Am. Soc. Nephrol. CJASN 12, 332–345. https://doi.org/10.2215/CJN.05000516
von Vietinghoff, S., Ley, K., 2010. Interleukin 17 in vascular inflammation. Cytokine Growth Factor Rev. 21, 463–469. https://doi.org/10.1016/j.cytogfr.2010.10.003

Vyklicky, V., Korinek, M., Smejkalova, T., Balik, A., Krausova, B., Kaniakova, M., Lichnerova, K., Cerny, J., Krusek, J., Dittert, I., Horak, M., Vyklicky, L., 2014. Structure, function, and pharmacology of NMDA receptor channels. Physiol. Res. 63 Suppl 1, S191-203.

Wada, J., Makino, H., 2016. Innate immunity in diabetes and diabetic nephropathy. Nat. Rev. Nephrol. 12, 13–26. https://doi.org/10.1038/nrneph.2015.175

Walker, K.A., Sims-Lucas, S., Bates, C.M., 2016. Fibroblast growth factor receptor signaling in kidney and lower urinary tract development. Pediatr. Nephrol. Berl. Ger. 31, 885–895. https://doi.org/10.1007/s00467-015-3151-1

Wallquist, C., Mansouri, L., Norrbäck, M., Hylander, B., Jacobson, S.H., Larsson, T.E., Lundahl, J., 2018. Associations of Fibroblast Growth Factor 23 with Markers of Inflammation and Leukocyte Transmigration in Chronic Kidney Disease. Nephron 138, 287–295. https://doi.org/10.1159/000485472

Wang, B., Zhang, A., Wang, H., Klein, J.D., Tan, L., Wang, Z.-M., Du, J., Naqvi, N., Liu, B.-C., Wang, X.H., 2019. miR-26a Limits Muscle Wasting and Cardiac Fibrosis through Exosome-Mediated microRNA Transfer in Chronic Kidney Disease. Theranostics 9, 1864–1877. https://doi.org/10.7150/thno.29579

Wang, F., Lu, X., Peng, K., Zhou, L., Li, C., Wang, W., Yu, X., Kohan, D.E., Zhu, S.-F., Yang, T., 2014. COX-2 mediates angiotensin II-induced (pro)renin receptor expression in the rat renal medulla. Am. J. Physiol. Renal Physiol. 307, F25-32. https://doi.org/10.1152/ajprenal.00548.2013

Wang, J., Fu, D., Senouthai, S., You, Y., 2019. Critical roles of PI3K/Akt/NF-κB survival axis in angiotensin II-induced podocyte injury. Mol. Med. Rep. 20, 5134–5144. https://doi.org/10.3892/mmr.2019.10733

Wang, P., Sun, B., Hao, D., Zhang, X., Shi, T., Ma, D., 2010. Human TMEM174 that is highly expressed in kidney tissue activates AP-1 and promotes cell proliferation. Biochem. Biophys. Res. Commun. 394, 993–999. https://doi.org/10.1016/j.bbrc.2010.03.109

Wang, W., Shen, J., Qi, C., Pu, J., Chen, H., Zuo, Z., 2020. The key candidate genes in tubulointerstitial injury of chronic kidney diseases patients as determined by bioinformatic analysis. Cell Biochem. Funct. cbf.3545. https://doi.org/10.1002/cbf.3545

Wang, X., Shaw, S., Amiri, F., Eaton, D.C., Marrero, M.B., 2002. Inhibition of the JAK/STAT Signaling Pathway Prevents the High Glucose-Induced Increase in TGF-β and Fibronectin Synthesis in Mesangial Cells. Diabetes 51, 3505–3509. https://doi.org/10.2337/diabetes.51.12.3505

Wang, X.-D., Huang, X.-F., Yan, Q.-R., Bao, C., 2014. Aberrant activation of the WNT/β-catenin signaling pathway in lupus nephritis. PloS One 9, e84852. https://doi.org/10.1371/journal.pone.0084852

Wang, X.-M., Yao, M., Liu, S.-X., Hao, J., Liu, Q.-J., Gao, F., 2014. Interplay between the Notch and PI3K/Akt pathways in high glucose-induced podocyte apoptosis. Am. J. Physiol. Renal Physiol. 306, F205-213. https://doi.org/10.1152/ajprenal.90005.2013

Wendt, T.M., Tanji, N., Guo, J., Kislinger, T.R., Qu, W., Lu, Y., Bucciarelli, L.G., Rong, L.L., Moser, B., Markowitz, G.S., Stein, G., Bierhaus, A., Liliensiek, B., Arnold, B., Nawroth, P.P., Stern, D.M., D'Agati, V.D., Schmidt, A.M., 2003. RAGE Drives the Development of Glomerulosclerosis and Implicates Podocyte Activation in the Pathogenesis of Diabetic Nephropathy. Am. J. Pathol. 162, 1123–1137. https://doi.org/10.1016/S0002-9440(10)63909-0

Wenger, R.H., Stiehl, D.P., Camenisch, G., 2005. Integration of oxygen signaling at the consensus HRE. Sci. STKE Signal Transduct. Knowl. Environ. 2005, re12. https://doi.org/10.1126/stke.3062005re12

Wernig, G., Chen, S.-Y., Cui, L., Van Neste, C., Tsai, J.M., Kambham, N., Vogel, H., Natkunam, Y., Gilliland, D.G., Nolan, G., Weissman, I.L., 2017. Unifying mechanism for different fibrotic diseases. Proc. Natl. Acad. Sci. 114, 4757–4762. https://doi.org/10.1073/pnas.1621375114

Whittier, E.O., 1925. Lactose. A Review. Chem. Rev. 2, 85–125. https://doi.org/10.1021/cr60005a003
Williams, V.R., Konvalinka, A., Song, X., Zhou, X., John, R., Pei, Y., Scholey, J.W., 2020. Connectivity mapping of a chronic kidney disease progression signature identified lysine deacetylases as novel therapeutic targets. Kidney Int. 98, 116–132. https://doi.org/10.1016/j.kint.2020.01.029
Wong, G.S., Rustgi, A.K., 2013. Matricellular proteins: priming the tumour microenvironment for cancer development and metastasis. Br. J. Cancer 108, 755–761. https://doi.org/10.1038/bjc.2012.592
Wrighton, K.H., Dai, F., Feng, X.-H., 2008. A new kid on the TGFbeta block: TAZ controls Smad nucleocytoplasmic shuttling. Dev. Cell 15, 8–10. https://doi.org/10.1016/j.devcel.2008.06.010
Wu, J., Saleh, M.A., Kirabo, A., Itani, H.A., Montaniel, K.R.C., Xiao, L., Chen, W., Mernaugh, R.L., Cai, H., Bernstein, K.E., Goronzy, J.J., Weyand, C.M., Curci, J.A., Barbaro, N.R., Moreno, H., Davies, S.S., Roberts, L.J., Madhur, M.S., Harrison, D.G., 2016. Immune activation caused by vascular oxidation promotes fibrosis and hypertension. J. Clin. Invest. 126, 50–67. https://doi.org/10.1172/JCI80761
Wu, M.-J., Wen, M.-C., Chiu, Y.-T., Chiou, Y.-Y., Shu, K.-H., Tang, M.-J., 2006. Rapamycin attenuates unilateral ureteral obstruction-induced renal fibrosis. Kidney Int. 69, 2029–2036. https://doi.org/10.1038/sj.ki.5000161
Xiao, L., Zhu, X., Yang, S., Liu, F., Zhou, Z., Zhan, M., Xie, P., Zhang, D., Li, J., Song, P., Kanwar, Y.S., Sun, L., 2014. Rap1 ameliorates renal tubular injury in diabetic nephropathy. Diabetes 63, 1366–1380. https://doi.org/10.2337/db13-1412
Xiao, Y.Q., Freire-de-Lima, C.G., Schiemann, W.P., Bratton, D.L., Vandivier, R.W., Henson, P.M., 2008. Transcriptional and Translational Regulation of TGF-β Production in Response to Apoptotic Cells. J. Immunol. 181, 3575–3585. https://doi.org/10.4049/jimmunol.181.5.3575
Xing, X., Yang, J., Yang, X., Wei, Y., Zhu, L., Gao, D., Li, M., 2013. IL-17A Induces Endothelial Inflammation in Systemic Sclerosis via the ERK Signaling Pathway. PLOS ONE 8, e85032. https://doi.org/10.1371/journal.pone.0085032
Xu, D., Young, J.H., Krahn, J.M., Song, D., Corbett, K.D., Chazin, W.J., Pedersen, L.C., Esko, J.D., 2013. Stable RAGE-Heparan Sulfate Complexes Are Essential for Signal Transduction. ACS Chem. Biol. 8, 1611–1620. https://doi.org/10.1021/cb4001553
Xu, K., Rosenstiel, P., Paragas, N., Hinze, C., Gao, X., Huai Shen, T., Werth, M., Forster, C., Deng, R., Bruck, E., Boles, R.W., Tornato, A., Gopal, T., Jones, M., Konig, J., Stauber, J., D'Agati, V., Erdjument-Bromage, H., Saggi, S., Wagener, G., Schmidt-Ott, K.M., Tatonetti, N., Tempst, P., Oliver, J.A., Guarnieri, P., Barasch, J., 2017. Unique Transcriptional Programs Identify Subtypes of AKI. J. Am. Soc. Nephrol. JASN 28, 1729–1740. https://doi.org/10.1681/ASN.2016090974
Xu, X.-H., Pan, W., Kang, L.-H., Feng, H., Song, Y.-Q., 2015. Association of annexin A2 with cancer development (Review). Oncol. Rep. 33, 2121–2128. https://doi.org/10.3892/or.2015.3837
Yamamoto, Y., Kato, I., Doi, T., Yonekura, H., Ohashi, S., Takeuchi, M., Watanabe, T., Yamagishi, S., Sakurai, S., Takasawa, S., Okamoto, H., Yamamoto, H., 2001. Development and prevention of advanced diabetic nephropathy in RAGE-overexpressing mice. J. Clin. Invest. 108, 261–268. https://doi.org/10.1172/JCI11771
Yamazaki, Y., Arita, K., Harada, S., Tokuyama, S., 2018. Activation of c-Jun N-terminal kinase and p38 after cerebral ischemia upregulates cerebral sodium-glucose transporter type 1. J. Pharmacol. Sci. 138, 240–246. https://doi.org/10.1016/j.jphs.2017.02.016
Yang, J.C., Cortopassi, G.A., 1998. dATP causes specific release of cytochrome C from mitochondria. Biochem. Biophys. Res. Commun. 250, 454–457. https://doi.org/10.1006/bbrc.1998.9333

Yang, Q., Ma, Y., Liu, Y., Liang, W., Chen, X., Ren, Z., Wang, H., Singhal, P.C., Ding, G., 2016. Angiotensin II down-regulates nephrin–Akt signaling and induces podocyte injury: roleof c-Abl. Mol. Biol. Cell 27, 197–208. https://doi.org/10.1091/mbc.E15-04-0223
Yang, Y., Kim, S.C., Yu, T., Yi, Y.-S., Rhee, M.H., Sung, G.-H., Yoo, B.C., Cho, J.Y., 2014. Functional Roles of p38 Mitogen-Activated Protein Kinase in Macrophage-Mediated Inflammatory Responses [WWW Document]. Mediators Inflamm. https://doi.org/10.1155/2014/352371
Yang, Y., Yang, Q., Yang, J., Ma, Y., Ding, G., 2017. Angiotensin II induces cholesterol accumulation and injury in podocytes. Sci. Rep. 7, 10672. https://doi.org/10.1038/s41598-017-09733-w
Yang, Z.-Z., Tschopp, O., Baudry, A., Dümmler, B., Hynx, D., Hemmings, B.A., 2004. Physiological functions of protein kinase B/Akt. Biochem. Soc. Trans. 32, 350–354. https://doi.org/10.1042/bst0320350
Yavuz, Y.C., Altınkaynak, K., Sevinc, C., Ozbek Sebin, S., Baydar, I., 2019. The cartonectin levels at different stages of chronic kidney disease and related factors. Ren. Fail. 41, 42–46. https://doi.org/10.1080/0886022X.2018.1561373
Yu, S., 2016. Role of nephrin in podocyte injury induced by angiotension II. J. Recept. Signal Transduct. Res. 36, 1–5. https://doi.org/10.3109/10799893.2014.963872
Yuan, H., Ren, Z.-L., Hu, F.-Q., Liang, W., Ding, G.-H., 2012. Renin induces apoptosis in podocytes through a receptor-mediated, angiotensin II-independent mechanism. Am. J. Med. Sci. 344, 441–446. https://doi.org/10.1097/MAJ.0b013e318245fdaa
Yu-Shengyou, null, Li, Y., 2013. Dexamethasone inhibits podocyte apoptosis by stabilizing the PI3K/Akt signal pathway. BioMed Res. Int. 2013, 326986. https://doi.org/10.1155/2013/326986
Zaiss, D.M.W., Gause, W.C., Osborne, L.C., Artis, D., 2015. Emerging functions of amphiregulin in orchestrating immunity, inflammation, and tissue repair. Immunity 42, 216–226. https://doi.org/10.1016/j.immuni.2015.01.020
Zavadil, J., Cermak, L., Soto-Nieves, N., Böttinger, E.P., 2004. Integration of TGF-beta/Smad and Jagged1/Notch signalling in epithelial-to-mesenchymal transition. EMBO J. 23, 1155–1165. https://doi.org/10.1038/sj.emboj.7600069
Zhang, B., Umbach, A.T., Chen, H., Yan, J., Fakhri, H., Fajol, A., Salker, M.S., Spichtig, D., Daryadel, A., Wagner, C.A., Föller, M., Lang, F., 2016. Up-regulation of FGF23 release by aldosterone. Biochem. Biophys. Res. Commun. 470, 384–390. https://doi.org/10.1016/j.bbrc.2016.01.034
Zhang, H., Chen, J., Liu, X., Awar, L., McMickle, A., Bai, F., Nagarajan, S., Yu, S., 2013. IL-17 induces expression of vascular cell adhesion molecule through signaling pathway of NF-κB, but not Akt1 and TAK1 in vascular smooth muscle cells. Scand. J. Immunol. 77, 230–237. https://doi.org/10.1111/sji.12030
Zhang, J., Ji, J.-Y., Yu, M., Overholtzer, M., Smolen, G.A., Wang, R., Brugge, J.S., Dyson, N.J., Haber, D.A., 2009. YAP-dependent induction of amphiregulin identifies a non-cell-autonomous component of the Hippo pathway. Nat. Cell Biol. 11, 1444–1450. https://doi.org/10.1038/ncb1993
Zhang, J., Wu, J., Gu, C., Noble, N.A., Border, W.A., Huang, Y., 2012. Receptor-mediated nonproteolytic activation of prorenin and induction of TGF-β1 and PAI-1 expression in renal mesangial cells. Am. J. Physiol. Renal Physiol. 303, F11-20. https://doi.org/10.1152/ajprenal.00050.2012
Zhang, J., Zhang, R., Wang, Y., Li, H., Han, Q., Wu, Y., Wang, T., Liu, F., 2019. The Level of Serum Albumin Is Associated with Renal Prognosis in Patients with Diabetic Nephropathy. J. Diabetes Res. 2019, 7825804. https://doi.org/10.1155/2019/7825804
Zhang, L., Z, R., Q, Y., G, D., 2016. Csk regulates angiotensin II-induced podocyte apoptosis. Apoptosis Int. J. Program. Cell Death 21, 846–855. https://doi.org/10.1007/s10495-016-1256-z

Zhang, W.-J., Frei, B., 2002. Albumin selectively inhibits TNFα-induced expression of vascular cell adhesion molecule-1 in human aortic endothelial cells. Cardiovasc. Res. 55, 820–829. https://doi.org/10.1016/S0008-6363(02)00492-3

Zhang, Yuan, Chen, Xiangfan, Yuan, L., Zhang, Yide, Wu, J., Guo, N., Chen, Xu, Liu, J., 2018. Down-regulation of IRAK1 attenuates podocyte apoptosis in diabetic nephropathy through PI3K/Akt signaling pathway. Biochem. Biophys. Res. Commun. 506, 529–535. https://doi.org/10.1016/j.bbrc.2018.09.175

Zhao, B., Tumaneng, K., Guan, K.-L., 2011. The Hippo pathway in organ size control, tissue regeneration and stem cell self-renewal. Nat. Cell Biol. 13, 877–883. https://doi.org/10.1038/ncb2303

Zhao, M., Bai, M., Ding, G., Zhang, Y., Huang, S., Jia, Z., Zhang, A., 2018. Angiotensin II Stimulates the NLRP3 Inflammasome to Induce Podocyte Injury and Mitochondrial Dysfunction. Kidney Dis. 4, 83–94. https://doi.org/10.1159/000488242

Zhou, L., Li, Y., Hao, S., Zhou, D., Tan, R.J., Nie, J., Hou, F.F., Kahn, M., Liu, Y., 2015a. Multiple Genes of the Renin-Angiotensin System Are Novel Targets of Wnt/β-Catenin Signaling. J. Am. Soc. Nephrol. 26, 107–120. https://doi.org/10.1681/ASN.2014010085

Zhou, L., Mo, H., Miao, J., Zhou, D., Tan, R.J., Hou, F.F., Liu, Y., 2015b. Klotho Ameliorates Kidney Injury and Fibrosis and Normalizes Blood Pressure by Targeting the Renin-Angiotensin System. Am. J. Pathol. 185, 3211–3223. https://doi.org/10.1016/j.ajpath.2015.08.004

Zhou, L.-T., Qiu, S., Lv, L.-L., Li, Z.-L., Liu, H., Tang, R.-N., Ma, K.-L., Liu, B.-C., 2018. Integrative Bioinformatics Analysis Provides Insight into the Molecular Mechanisms of Chronic Kidney Disease. Kidney Blood Press. Res. 43, 568–581. https://doi.org/10.1159/000488830

Zhou, M., Veenstra, T.D., 2006. Multiplexed immunofluorescence microscopy for the interrogation of cellular protein complexes. Expert Rev. Proteomics 3, 581–583. https://doi.org/10.1586/14789450.3.6.581

Zhou, P., Wan, X., Zou, Y., Chen, Z., Zhong, A., 2020. Transforming growth factor beta (TGF-β) is activated by the CtBP2-p300-AP1 transcriptional complex in chronic renal failure. Int. J. Biol. Sci. 16, 204–215. https://doi.org/10.7150/ijbs.38841

Zhou, T., Luo, M., Cai, W., Zhou, S., Feng, D., Xu, C., Wang, H., 2018. Runt-Related Transcription Factor 1 (RUNX1) Promotes TGF-β-Induced Renal Tubular Epithelial-to-Mesenchymal Transition (EMT) and Renal Fibrosis through the PI3K Subunit p110δ. EBioMedicine 31, 217–225. https://doi.org/10.1016/j.ebiom.2018.04.023

Zhu, B., Cao, A., Li, J., Young, J., Wong, J., Ashraf, S., Bierzynska, A., Menon, M.C., Hou, S., Sawyers, C., Campbell, K.N., Saleem, M.A., He, J.C., Hildebrandt, F., D'Agati, V.D., Peng, W., Kaufman, L., 2019. Disruption of MAGI2-RapGEF2-Rap1 signaling contributes to podocyte dysfunction in congenital nephrotic syndrome caused by mutations in MAGI2. Kidney Int. 96, 642–655. https://doi.org/10.1016/j.kint.2019.03.016

Zhu, J., Sun, N., Aoudjit, L., Li, H., Kawachi, H., Lemay, S., Takano, T., 2008. Nephrin mediates actin reorganization via phosphoinositide 3-kinase in podocytes. Kidney Int. 73, 556–566. https://doi.org/10.1038/sj.ki.5002691

Zoccali, C., Vanholder, R., Massy, Z.A., Ortiz, A., Sarafidis, P., Dekker, F.W., Fliser, D., Fouque, D., Heine, G.H., Jager, K.J., Kanbay, M., Mallamaci, F., Parati, G., Rossignol, P., Wiecek, A., London, G., on behalf of the European Renal and Cardiovascular Medicine (EURECA-m) Working Group of the European Renal Association – European Dialysis Transplantation Association (ERA-EDTA), 2017. The systemic nature of CKD. Nat. Rev. Nephrol. 13, 344–358. https://doi.org/10.1038/nrneph.2017.52

Zrazhevskiy, P., Gao, X., 2013. Quantum dot imaging platform for single-cell molecular profiling. Nat. Commun. 4, 1619. https://doi.org/10.1038/ncomms2635

Zsurka, G., Gregán, J., Schweyen, R.J., 2001. The human mitochondrial Mrs2 protein functionally substitutes for its yeast homologue, a candidate magnesium transporter. Genomics 72, 158–168. https://doi.org/10.1006/geno.2000.6407

Zur, R., Garcia-Ibanez, L., Nunez-Buiza, A., Aparicio, N., Liappas, G., Escós, A., Risco, A., Page, A., Saiz-Ladera, C., Alsina-Beauchamp, D., Montans, J., Paramio, J.M., Cuenda, A., 2015. Combined deletion of p38γ and p38δ reduces skin inflammation and protects from carcinogenesis. Oncotarget 6, 12920–12935. https://doi.org/10.18632/oncotarget.4320